Report No. **285**

epa Research
Climate - Water - Sustainability
Identifying pressures • Informing policy • Developing solutions

Nutrient Dynamics and Ecophysiology of Opportunistic Macroalgal Blooms in Irish Estuaries and Coastal Bays (Sea-MAT)

Authors: Ricardo Bermejo, Svenja Heesch, Moya O'Donnell, Nessa Golden, Michéal MacMonagail, Maeve Edwards, Edna Curley, Owen Fenton, Eve Daly and Liam Morrison

www.epa.ie

Rialtas na hÉireann
Government of Ireland

ENVIRONMENTAL PROTECTION AGENCY

The Environmental Protection Agency (EPA) is responsible for protecting and improving the environment as a valuable asset for the people of Ireland. We are committed to protecting people and the environment from the harmful effects of radiation and pollution.

The work of the EPA can be divided into three main areas:

Regulation: *We implement effective regulation and environmental compliance systems to deliver good environmental outcomes and target those who don't comply.*

Knowledge: *We provide high quality, targeted and timely environmental data, information and assessment to inform decision making at all levels.*

Advocacy: *We work with others to advocate for a clean, productive and well protected environment and for sustainable environmental behaviour.*

Our Responsibilities

Licensing

We regulate the following activities so that they do not endanger human health or harm the environment:

- waste facilities *(e.g. landfills, incinerators, waste transfer stations)*;
- large scale industrial activities (*e.g. pharmaceutical, cement manufacturing, power plants)*;
- intensive agriculture *(e.g. pigs, poultry)*;
- the contained use and controlled release of Genetically Modified Organisms *(GMOs)*;
- sources of ionising radiation *(e.g. x-ray and radiotherapy equipment, industrial sources)*;
- large petrol storage facilities;
- waste water discharges;
- dumping at sea activities.

National Environmental Enforcement

- Conducting an annual programme of audits and inspections of EPA licensed facilities.
- Overseeing local authorities' environmental protection responsibilities.
- Supervising the supply of drinking water by public water suppliers.
- Working with local authorities and other agencies to tackle environmental crime by co-ordinating a national enforcement network, targeting offenders and overseeing remediation.
- Enforcing Regulations such as Waste Electrical and Electronic Equipment (WEEE), Restriction of Hazardous Substances (RoHS) and substances that deplete the ozone layer.
- Prosecuting those who flout environmental law and damage the environment.

Water Management

- Monitoring and reporting on the quality of rivers, lakes, transitional and coastal waters of Ireland and groundwaters; measuring water levels and river flows.
- National coordination and oversight of the Water Framework Directive.
- Monitoring and reporting on Bathing Water Quality.

Monitoring, Analysing and Reporting on the Environment

- Monitoring air quality and implementing the EU Clean Air for Europe (CAFÉ) Directive.
- Independent reporting to inform decision making by national and local government *(e.g. periodic reporting on the State of Ireland's Environment and Indicator Reports)*.

Regulating Ireland's Greenhouse Gas Emissions

- Preparing Ireland's greenhouse gas inventories and projections.
- Implementing the Emissions Trading Directive, for over 100 of the largest producers of carbon dioxide in Ireland.

Environmental Research and Development

- Funding environmental research to identify pressures, inform policy and provide solutions in the areas of climate, water and sustainability.

Strategic Environmental Assessment

- Assessing the impact of proposed plans and programmes on the Irish environment *(e.g. major development plans)*.

Radiological Protection

- Monitoring radiation levels, assessing exposure of people in Ireland to ionising radiation.
- Assisting in developing national plans for emergencies arising from nuclear accidents.
- Monitoring developments abroad relating to nuclear installations and radiological safety.
- Providing, or overseeing the provision of, specialist radiation protection services.

Guidance, Accessible Information and Education

- Providing advice and guidance to industry and the public on environmental and radiological protection topics.
- Providing timely and easily accessible environmental information to encourage public participation in environmental decision-making *(e.g. My Local Environment, Radon Maps)*.
- Advising Government on matters relating to radiological safety and emergency response.
- Developing a National Hazardous Waste Management Plan to prevent and manage hazardous waste.

Awareness Raising and Behavioural Change

- Generating greater environmental awareness and influencing positive behavioural change by supporting businesses, communities and householders to become more resource efficient.
- Promoting radon testing in homes and workplaces and encouraging remediation where necessary.

Management and structure of the EPA

The EPA is managed by a full time Board, consisting of a Director General and five Directors. The work is carried out across five Offices:

- Office of Environmental Sustainability
- Office of Environmental Enforcement
- Office of Evidence and Assessment
- Office of Radiation Protection and Environmental Monitoring
- Office of Communications and Corporate Services

The EPA is assisted by an Advisory Committee of twelve members who meet regularly to discuss issues of concern and provide advice to the Board.

EPA RESEARCH PROGRAMME 2014–2020

Nutrient Dynamics and Ecophysiology of Opportunistic Macroalgal Blooms in Irish Estuaries and Coastal Bays (Sea-MAT)

(2015-W-MS-20)

EPA Research Report

Prepared for the Environmental Protection Agency

by

National University of Ireland, Galway

Authors:

Ricardo Bermejo, Svenja Heesch, Moya O'Donnell, Nessa Golden, Michéal MacMonagail, Maeve Edwards, Edna Curley, Owen Fenton, Eve Daly and Liam Morrison

ENVIRONMENTAL PROTECTION AGENCY
An Ghníomhaireacht um Chaomhnú Comhshaoil
PO Box 3000, Johnstown Castle, Co. Wexford, Ireland

Telephone: +353 53 916 0600 Fax: +353 53 916 0699
Email: info@epa.ie Website: www.epa.ie

ACKNOWLEDGEMENTS

This report is published as part of the EPA Research Programme 2014–2020. The EPA Research Programme is a Government of Ireland initiative funded by the Department of Communications, Climate Action and Environment. It is administered by the Environmental Protection Agency, which has the statutory function of co-ordinating and promoting environmental research.

The authors would like to acknowledge the members of the project steering committee, namely Robert Wilkes (EPA), Christine Maggs (Bournemouth University), Claire Young (Department of the Environment, NI), David Lyons (Department of Culture, Heritage and the Gaeltacht), Nadège Rossi (Centre d'Étude et de Valorisation des Algues; CEVA, France), Sylvain Ballu (CEVA, France), Sophie Richier (CEVA, France), Bryan Deegan (Irish Water), Serena Keane (Irish Water) and Karen Roche (Project Manager on behalf of EPA Research). In addition, the authors would like to acknowledge the contributions to the Sea-MAT Project of Ana Mendes, Eoin McGillicuddy, Owen Doherty, Shane Rooney, Paul Naessens, Charlène Linderhof, Andrew Niven, María Galindo Ponce, Claudia Cara, Guillaume Bernard, Gabrille Tragin, Teresa Fernandez and Nicole Keogh.

EPA RESEARCH PROGRAMME 2014–2020
Published by the Environmental Protection Agency, Ireland

ISBN: 978-1-84095-847-8 August 2019

Price: Free Online version

Project Partners

Dr Liam Morrison (Principal Investigator)
Earth and Ocean Sciences and Ryan Institute
School of Natural Sciences
National University of Ireland, Galway
Ireland
Tel.: 00 353 (0)91 493200
Email: liam.morrison@nuigalway.ie

Dr Ricardo Bermejo (Researcher)
Earth and Ocean Sciences and Ryan Institute
School of Natural Sciences
National University of Ireland, Galway
Ireland
Tel.: 00 353 (0)91 493920
Email: ricardo.bermajo@uca.es

Dr Edna Curley (Researcher)
Earth and Ocean Sciences and Ryan Institute
School of Natural Sciences
National University of Ireland, Galway
Ireland
Tel.: 00 353 (0)91 493920
Email: edna.curley@nuigalway.ie

Ms Moya O' Donnell (Researcher)
Earth and Ocean Sciences and Ryan Institute
School of Natural Sciences
National University of Ireland, Galway
Ireland
Tel.: 00 353 (0)91 493920
Email: odonnellmoya@gmail.com

Mr Michéal MacMonagail (Researcher)
Earth and Ocean Sciences and Ryan Institute
School of Natural Sciences
National University of Ireland, Galway
Ireland
Tel.: 00 353 (0)91 494135
Email: michealmacmonagail2@gmail.com

Ms Nessa Golden (Researcher)
Earth and Ocean Sciences and Ryan Institute
School of Natural Sciences
National University of Ireland, Galway
Ireland
Tel.: 00 353 (0)91 494135
Email: N.Golden1@nuigalway.ie

Dr Eve Daly (Co-investigator)
Earth and Ocean Sciences and Ryan Institute
School of Natural Sciences
National University of Ireland, Galway
Ireland
Tel.: 00 353 (0)91 492183
Email: eve.daly@nuigalway.ie

Dr Maeve Edwards (Co-investigator)
Zoology
School of Natural Sciences
National University of Ireland, Galway
Ireland
Tel.: 00 353 (0)91 492611
Email: maeve.edwards@nuigalway.ie

Dr Owen Fenton (Co-investigator)
Teagasc
Johnstown Castle
Co. Wexford
Ireland
Tel.: 00 353 (0)53 9171271
Email: owen.fenton@teagasc.ie

Dr Svenja Heesch (Co-investigator)
Algal Genetics
Station Biologique de Roscoff
Roscoff
France
Tel.: 00 33 2 98 29 23 68
Email: Svenja.Heesch@gmx.de

Contents

List of Figures

List of Tables

Executive Summary

The Sea-MAT project aimed to understand the role of local environmental conditions in the development of green tides in Ireland. To achieve this aim, five of the largest macroalgal blooms in Irish estuaries were studied and monitored using novel and innovative methodologies and approaches. The utilisation of molecular tools for the identification of seaweeds revealed the multispecific composition of Irish green tides, confirmed the presence of the alien species *Gracilaria vermiculophylla* along Irish coasts, and identified *Pylaiella littoralis* as the main species producing the golden tide at Killybegs.

Remote sensing techniques were used to accurately define the spatial extent of the bloom event in Clonakilty Bay. Both high-resolution imagery and multispectral photogrammetry acquired from an unmanned aerial vehicle were used in the production of classification maps of the *Ulva* bloom in the Clonakilty estuary.

The assessment of the spatial and temporal scales of biomass variability showed a clear seasonal pattern in red and green tides at the estuaries of Clonakilty, Argideen and Tolka, but no seasonality was observed in the golden tide at Killybegs. Regarding green tides, this assessment suggested that the biomass of tubular morphologies (e.g. *Ulva compressa* and *U. prolifera*) may be less susceptible to being transported out of the estuary than laminar *Ulva* (e.g. *U. rigida*). Furthermore, tubular morphologies appear to be buried at the end of the bloom, favouring the accumulation of organic matter and nutrients in sediments, which could act as a source of nutrients for the subsequent bloom, perpetuating the eutrophication problems.

The monitoring of physicochemical parameters of seawater and sediments in areas affected by seaweed tides suggested an important biofiltration capacity of dissolved inorganic nutrients in quantities that can reduce the nutrient concentration in surrounding seawaters at medium scales. This monitoring also revealed important differences in environmental conditions between different seaweed tides (i.e. green, golden and red), indicating relevant differences in ecophysiological traits. Moreover, the low organic content found in sediments at Tolka and Clonakilty may make feasible the development of seagrass restoration actions. The results of analysis of tissue nitrogen content in seaweeds (> 2% nitrogen) suggest that seaweed tides are not limited by nutrients at any time of the year, as these values were higher than the critical quota (approx. 2%). Thus, other environmental factors (e.g. meteorological or climatological conditions) and biological constraints may play a more important role than previously thought, controlling the potential development of Irish blooms.

Various experiments were conducted to identify the mechanism(s) determining the seasonal succession observed in Irish green tides between tubular (i.e. *U. compressa*) and laminar (*U. rigida*) morphologies and predict the future development of Irish green tides in the context of global warming and eutrophication. The results obtained indicated that the growth of *U. rigida* was controlled by temperature, whereas the growth of *U. compressa* was determined by the photoperiod. Thus, considering the scenario of global warming proposed by the Intergovernmental Panel on Climate Change for Irish coastal waters and the expected increase in nutrient loadings, earlier development of the laminar bloom is expected, which could have significant consequences for biomass balance in Irish estuaries and the maximum accumulated biomass during peak bloom.

Different recommendations to reduce the impact of seaweed tides and control their development are proposed. These include the development of an index based on the ecophysiological status of seagrasses or saltmarsh plants to assess the ecological status of estuarine waters; the reduction of nutrient loadings; the harvesting or cultivation of seaweeds, which may help to remove nutrients and biomass from the estuary; and the cultivation or restoration of oyster beds, which might enhance denitrification processes.

1 Introduction

1.1 Background

Eutrophication is one of the most important pressures affecting European coastal waters (Hering *et al*., 2010). In transitional waters, such as coastal lagoons or estuaries, one of the most evident signs of eutrophication is the development of “seaweed tides” (Valiela *et al*., 1997; Teichberg *et al*., 2010). These seaweed tides, or “macroalgal blooms”, are accumulations of a large biomass of fast-growing, opportunistic macroalgae as a consequence of their overgrowth. They are named according to the colour of the main species present, that is, as green tides (e.g. *Ulva*, *Cladophora*, *Chaetomorpha* or *Ulvaria*), golden tides (e.g. *Sargassum* or Ectocarpaceae) or, in the case of red macroalgae, red tides (e.g. *Gracilaria*) (Smetacek and Zingone, 2013). Although these bloom-forming species are per se not toxic for humans, their excessive growth, accumulation and subsequent degradation can cause serious amenity and public health impacts as a consequence of oxygen depletion and the release of sulfur compounds, which can be harmful for humans and wildlife (Valiela *et al*., 1997; Sfriso *et al*., 2003).

In the context of the Water Framework Directive (WFD; 2000/60/EC), one of the biological quality elements selected to assess the ecological status of transitional waters in Ireland is the monitoring of opportunistic macroalgal blooms (Clabby, 2008). This monitoring tool is described in Scanlan *et al*. (2007) and uses the extent of the bloom (% suitable substrate in the estuary affected by the bloom) and biomass (fresh weight of seaweed m^{-2}) to classify water bodies relative to undisturbed conditions. The WFD aims to prevent further deterioration of aquatic ecosystems associated with European waters and promote the restoration of degraded water bodies. To address this aim, the WFD states that the ecological status of all European water bodies had to be assessed, with water bodies having to achieve good ecological status by 2015; otherwise, management actions should be taken to reach good ecological status. Thus, to comply with the WFD, the management and control of macroalgal tides is key. Currently in Ireland, nine of the 17 estuaries assessed (including Tolka, Clonakilty and Argideen) using the opportunistic green algal assessment tool showed an ecological status that was moderate or lower, requiring necessary specific actions to bring these areas up to the required ecological standard (Task Force, 2010).

Nutrient enrichment of estuarine and coastal waters plays a key role in the development of macroalgal blooms (Valiela *et al*., 1997; Nelson *et al*., 2003; Teichberg *et al*., 2010). However, the extent, distribution and species composition of blooms vary strongly among systems of similar nutrient load, which compromises our ability to predict such events based on information about nutrient status alone (Bonsdorff, 1992; Malta and Verschuure, 1997; Lotze *et al*., 2000). Additional factors may play a role in the development of macroalgal blooms, such as local coastal geomorphology, hydrological regimes, irradiance, water temperature, grazing, species pool or propagule bank size (Lotze *et al*., 2000; Nelson *et al*., 2008; Thornber *et al*., 2017). These factors may lead systems to respond differently for a similar anthropogenic pressure or management action. For instance, using a modelling approach and a long-term data series of seaweed biomass and nutrients, Ní Longphuirt *et al*. (2015a) showed that similar reductions in nitrogen (N) and phosphorus (P) inputs in two Irish estuaries with similar nutrient loadings (the Argideen and the Black Water estuaries) had contrasting effects on the development of macroalgal tides as a consequence of the specific hydrological regimes of each estuary. In another two cases from Japan, the arrival of cryptic non-native species could account for the occurrence of macroalgal tides in places where nutrient conditions have remained more or less constant (e.g. Yabe *et al*., 2009; Yoshida *et al*., 2015). Moreover, sediments in areas affected by macroalgal blooms could act as a nutrient reservoir, fuelling the next blooms, which could make seaweed tides less sensitive to reductions in nutrient loadings (Corzo *et al*., 2009; Robertson and Savage, 2018). Therefore, for effective management of macroalgal tides, each case needs to be assessed individually to identify the most suitable actions. This requires an in-depth knowledge of the processes and mechanisms controlling the development of macroalgal blooms, as

well as monitoring of the physicochemical attributes of the affected areas.

1.2 Project Objectives

1. To develop and implement methods for a better understanding of the local environmental conditions that result in the development of opportunistic macroalgal blooms in Ireland.
2. To determine the physicochemical and ecophysiological characteristics, along with the temporal and spatial variations in environmental conditions, that influence the development, abundance and species composition of opportunistic macroalgal blooms in Ireland.
3. To provide a guidance report, based on objectives 1 and 2, to inform water management decisions to control opportunistic macroalgal blooms in Irish coastal bays and estuaries.

2 Identifying Species Forming Macroalgal Blooms in Irish Estuaries

2.1 Background

Opportunistic bloom-forming seaweeds, belonging to the orders Ulvales, Gracilariales or Ectocarpales, often show a very simple morphology, hindering accurate identification based on morphological traits (Steentoft *et al*., 1995; Malta *et al*., 1999; Rueness, 2005). Because of difficulties in the identification of bloom-forming seaweeds, the study of the species composition of macroalgal blooms and its importance for their development has usually been overlooked, and the arrival of cryptic alien species able to produce seaweed tides may have gone unnoticed. However, the development of new molecular identification tools allows these taxonomic challenges to be overcome. Recent evidence indicates that multispecific green tides are more common than previously thought (Nelson *et al*., 2003; Guidone *et al*., 2013), and the presence of seaweed tides formed by unnoticed alien species has been confirmed (e.g. Rueness, 2005; Baamonde-López *et al*., 2007; Yoshida *et al*., 2015).

The co-existence of different species in seaweed tides could stimulate the duration and extension of macroalgal blooms through spatial and temporal successions between species with different ecological requirements. This hypothesis is supported by the occurrence of macroalgal tides as a consequence of the arrival of alien species in estuaries previously unaffected by such phenomena (Weinberger *et al*., 2008; Yabe *et al*., 2009; Yoshida *et al*., 2015), by the changes in dominant species forming green tides as a result of alterations in environmental conditions (Lavery *et al*., 1991), and by the habitat segregation observed between cryptic sheet-like species belonging to the genus *Ulva* (intertidal) and the genus *Ulvaria* (subtidal) (Nelson *et al*., 2008). This highlights the importance of knowledge about the species composition of seaweed blooms and their ecophysiological performance.

The genus *Ulva* is notorious for producing green tides (Valiela *et al*., 1997; Wang *et al*., 2015; Thornber *et al*., 2017). Green seaweeds belonging to the *Ulva* genus have a simple morphology, consisting of either a monostromatic tubular thallus (formerly *Enteromorpha* genus; Hayden *et al*., 2003) or a distromatic laminar thallus. Although in some cases microscopic traits can be useful for taxonomic identification, the high plasticity and the lack of reliable traits, especially in detached specimens forming *Ulva* blooms (e.g. lack of the basal part, intermediate size of cells or numbers of pyrenoids), confound accurate identification (Malta *et al*., 1999; Guidone and Thornber, 2013). Molecular genetic information provides a powerful tool to overcome these challenges. The large subunit of the plastid-encoded ribulose-1,5-bisphosphate carboxylase/oxygenase (*rbc*L) has been shown to amplify with published primers reliably and to provide enough variation to distinguish species within the genus *Ulva* (e.g. Hayden *et al*., 2003; Heesch *et al*., 2009; Wan *et al*., 2017).

The *rbc*L marker has been used to unravel numerous taxonomic issues within the phylum Rhodophyta, providing useful information for species delimitation in problematic taxa (Wilson-Freshwater and Rueness, 1994; Wilkes *et al*., 2006; Yang *et al*., 2015). In the case of gracilarioids, where morphological identification is especially difficult, this marker has been widely used for species identification (Rueness, 2005; Guillemin *et al*., 2008) and confirmed for the first time in Europe the presence of the cryptic alien species *Gracilaria vermiculophylla* (Ohmi) Papenfuss (Rueness, 2005).

A third group of opportunistic algae encountered in blooms, members of the phaeophycean order Ectocarpales, likewise shows simple morphologies, making identification using molecular genetic markers desirable (e.g. Geoffroy *et al*., 2015). In brown algae, because of low variation in encoding regions (Kucera and Saunders, 2008) or extensive hybridisation (Billard *et al*., 2005; Neiva *et al*., 2010; Geoffroy *et al*., 2015), organellar markers often do not allow unambiguous identification to species or even genus level, whereas nuclear intron regions such as the internal transcribed spacers of the nuclear-encoded ribosomal operon (ITS) may allow a distinction between entities (McDevit and Saunders, 2009; Saunders and Kucera, 2010).

Thus, the objective of this chapter was to use genetic markers to assess the species composition of five seaweed tides affecting four Irish estuaries.

2.2 Methodology

Representative specimens of the main bloom-forming species were collected on five sampling occasions (see section 4.2 for further details). Specimens of *Ulva* were sorted by morphotypes using macroscopic traits (e.g. tubular or laminar morphology, presence or absence of teeth on the margins, branching density) and distinguishing cellular features (e.g. cell size and shape, number of pyrenoids, shape and position of chloroplasts). Where necessary, microscopic observations were carried out using a Nikon Optiphot II microscope (Nippon Kogakukk), with a stage micrometre used to determine cell size. In all cases, a part of each specimen was then stored in dry silica gel for genetic analysis; for specimens of sufficient size, the remainder was prepared as a herbarium voucher.

The plastid-encoded marker *rbc*L was employed to genetically identify samples of *Ulva* and red algae, whereas the more variable ITS1 was used to identify brown algae. Whole genomic deoxyribonucleic acid (DNA) was extracted from approx. 5–20 mg of the silica-dried tissue using a commercial kit (NucleoSpin® Plant II, Macherey-Nagel). Target regions were amplified in polymerase chain reactions (PCRs) using published primers SHF1 and SHR4 (Heesch *et al*., 2009) for *Ulva* specimens, primers F8 or F57 and R1150 (Wilson-Freshwater and Rueness, 1994; Mineur *et al*., 2010) for red algal samples and primers AFP4LF and 5.8S1R (Burkhardt and Peters, 1998) for ectocarpalean brown algae, at an annealing temperature of 50°C. Protocols for PCR amplification, purification of the products and sequencing are given in Heesch *et al*. (2016). Sequence treatment (quality control and alignment), as well as data analysis under the maximum likelihood (ML) criterion, followed methods provided in Heesch *et al*. (2016). Identifications were verified using the Standard Nucleotide Basic Local Alignment Search Tool (BLAST; http://www.ncbi.nlm.nih.gov/). Algal nomenclature followed that in AlgaeBase (Guiry and Guiry, 2018).

2.3 Results

A total of 126 *Ulva* specimens were successfully sequenced and identified. Representative sequences from all estuaries were included in an alignment of 1252 bases in length, containing 65 sequences in total, including 22 newly generated sequences for the genus *Ulva* and an outgroup comprising eight sequences, six of the related genus *Umbraulva* and one each of the genera *Gemina* and *Ulvaria* (see Figure 2.1 for the GenBank accession numbers). A total of eight *Ulva* species were encountered in the samples (Figure 2.1), with most specimens belonging to three species: *U. compressa* L. ($n = 41$), *U. prolifera* O.F.Müller ($n = 40$) and *U. rigida* C.Agardh ($n = 33$). The other species were represented by only a few specimens each: *U. clathrata* (Roth) C.Agardh ($n = 1$), *U. gigantea* (Kützing) Bliding ($n = 2$), *U. intestinalis* L. ($n = 2$), *U. lactuca* L. ($n = 3$) and *U. procera* (K.Ahlner) Hayden *et al*. ($n = 4$).

Of the 14 red algal samples, 12 were successfully amplified and included in an *rbc*L alignment of 1419 bases in length, containing 72 sequences in total. Most of the specimens were identified as belonging to the genus *Gracilaria* (order Gracilariales), with one specimen of *G. gracilis* (Stackhouse) M.Steentoft, L.M.Irvine and W.F.Farnham and nine of *G. vermiculophylla* from the Clonakilty and Argideen estuaries. The remaining two specimens belonged to the related species *Gracilariopsis longissima* (S.G.Gmelin) Steentoft, L.M.Irvine and Farnham.

Despite several attempts, four of the eight brown algal samples could not be amplified. Because of the use of primers that were not specific enough to allow uncontaminated amplification of only the brown algal species, sequencing of the cytochrome C oxidase subunit I (cox1/COI-5P) marker was abandoned and ITS sequences were employed instead. However, no comparable sequences of *Pylaiella* currently exist in GenBank. Moreover, because of the high variability of the non-coding ITS region, a sequence alignment with related Ectocarpales species was not feasible. Instead, the sequences of the remaining two samples were directly compared with the ITS sequence of a known strain of *Pylaiella littoralis* (U 1.48, isolated and identified by the senior author of Geoffroy *et al*., 2015) and could thus be unambiguously identified as *P. littoralis* (L.) Kjellman.

2.4 Discussion

The species composition of the five macroalgal blooms assessed is shown in Table 2.1. This study indicated that three of the largest green tides in

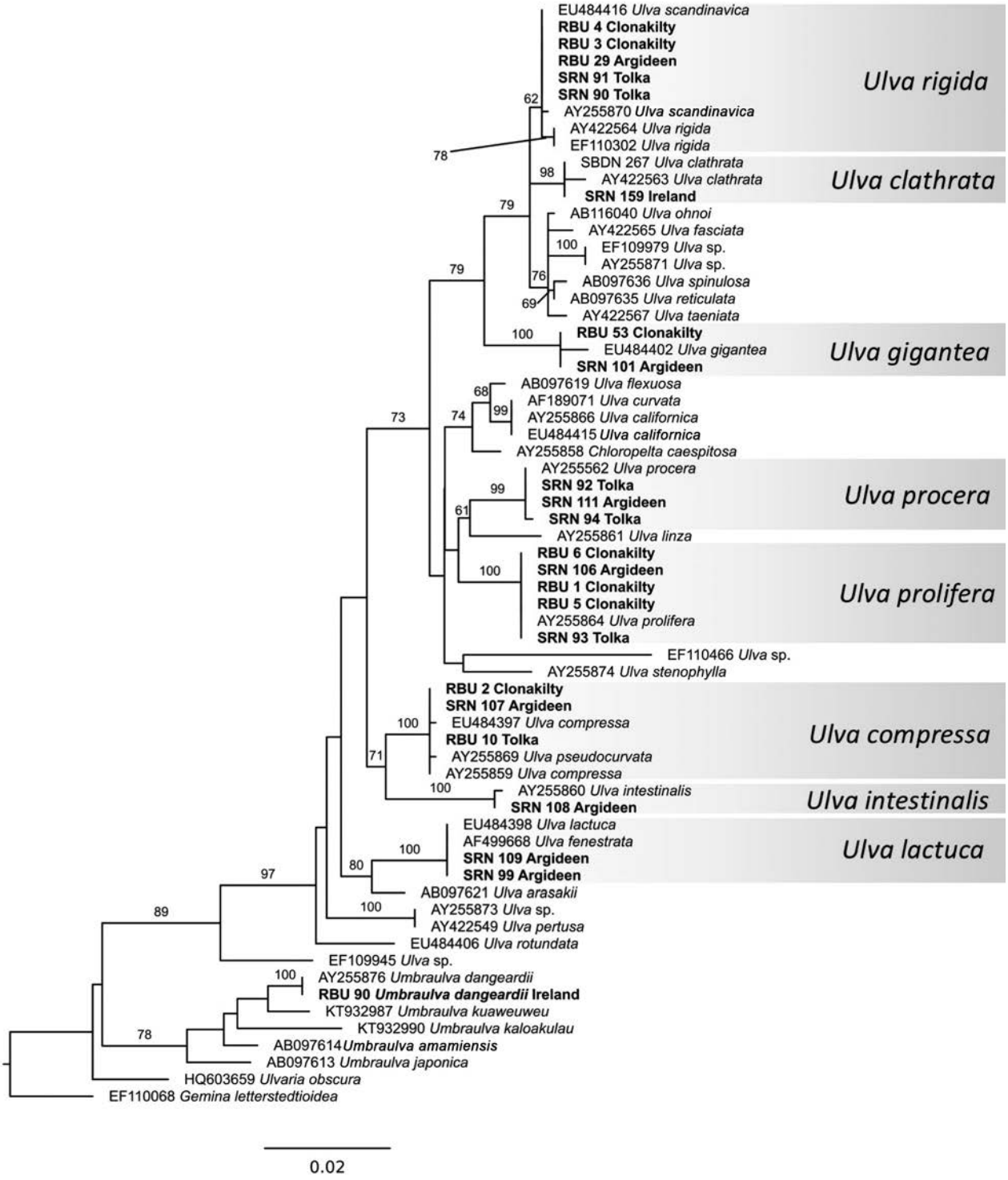

Figure 2.1. Phylogenetic tree inferred from a ML analysis of partial *rbc*L sequences of *Ulva* species. Numbers next to nodes indicate bootstrap support values (branches without numbers received 60% support). Where appropriate, species names are preceded by the GenBank accession number; representative new sequences are in bold.

Ireland (Argideen, Clonakilty and Tolka) showed a similar species composition, being dominated by three species (*U. compressa*, *U. prolifera* and *U. rigida*). Furthermore, a seasonal successional pattern common to the Tolka and Argideen estuaries was observed (see Chapters 4 and 5). The molecular

Table 2.1. Species identified in the five seaweed blooms assessed using molecular identification tools

Argideen (green)	Clonakilty (green)	Clonakilty (red)	Tolka (green)	Killybegs (golden)
U. compressa	*U. compressa*	*G. gracilis*	*U. clathrata*	*P. littoralis*
U. gigantea	*U. gigantea*	*G. vermiculophylla*	*U. compressa*	
U. intestinalis	*U. prolifera*		*U. procera*	
U. lactuca	*U. rigida*		*U. prolifera*	
U. procera			*U. rigida*	
U. prolifera				
U. rigida				

identification of *Gracilaria* specimens from Clonakilty confirms, for the first time in Ireland, the presence of a seaweed tide formed by the alien species *G. vermiculophylla*, which was reported previously in different localities in Europe (e.g. Rueness, 2005; Weinberger *et al*., 2008; Sfriso *et al*., 2012) and the UK (Krueger-Hadfield *et al*., 2017). Finally, the molecular analysis of some samples of ectocarpoids from the seaweed tide affecting the Killybegs estuary suggests that *P. littoralis* is the main component of this bloom. This species is known to form important golden tides in the Baltic, where its ecological performance and interaction with grazers have been intensively studied (Lotze *et al*., 1999, 2000, 2001; Paalme and Kukk, 2003).

Similar to other recent studies concerning the species composition of problematic macroalgal blooms (e.g. Nelson *et al*., 2003; Guidone and Thornber, 2013), our results revealed that the green tides contained multiple species of *Ulva* (see Figure 2.1), with *U. compressa*, *U. prolifera* and *U. rigida* being the most frequent and abundant entities in both the Argideen and the Tolka estuaries. Wan *et al*. (2017) stated that *Ulva* blooms in seven estuaries in Ireland (from one sampling occasion each, including the Tolka, Clonakilty and Argideen estuaries) primarily consisted of *U. rigida*. Although *U. rigida* appears to be the dominant laminar species of *Ulva* in Irish green tides, reaching important biomass densities in late summer and autumn (33% and 24% of the total biomass during August and October in the Argideen and Tolka estuaries, respectively; see Chapter 4), the results obtained in the present study showed that the tubular *U. prolifera* and *U. compressa* are more abundant and are the main species forming green tides in the Argideen, Clonakilty and Tolka estuaries. This finding is in accordance with a report by Jeffrey *et al*. (1995), who identified two tubular species, *U. prolifera* and *U. flexuosa*, as the main components of the macroalgal blooms occurring in the Tolka estuary between June 1989 and September 1990. The differences between the present study and that by Wan *et al*. (2017) were due to sampling bias, as that study collected only laminar specimens of *Ulva* for molecular identification on a single sampling occasion.

In 2005, Rueness (2005) confirmed for the first time the presence of *G. vermiculophylla* on European coasts, widely distributed from Sweden to southern Portugal. Since then, further studies have recorded this species in different estuarine habitats, from the Baltic Sea (Weinberger *et al*., 2008) to southern Spain (Bárbara *et al*., 2012), the Mediterranean Sea (Sfriso *et al*., 2012) and Morocco (Guillemin *et al*., 2008), where it produces seaweed tides in nutrient over-enriched areas. However, considering the expansion of this species, the existence of previous records based on morphological characteristics (Mollet *et al*., 1998) and descriptions of free-living specimens of *G. gracilis* thriving in muddy estuarine areas from the mid 1990s in the northern Iberian Peninsula (Ignacio Bárbara, University of A Coruña, Spain, 2012, personal communication), this invasion has probably gone unnoticed for a long time. Two factors may have contributed to this: the taxonomy of gracilarioids remained unsolved for a long time (Steentoft *et al*., 1995; Rueness, 2005) and estuarine areas are usually under-sampled by macroalgal phycologists because of a lack of habitats suitable for macroalgae (Krueger-Hadfield *et al*., 2018). In the UK, *G. vermiculophylla* has been recently recorded in numerous localities, being at least present from 2008 in Northern Irish estuaries (Krueger-Hadfield *et al*., 2017). Oyster culture is proposed as one of the main vectors for the introduction and spread of this species (Mollet *et al*., 1998; Rueness, 2005; Krueger-Hadfield *et al*., 2018). Thus, considering

the geographical location of these new records on the southernmost Irish coast (i.e. Argideen and Clonakilty; Figure 2.2), and that there are many estuaries where oysters are cultivated, it is likely that the distribution of this species is more extensive along the Irish coast than currently known, as has been suggested by Krueger-Hadfield *et al*. (2017).

Figure 2.2. *G. vermiculophylla* bloom at Clonakilty in September 2017 (*Ulva* bloom can be seen in the background).

3 The Potential Application of Unmanned Aerial Vehicle Remote Sensing Techniques in the Spatial and Temporal Determination of *Ulva* Species Blooms in South-west Ireland

3.1 Introduction

The effective monitoring of green tides (*Ulva* spp.) is important, particularly as bloom events are considered a global ecological issue that is increasing in both magnitude and frequency (Van Alstyne *et al*., 2015). The abnormal proliferation of *Ulva* spp. blooms in eutrophic coastal waters has been reported in numerous countries, including the USA (Nelson *et al*., 2003; Jorgensen *et al*., 2010), France (Merceron *et al*., 2007), Japan (Yabe *et al*., 2009) and China (Hu *et al*., 2010; Pang *et al*., 2010). There are significant negative ecological impacts associated with *Ulva* spp. blooms (Nelson *et al*., 2003), including the potential to cause marine fish and mammal mortalities (Smayda, 1997) and significant impacts to the local economy and tourism (Smetacek and Zingone, 2013).

Defining accurately *Ulva* spp. bloom extent (both spatially and temporally) is difficult using traditional field sampling techniques. Typically, ground-based surveys carried out by highly trained field scientists are the most common method of bloom detection and monitoring. Ground-based surveys, however, are typically laborious and time-consuming and often particularly limited because of difficult working environments and costs (Wan *et al*., 2017). There is increasing interest in the potential application of remote sensing (RS) techniques, including the use of unmanned aerial vehicles (UAVs), in mapping coastal environments (Rapinel *et al*., 2014). The types of visual imagery created from these platforms include very high-resolution photogrammetry, with centimetre resolution in the case of UAV photogrammetry (Setyawidati *et al*., 2018), and multispectral and hyperspectral imagery (traditionally from low-resolution satellite imagery but increasingly available on UAV platforms).

In Ireland, cloud cover is a known inhibitor of satellite-based visual imagery. Therefore, UAV sensors that fly below the clouds allow very high spatial resolution, and more on-demand temporal resolution could be a viable tool in bloom monitoring. Several studies utilising UAVs (also known as drones) for coastal management have been carried out. For example, Mancini *et al*. (2013) and Gonçalves and Henriques (2015) have shown the potential of light detection and ranging (LiDAR) coupled with UAVs to produce high-quality digital surface models (DSMs) for coastal management practices, whereas Long *et al*. (2016) have shown the effectiveness of using drones in producing high-quality topographic maps in tidal reefs. When applied to green tide monitoring, the use of UAVs can improve knowledge relating to *Ulva* spp. bloom spatial extent and species abundance, and act as a complementary technique alongside traditional field ground truthing.

This study aimed to examine the potential of using both high-resolution and multispectral photogrammetry acquired from UAVs in the production of classification maps of the *Ulva* spp. blooms in the Clonakilty estuary. The techniques developed in this pilot study can be applied to other coastal regions of Ireland affected by these blooms, thereby providing policymakers with data that may help in the establishment of *Ulva* spp.-specific management plans in Ireland.

3.2 Materials and Methods

3.2.1 Study area/seaweed sampling

On two dates in 2018 (May and August), high-resolution aerial surveys were carried out on an annually occurring *Ulva* spp.-dominated bloom in Clonakilty Bay, County Cork, located in the south-west of Ireland (51°36′25.0″N 8°51′44.0″W) (see Figure 3.1). A detailed site description is provided in Wan *et al*. (2017). Seaweed samples were collected on 27 August 2018, to be used as training data for the classification process discussed later. A section of the bloom was chosen for representative *Ulva* spp. sampling. For field validation, three 20 m transects were randomly placed along the bloom at low tide and visual observations were taken every 2 m. Three quadrats were randomly placed along the transect

and seaweeds were identified. The location of the quadrats was recorded with a Garmin GPSMAP 64s global positioning system (GPS). Seaweed species identified were *U. rigida* (laminar morphology), *U. compressa* (tubular morphology), *U. prolifera* (tubular morphology) and *G. vermiculophylla*. Seaweeds were removed and stored in a clean Ziploc bag between moist tissue paper before transporting to the laboratory. Reflectance measurements were taken using an Ocean Optics USB4000 spectrometer (200–1100 nm spectral range). Reflectance values are converted into spectral signatures and are used to help constrain the supervised classification scheme of the multispectral dataset (Son *et al*., 2012; Van der Wal *et al*., 2014). Species collected were visually inspected and taxonomically identified in the laboratory prior to radiometric analysis.

3.2.2 High-resolution photogrammetry from the UAV

Unmanned aerial vehicle high-resolution photogrammetry was acquired using a DJI Zenmuse X5 camera coupled to a UAV (DJI Inspire) to create an orthomosaic of the *Ulva* spp. bloom [ground sampling distance (GSD) of < 2.5 cm] (Figure 3.1) (Vallet *et al*., 2012). The UAV was controlled using DroneDeploy software (Infatics Inc.), which allows for autonomous pre-planned flights. Images were automatically acquired every 1.5 seconds. All images were taken near solar high noon during low tide periods with low wind speeds (< 15 kph) and geotagged using Mission Planner (v1.3.11; http://planner.ardupilot.com/). Ground control points (GCPs; $n = 8$) were used to improve the geo-referenced accuracy of all images (Figure 3.2a). Specific

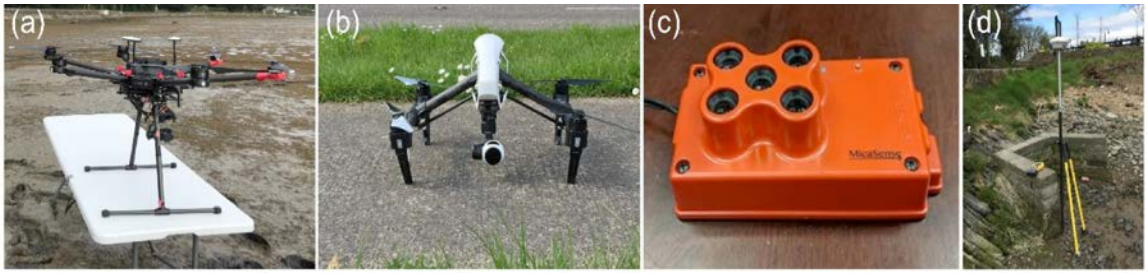

Figure 3.1. (a) DJI Matrice 600, (b) DJI Inspire, (c) MicaSense RedEdge multispectral camera and (d) real-time kinematic positioning.

Figure 3.2. Location of the Clonakilty Bay study area and planned UAV multispectral flight plans highlighting (a) distribution of the GCPs and seaweed sampling points, (b) flight plan 1 – north Clonakilty Bay and (c) flight plan 2 – south Clonakilty Bay.

permanent GCPs were recorded using a real-time kinematic (RTK) GPS (< 1 cm precision *x*, *y*, *z*) and base station. Full processing and stitching of high-resolution imagery was carried out using Pix4Dmapper software (v.1.2.2 X). A digital elevation model was also produced as an output of the processing (Figure 3.3a).

Technical information on both the UAV and the imager is provided in Table 3.1.

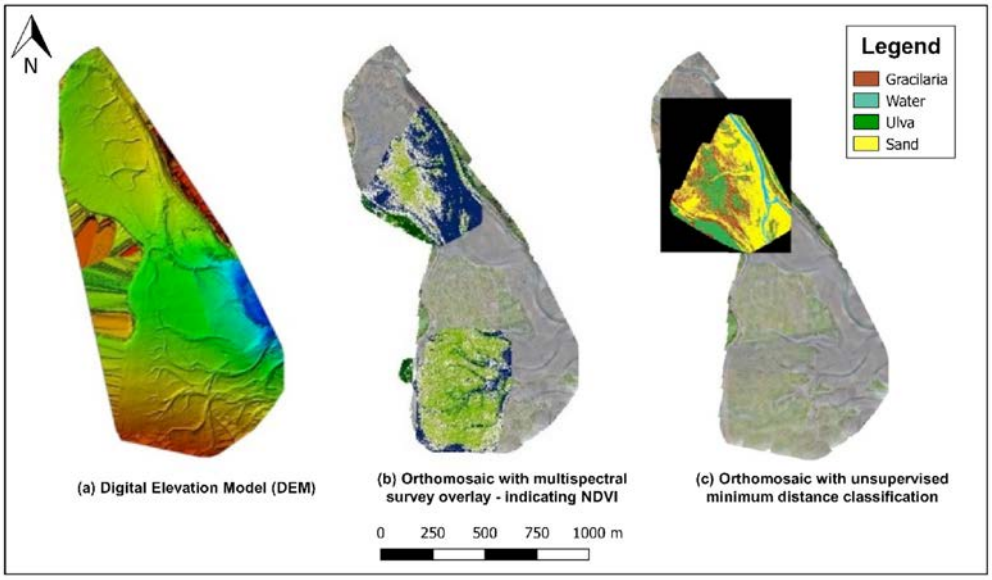

Figure 3.3. Multispectral and high-resolution photogrammetry survey, featuring (a) a digital elevation model, (b) an orthomosaic with overlaid multispectral surveys (showing the normalised difference vegetation index) and (c) an orthomosaic with a supervised classification of the multispectral survey (August 2018).

Table 3.1. Technical summary table

Technical details	High-resolution camera	Multispectral imager
Imager	Zenmuse X5	MicaSense RedEdge
Acquisition time	11.10.2018 11:31	12.10.2018 12:06
Size	17.3 × 13.0 mm	9.4 cm × 6.3 cm × 4.6 cm
Weight	526 g	150 g
Megapixels	16	–
Lens and focal length	20 cm	5.4 mm
Lens field of view	72°	47.9°
Spectral bands	RGB	RGB, RE, NIR
Image files (RAW or JPG)	MP4/MOV	JPG
GSD	2.48 cm	6.98 cm
Flying altitude	102 m	102 m
Overlap (side/front)	75%/85%	75%/85%
Area covered	102.514 ha	48.68 ha

NIR, near infrared; RE, red edge; RGB, red, green, blue.

3.2.3 High-resolution photogrammetry classification models: supervised and unsupervised classification

To determine the green tide cover, classification of the *Ulva* spp. bloom was carried out on the high-resolution UAV orthomosaic using both a supervised ML classifier based on a pixel-based approach and an unsupervised minimum distance (MD) classifier (Figure 3.4). For the ML classifier, 20 regions of interest for each class (*Ulva*, *Gracilaria*, vegetation, water sand, diatoms, urban) were selected in the training data. The ML classifier calculates the average variance of the spectral training data to estimate the likelihood of a pixel belonging to each class (Foody, 1992). The use of ML classifiers is a common approach in both vegetation (Zhao *et al*., 2015) and marine (Uhl *et al*., 2016) mapping. The MD classifier utilises Euclidean distances in (spectral) feature space between the pixels to be classified and the class means (Atkinson and Lewis, 2000).

3.2.4 Multispectral photogrammetry from the UAV

A multispectral camera (MicaSense RedEdge) was mounted nadir facing on a UAV (DJI Matrice 600) (Figure 3.1a and c). The multispectral imager captured the study areas in five bands (blue, 475 nm; green, 560 nm; red, 668 nm; near infrared, 840 nm; red edge, 717 nm). The camera was triggered to capture multispectral images every 1.2 seconds, with a GSD of < 7.0 cm. The flight plans from this survey are shown in Figure 3.2b and c. Pre- and post-flight calibration of multispectral images was carried out using reflectance panels to improve the accuracy of reflectance data and account for any shift in illumination during the survey.

Multispectral images were photogrammetrically processed using ENVI (v. 5.3.1; Research Systems). Atmospheric correction of UAV imagery was not required because of minimal atmospheric disturbance when flying at heights of 100–500 m (Jensen *et al*., 2014).

3.2.5 Multispectral photogrammetry classification models: normalised difference vegetation index and ML classification

Several vegetation indices, in particular the normalised difference vegetation index (NDVI), have been shown to be useful in vegetation surveying and mapping. For example, the NDVI has successfully been used to classify different land cover types (Defries and Townshend, 1994; Hansen *et al*., 2000), in vegetation

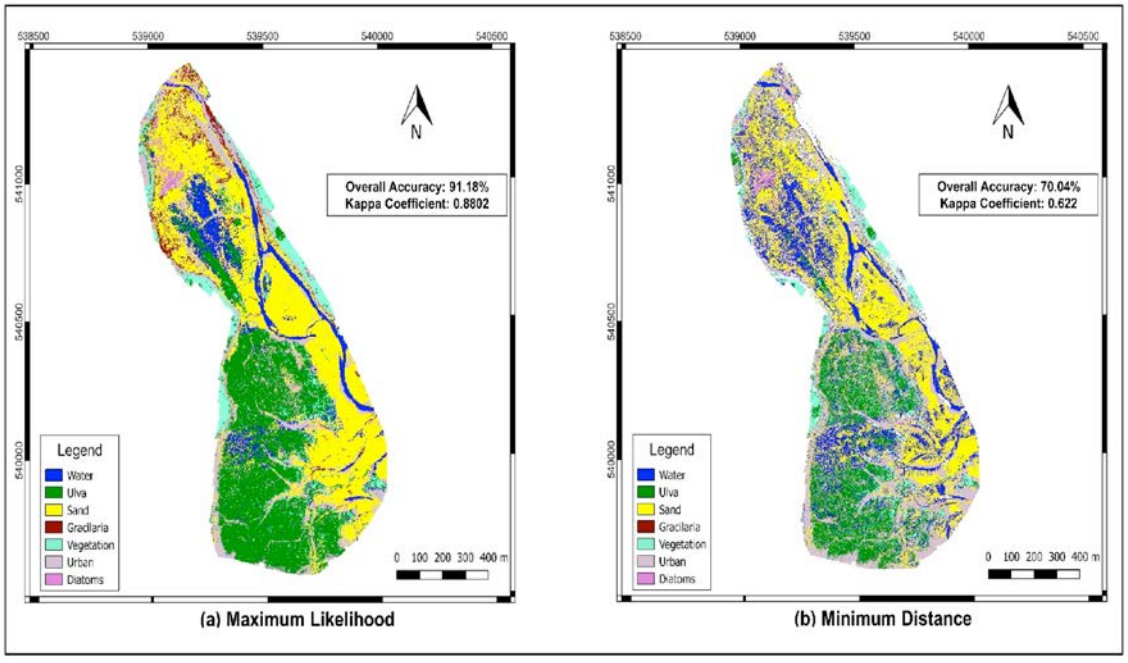

Figure 3.4. Classification outputs of the UAV high-resolution survey showing (a) the supervised ML classification and (b) the unsupervised MD classification.

classification and change detection (Gandhi *et al*., 2015) and in severe drought monitoring (West *et al*., 2018). NDVIs were applied to multispectral UAV data to assess the green tide. The ability of the NDVI to highlight the strong contrast between photosynthetically active vegetation and water (Sims and Gamon, 2003), as well as its ability to determine the state of photosynthesis and vegetation health (Kogan *et al*., 2004) and biomass (Wessels *et al*., 2006), makes it a powerful tool in ecological assessment.

Further to this, a ML classification was carried out on the multispectral survey data (northern survey only). Validation of the supervised classification was based on spectral signatures taken from radiometric measurements of the three seaweeds sampled under laboratory conditions. Outputs of the NDVI and ML classifications are shown in Figure 3.5.

3.3 Results

3.3.1 High-resolution photogrammetry classification outputs

When comparing classifiers, the supervised ML classification resulted in an overall accuracy of 91.18%, with a kappa coefficient of 0.880, whereas the unsupervised MD classification resulted in an overall accuracy of 70.04%, with a kappa coefficient of 0.622. The value of the kappa lies between 0 and 1, with 0 representing agreement resulting from chance only and 1 representing complete agreement between the two datasets (Ismail and Jusoff, 2008). The ML classifier results in a highly accurate classification output with good discrimination between the classes, whereas the MD classifier shows significant mixing of pixels between classes, with particular inaccuracies when discriminating between diatoms, *Gracilaria* and sand.

3.3.2 Multispectral photogrammetry classification outputs

Figure 3.3b shows the results of the NDVI analysis superimposed on the multispectral surveys. The NDVI expresses areas of greater photosynthetic activity as darker areas. The maximum NDVI value recorded was 0.398 and the minimum value recorded was 0.301. The average NDVI value of the *Ulva* bloom was 0.383. These values are in line with those of other studies (NDVI of *Ulva* bloom during May–June of between 0.2 and 0.75; Liu *et al*., 2015). An unsupervised MD classification of the multispectral survey resulted in poor discrimination between classes (Figure 3.3c). Pixel mixing resulted in inaccuracies in defining classes, and the multispectral imager was spectrally too coarse to distinguish between diatoms, urban or vegetation. The use of the ML classifier with improved pixel training will improve the accuracy of this classification, and this work is currently underway.

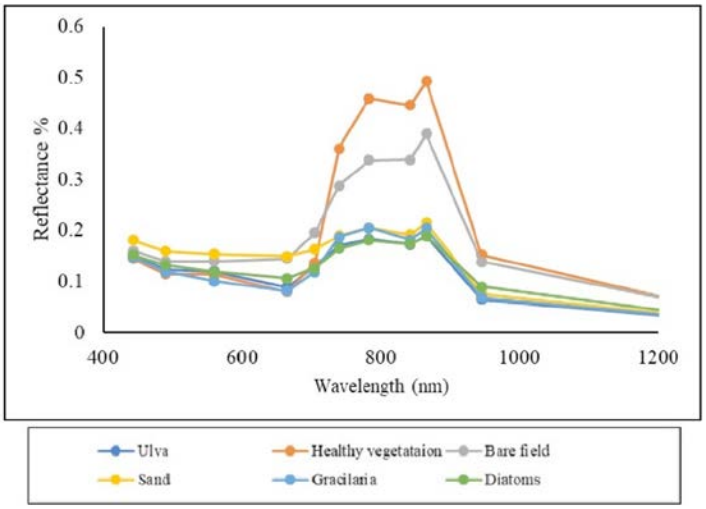

Figure 3.5. Recorded spectra of substrates within the study site (showing the near-infrared band).

3.3.3 Multispectral classification: supervised ML classification

As mentioned earlier, the initial supervised classification of multispectral imagery shows relatively poor discrimination between different substrates. Figure 3.5 highlights the spectral similarities between a number of classes analysed. Classes including *Ulva*, *Gracilaria*, sand and diatoms all show similar reflectance at around 800 nm (maximum 20% reflectance), indicating that multispectral imagery may require improved pixel training or, perhaps, lacks the spectral sensitivity to discriminate between these substrates as a result of spectral mixing. This is currently being assessed.

3.4 Discussion

Although the results are preliminary, the application of high-resolution aerial photogrammetry and multispectral RS techniques in this study shows considerable potential in the enhanced future monitoring of green tide events in Ireland.

When applied to high-resolution imagery, the ML classifier proved highly effective in accurately categorising substrates into specific classes. Improved pixel training of the ML classifier may also improve overall accuracy. The MD classifier was shown to be less accurate when applied to both high-resolution and multispectral imagery.

It is crucial that the appropriate imager is chosen for specific tasks. For example, because of the spectral limitations of the multispectral imager and the spectral similarities of *Ulva* spp., it was difficult in this study to differentiate many classes confidently. The use of hyperspectral imagery, with its narrow contiguous bands, may be a solution to this.

Further analysis of multispectral data, and the application of more green algae-specific classification indices, such as the Floating Algae Index (FAI) or the Scaled Algae Index (SAI), will improve the accuracy of classification data (Hu, 2009; Garcia *et al*., 2013). The production of a highly accurate digital elevation model, meanwhile, may provide relevant information when defining the structural complexity of tidal environments, which may influence the propagation of green tide events.

3.4.1 Further work

The next phase of this work is to survey the study area with a hyperspectral imager coupled to a UAV. A number of studies have highlighted the application of hyperspectral RS in the study of seaweeds and other marine vegetation (Dekker *et al*., 2006; Silva *et al*., 2008; Mehrtens *et al*., 2009). A hyperspectral imager may have a greater ability to differentiate spectrally similar substrates, considering the narrower contiguous bands available.

Following this, a temporal analysis of the green tide event in Clonakilty Bay will be mapped and surveyed using Sentinel-2 satellite data. A temporal series of Sentinal-2 images from April to November 2018 have already been acquired and processed. The ability to capture time series images of the bloom may be important in understanding the growth dynamics of the green tide throughout its growing period. The next step is to build a regression model to predict the relative abundance of current and future green tide events in Clonakilty Bay. The production of accurate prediction models will provide enhanced surveying techniques in the context of green tide management in Ireland.

4 Assessing the Most Relevant Scales of Variability in Irish Seaweed Tides

4.1 Background

Estuaries are highly dynamic and complex ecosystems that are subjected to significant fluctuations in physicochemical conditions as a result of natural and anthropogenic processes, which produce an important variability in the structure and composition of natural assemblages (Nelson *et al*., 2003; Carvalho *et al*., 2011). In the case of seaweed tides, significant variations in biomass distribution and abundance have been observed at different temporal and spatial scales. This has been explained by diverse biotic and abiotic processes, such as desiccation, time availability for nutrient uptake and photosynthesis, grazing, salinity gradients, and geomorphological characteristics in relation to prevailing winds, currents and tidal dynamics, which favour or preclude the accumulation of drift seaweeds (Aldridge and Trimmer, 2009; Park *et al*., 2014; Lanari and Copertino, 2017).

The study of spatial and temporal patterns of variation in natural assemblages can be helpful to identify or infer the most important processes or factors controlling the development and variability of benthic assemblages (e.g. Benedetti-Cecchi *et al*., 2001; Terlizzi *et al*., 2007; Bermejo *et al*., 2015, 2019). The identification of relevant scales of spatial and temporal variation is a necessary prerequisite before explanatory models can be proposed and tested (Andrew and Mapstone, 1987). The objective of this study was to infer the most likely factors controlling the development and persistence of two green tides in the Tolka and the Argideen estuaries, a red seaweed tide affecting the Clonakilty estuary and a golden tide occurring in the Killybegs estuary, by assessing spatial and temporal patterns of biomass distribution in these estuaries.

4.2 Methodology

In order to identify the most relevant spatial and temporal scales of seaweed biomass variability, a hierarchical spatial sampling design was used in the four Irish estuaries (Figure 4.1) over seven sampling occasions between June 2016 and August 2017. To avoid temporal effects that may confound any spatial variation, the four estuaries were sampled within a maximum period of 1 week on each sampling occasion. For logistical reasons, the first sampling was performed within a larger period (i.e. 1.5 months).

These estuaries were divided into two sections, one close to the open sea (“outer section”) and another 1 km upstream towards the freshwater–tidal limit (“inner section”). In each section, two sampling sites separated by 100 m were selected. One or two random transects separated by 10 m, and perpendicular to the main channel, were sampled per site (see Figure 4.1). Along each transect, three sampling stations were positioned in the upper, middle and lower part of the intertidal covered by the bloom during its maximum extension, which usually occurs in June or July in cold-temperate north-eastern Atlantic estuaries (e.g. Jeffrey *et al*., 1995; Malta and Verschuure, 1997; Lyngby *et al*., 1999; Scanlan *et al*., 2007). The sampling stations were pre-determined using Google Earth images of blooms from previous years. The pre-defined sampling stations were located in the field using a GPS (Magellan Triton 400). At each sampling station, three quadrats (25 × 25 cm) were used to assess the abundance of seaweed. All living material present in each quadrat was collected, placed in a labelled plastic bag and transported to the laboratory.

Once in the laboratory, seaweed biomass was rinsed with freshwater to remove adherent sedimentary and particulate material, debris and other organisms. Seaweeds were sorted at the lowest taxonomical level possible based on macroscopic traits (*Ulva* specimens were classified as tubular or laminar morphologies) and their mass was recorded after the removal of the excess water using a manually operated low-speed centrifuge (i.e. salad spinner). Subsequently, biomass was standardised to grams per square metre by multiplying the obtained weight in the 25 × 25 cm quadrat by 16. Finally, subsamples of morphologically representative specimens of the main bloom-forming species were collected for

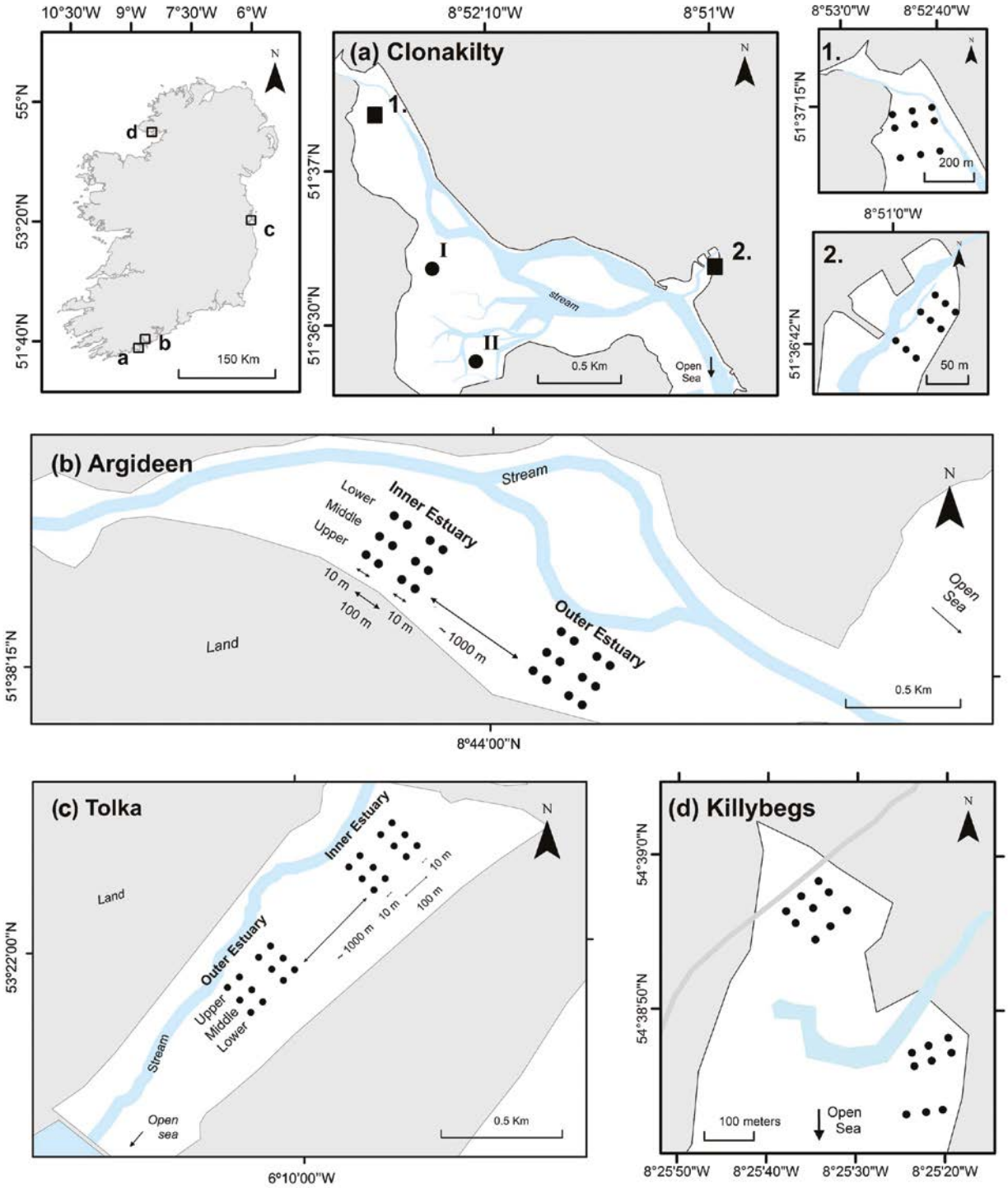

Figure 4.1. Geographical location of the four estuaries studied in Ireland. Detailed maps of (a) the Clonakilty estuary (1, 2, *Gracilaria* bloom; I, II, *Ulva* bloom), (b) the Argideen estuary, (c) the Tolka estuary and (d) the Killybegs estuary, showing a schematic representation of the spatial sampling design.

further microscopic and molecular identification (see Chapter 2).

In the case of the estuaries affected by green tides (Tolka and Argideen), multivariate six-way permutational analysis of variance (PERMANOVA; Anderson *et al*., 2008) was performed based on the Euclidean distances between quadrats, considering the biomass of tubular or laminar morphologies. The six factors considered (three fixed and three random) were sampling occasion (fixed; seven levels: "June 16", "August 16", "October 16", "February 17", "April 17", "June 17" and "August 17"); position in the bloom

(fixed; three levels: “upper”, “middle” and “lower”); estuary (fixed; two levels: “Tolka” and “Argideen”); section (random; two levels nested in estuary: “inner” and “outer”); site (random; two levels nested in the interaction between section and sampling occasion); and sampling station (random; two levels nested in the interaction between site and position). In case of significant effects for a factor, a permutational distance-based test for homogeneity of multivariate dispersion (PERMDISP; Anderson *et al*., 2008) and a pairwise PERMANOVA test (Anderson *et al*., 2008) were performed to interpret patterns.

In the case of the Clonakilty estuary, which was affected by a red seaweed tide, a similar approach was followed, but the factor “estuary” was removed from the analyses, with a five-way model followed instead of a six-way model. In the case of the Killybegs estuary, which was affected by a golden tide, the design used to assess the spatial-temporal variability was also modified because of some missing data as a result of rough weather in February (all three transects from the inner section) and June (two transects from the outer section) 2017. Thus, the two sections were analysed independently to assess the temporal and spatial variability. In each section, the effects of sampling occasion [fixed; seven (outer) or six (inner) levels], position in the seaweed tide (fixed; three levels), site (random; two levels nested in sampling occasion) and sampling station (random; two levels nested in the interaction between position and site) were assessed. Subsequently, another PERMANOVA following the design used to assess the spatial and temporal variability in the Clonakilty estuary was performed, but data from February and June 2017 were excluded.

Statistical analyses were performed using the Vegan package (Oksanen *et al*., 2012) for R and PERMANOVA+ add-on PRIMER 6 (Plymouth Routines in Multivariate Ecological Research) software. In all statistical analyses, significance was set at a probability of $p < 0.05$ and, when necessary, was based on 1999 permutations. As biomass data usually failed when tested for normality and homoscedasticity, PERMANOVA was performed instead of the traditional analysis of variance (ANOVA).

4.3 Results

4.3.1 Green tides: the cases of the Argideen and Tolka estuaries

The PERMANOVA results for the biomass of tubular *Ulva* revealed significant differences between estuaries, sampling occasions and positions (Table 4.1). Significant interactions were observed between sampling occasion and most of the spatial scales of variation assessed for temporal interactions (i.e. estuary × sampling occasion, sampling occasion × section). The annual peaks of biomass were detected in June for both estuaries, with significant differences between June 2016 and June 2017 for both estuaries (Figure 4.2). In June 2016, the median values for biomass of tubular *Ulva* were 1193.6 g m^{-2} and 3345.6 g m^{-2} for the Argideen and Tolka estuaries, respectively. In June 2017, the median values for biomass of tubular *Ulva* were 676.8 g m^{-2} for the Argideen estuary and 1558 g m^{-2} for the Tolka estuary. The maximum values for biomass were measured in June 2016 for both estuaries, reaching 12,398.4 g m^{-2} in the Tolka estuary and 7140.8 g m^{-2} in the Argideen estuary. Overall, the Tolka estuary had a greater biomass of *Ulva* than the Argideen estuary, with the exception of April 2017, when the opposite trend was observed. In relation to shore position of the green tide, significant differences occurred for this morphology between the upper and middle positions. Overall, higher biomass was found on the middle shore than in the upper reaches of the bloom.

At smaller spatial scales of variation, significant differences were observed between sites (see Table 4.1). Moreover, a significant interaction between site and position was identified. No relevant scales of variation were found at scales of variation smaller than 100 m (i.e. sampling stations).

The annual peaks of biomass for the laminar morphology were observed during August in the Argideen estuary and during October in the Tolka estuary (Figure 4.3), with median values of 180.0 g m^{-2} and 322.4 g m^{-2}, respectively. No significant differences in biomass abundance during the peak bloom were found between the estuaries. The maximum values of biomass abundance were measured in the Tolka estuary during October 2016 (1652.8 g m^{-2}) and in the Argideen estuary in August 2017 (2369.6 g m^{-2}). During

Table 4.1. Results of six-way PERMANOVA testing the effects of the six factors[a] on the tubular and laminar biomass densities of *Ulva*

Tubular				Laminar			
Source	**df**	**MS (×10⁵)**	**Ps-F**	**Source**	**df**	**MS (×10⁵)**	**Ps-F**
Estuary (Es)	1	1133.00	69.10*	Estuary (Es)	1	0.30	0.17
Sampling occasion (SO)	6	1080.50	22.96***	Sampling occasion (SO)	6	19.17	8.01***
Position (Po)	2	160.22	12.66*	Position (Po)	2	1.19	2.08
Section (Se)	2	16.40	0.92	Section (Se)	2	1.77	7.05**
EsxSO	6	236.97	5.03*	EsxSO	6	11.25	4.70**
EsxPo	2	22.99	1.82	EsxPo	2	1.77	3.10
SOxPo	12	70.54	2.46	SOxPo	12	1.09	1.15
SOxSe(Es)	12	47.22	2.63*	SOxSe(Es)	12	2.40	9.62***
Se(Es)xPo	4	12.65	0.58	Se(Es)xPo	4	0.57	0.55
EsxSOxPo	12	22.19	0.77	EsxSOxPo	12	1.24	1.31
Site(Se(Es)xSO)	28	17.95	1.89*	Site(Se(Es)xSO)	28	0.25	0.82
SOxSe(Es)xPo	24	28.76	1.31	SOxSe(Es)xPo	24	0.95	0.90
PoxSi(Se(Es) xSO)	56	22.03	2.33***	PoxSi(Se(Es) xSO)	56	1.06	3.49***
St(Si(Se(Es) xSO))	162	9.47	1.03	St(Si(Se(Es) xSO))	162	0.30	1.63**
Residual	660	9.20		Residual	660	0.19	
Total	989			Total	989		

[a]The six factors were "estuary" (Es – fixed, two levels), "sampling occasion" (SO – fixed, seven levels), "position in the bloom" (Po – fixed, three levels), "section" (Se – random, nested in "Es"), "site" (Si – random, nested in "SexSO") and "sampling station" (St – random, nested in "SixPo").

df, degrees of freedom; MS, mean squares; Ps-F, pseudo F.

***p*<0.05; *******p*<0.01; ********p*<0.001.**

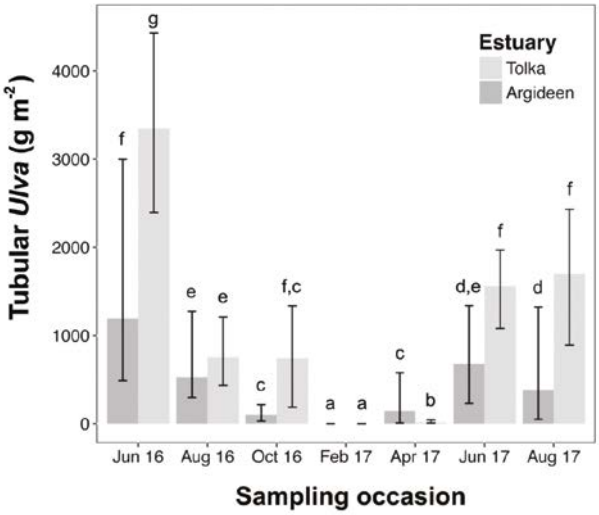

Figure 4.2. Median values for biomass (wet weight) of tubular *Ulva* according to estuary and sampling occasion (*n*=72, except for Tolka, June 2016, when *n*=54) . Lower and upper error bars represent the 25th and 75th percentiles, respectively; letters over the bars represent significant differences. The PERMANOVA results regarding the biomass of laminar *Ulva* indicated significant differences between sampling occasions, sections and sampling stations. Significant interactions between sampling occasion and estuary, sampling occasion and section, and position and site were also identified (see Table 4.1). Reproduced from Bermejo *et al.*, 2019.

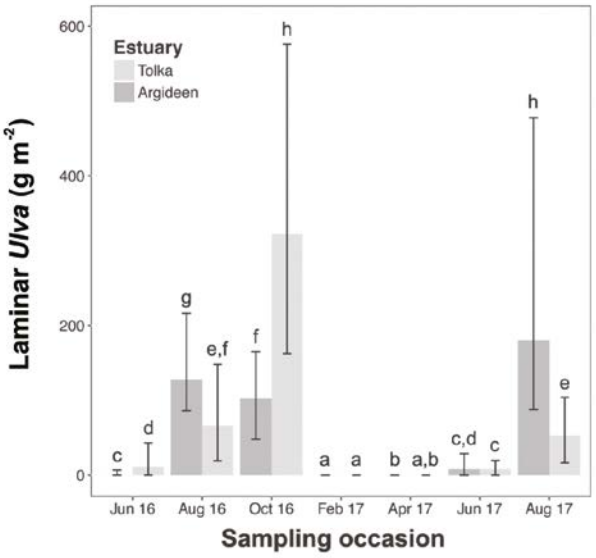

Figure 4.3. Median values for biomass (wet weight) of laminar *Ulva* according to estuary and sampling occasion (*n* = 72, except for Tolka, June 2016, when *n* = 54) . Lower and upper error bars represent the 25th and 75th percentile, respectively; letters over the bars represent significant differences. Reproduced from Bermejo *et al.*, 2019.

February and April, the biomass of laminar *Ulva* was negligible for both estuaries.

On the other hand, the differences between sections varied through the bloom season. Before and after the peak bloom of laminar *Ulva*, no differences in biomass densities between sections (Tolka: June 16, June 17 and August 17; Argideen: June 16 and June 17), or higher levels of biomass in the outer part of the estuary (Tolka: August 17; Argideen: October 16), were observed; however, during peak bloom conditions, the biomass density was significantly higher in the inner section in both estuaries.

4.3.2 Red seaweed tide: Clonakilty

The PERMANOVA results for the biomass of *Gracilaria* in the Clonakilty estuary indicated significant differences between sections of the estuary, sampling occasions and positions (Table 4.2). The annual peaks of biomass occurred in July–August, with the minimum density of biomass in February for both sections (Figure 4.4). In August 2016 and 2017, the median values for biomass of *Gracilaria* were 2345.28 g m^{-2} and 2161.60 g m^{-2} for the inner section and 942.24 g m^{-2} and 1627.20 g m^{-2} for the outer section, respectively. The maximum value for biomass was measured in July 2016 in the inner section, reaching 5438.08 g m^{-2}. Overall, the inner section reached a greater density of biomass of *Gracilaria* than the outer section (see Figure 4.4). In relation to shore position, a significant effect of this factor for *Gracilaria* was detected. However, this pattern was not spatially consistent, as suggested by the significant interactions observed between position in the red tide and section and site (see Table 4.2). The middle position usually showed a higher biomass than the lower and upper positions, but these differences were significant only in the case of the inner section between the lower and the middle positions (*t*-value = 4.07; *p* = 0.006). Marginal differences were found between the middle and the upper positions in the inner section (*t*-value = 2.10, *p* = 0.077).

Significant differences were also observed between sites (see Table 4.2), suggesting a patchy pattern of biomass distribution.

4.3.3 Golden tide: Killybegs

The results obtained for the biomass of the ectocarpoid (i.e. *P. littoralis*) forming a golden tide in the Killybegs estuary revealed significant differences between sampling stations in the outer section (Table 4.3). No significant effects were found for any factor or interactions between factors in the inner section. When the analysis was repeated excluding data from February and June 2017,

Table 4.2. Results of five-way PERMANOVA testing the effects of the five factors[a] on the biomass of *G. vermiculophylla* in the Clonakilty estuary

Source	df	MS($\times 10^5$)	Ps-F
Sampling occasion (SO)	6	204.50	19.59***
Section (Se)	1	112.99	10.83**
Position (Po)	2	61.78	7.01**
SOxSe	6	28.59	2.74
SOxPo	12	12.20	1.38
SexPo	2	55.24	6.27**
Site (Si(SOxSe))	14	10.44	2.52*
SOxSexPo	12	16.76	1.90
PoxSi(SOxSe)	28	8.81	2.13*
St(PoxSi(SOxSe))	42	4.14	1.42
Residual	252	2.91	
Total	377		

[a]The five factors were "sampling occasion" (SO – fixed, seven levels), "position in the bloom" (Po – fixed, three levels), "section" (Se – fixed, two levels), "site" (Si – random, nested in "SexSO"), and "sampling station" (St – random, nested in "SixPo").

df, degrees of freedom; MS, mean squares; Ps-F, pseudo F.

***p*<0.05; ****p*<0.01; *****p*<0.001.**

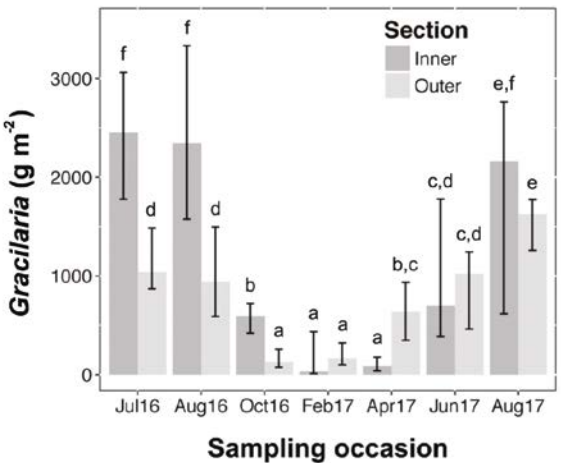

Figure 4.4. Median values for biomass (wet or fresh weight) of *G. vermiculophylla* according to section and sampling occasion in the Clonakilty estuary (*n*=54). Lower and upper error bars represent the 25th and 75th percentiles, respectively; letters over the bars represent significant differences.

significant differences were found between sections and sampling stations (see Table 4.3). Overall, the inner section reached a higher biomass (median 3598.40 g m^{-2}) than the outer section (median 1400.16 g m^{-2}). Although the effect of sampling occasion was not found to be significant, Figure 4.5 shows that the annual minimum biomass occurred in February in the outer section. No data were recorded for the inner section during this sampling occasion. In the outer section, two peaks of biomass were observed in July 2016 (median 2248.2 g m^{-2}) and October 2016 (median 2934.4 g m^{-2}). The annual peak of biomass was observed between June and July in the inner section (median 7046.4 and 5515.2 g m^{-2} for July 2016 and June 2017, respectively).

Table 4.3. Results of PERMANOVA assessing the most relevant scales of temporal and spatial variability in the biomass of *P. littoralis* in the Killybegs estuary[a]

Source	Inner section			Source	Outer section			Source	Full[b]		
	df	MS (×10⁶)	Ps-F		df	MS (×10⁶)	Ps-F		df	MS (×10⁶)	Ps-F
SO	5	52.44	2.54	SO	6	19.5	0.8	SO	4	32.74	1.47
Po	2	43.18	1.54	Po	2	7.93	1.01	Po	2	34.07	1.90
Si(SO)	6	20.63	1.70	Si(SO)	6	24.84	2.69	Se	1	431.49	19.35***
SOxPo	10	24.98	0.89	SOxPo	12	9.94	1.28	SOxPo	8	24.17	1.35
PoxSi(SO)	12	28.09	2.31	PoxSi(SO)	12	7.71	0.84	SOxSe	4	42.73	1.92
St(PoxSi(SO))	16	11.85	1.67	St(PoxSi(SO))	18	9.22	5.49***	PoxSe	2	14.34	0.80
Residual	110	7.11		Residual	114	1.68		Si(SOxSe)	10	22.30	1.92
Total	161			Total	170			SOxPoxSe	8	17.91	1.00
								PoxSi(SOxSe)	20	17.95	1.55
								St(PoxSi(SOxSe))	28	11.42	2.87***
								Residual	182	3.97	
								Total	269	3.97	

[a]**The factors considered were "sampling occasion" (SO), "position in the bloom" (Po), "section" (Se), "site" (Si) and "sampling station" (St).**

[b]**Considers the entire estuary but excluding data from February and June 2017.**

df, degrees of freedom; MS, mean squares; Ps-F, pseudo F.

***$p<0.05$; **$p<0.01$; ***$p<0.001$.**

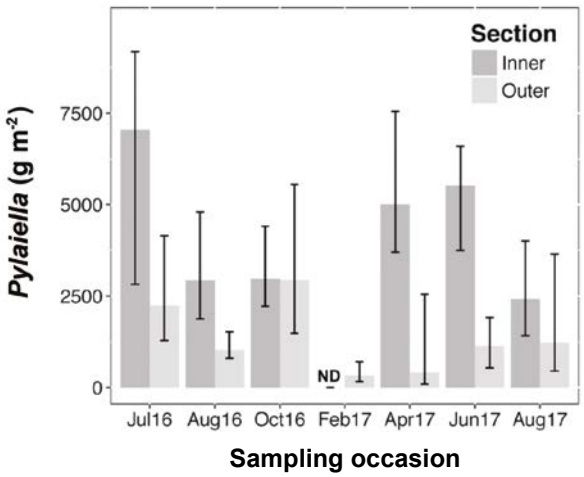

Figure 4.5. Median values of biomass (wet or fresh weight) of *P. littoralis* according to section and sampling occasion in the Killybegs estuary ($n=54$, except for February 2017 and June 2017, when $n=27$ and $n=42$, respectively). Lower and upper error bars represent the 25th and 75th percentiles, respectively. ND, no data.

4.4 Discussion

A significant temporal and spatial variability was observed in the red and green tides studied in Ireland (see Tables 4.1 and 4.2). In the case of the golden tide affecting the Killybegs estuary, significant spatial variability was observed, but not temporal variability (see Table 4.3). Regarding the spatial variability,

tubular *Ulva* and *Gracilaria* showed significant biomass variability associated with bigger spatial scales of variation (i.e. estuaries and sections) compared with laminar *Ulva* and *Pylaiella* (their biomass distribution was better explained at smaller scales of variability, i.e. sites and sampling stations). The contrasting patterns observed for the different seaweeds, and especially between the morphologies of *Ulva*, suggest that the mechanisms determining the distribution of laminar *Ulva* and *Pylaiella* and tubular *Ulva* and *Gracilaria* were different. Considering that tubular *Ulva* and *Gracilaria* were usually anchored in the sedimentary substrate as a result of the burial of their basal part (Schories and Reise, 1993; Robertson and Savage, 2018; this study), whereas laminar *Ulva* and *P. littoralis* were usually observed free-floating or weakly anchored, these differences could be explained by a differential influence of wind and wave action. In the case of the temporal variability, the obtained results indicated a relevant seasonality in the total biomass found in the red and green tides studied from Ireland. These blooms showed their annual peaks of biomass during the summer, with the minimum biomass seen in winter (see Figures 4.2–4.4). Furthermore, a seasonal succession common to both green tides from the Tolka and the Argideen estuaries was identified, with the bloom dominated by tubular species during spring and early summer and co-dominated by tubular and laminar morphologies during late summer and autumn. Although long-term changes in the species composition of green tides (Lavery *et al*., 1991), or differences in spatial distribution between different species, has been previously reported for *Ulva* blooms (Hernandez *et al*., 1997; Nelson *et al*., 2003; Guidone and Thornber, 2013), this seasonal pattern, which is common to both estuaries and both years, has not been previously described for other European estuaries. However, in California, a relatively similar temporal succession was observed between *U. intestinalis* and *U. expansa* (Fong *et al*., 1996). It is also important to note that green tides in Ireland were dominated by tubular morphologies and not laminar morphologies (i.e. *U. rigida*), as previously stated by Wan *et al*. (2017). When the median seaweed biomass per square metre during the peak bloom was compared, the inner section of the Killybegs estuary showed the highest value (median 7046.4 g of ectocarpoid m^{-2}), followed by the Tolka estuary (median 3345.6 g of *Ulva* m^{-2}), the inner section of the Clonakilty estuary (median 2345.28 g of *Gracilaria* m^{-2}) and finally the Argideen estuary (median 1193.6 g of *Ulva* m^{-2}).

4.4.1 Spatial variability

Our findings support the existence of an important spatial variability in the studied blooms, suggesting a patchy distribution similar to those observed in other macroalgal blooms (e.g. Malta and Verschuure, 1997; Nelson *et al*., 2003; Thornber *et al*., 2017). Marked differences in spatial variability were found between seaweed anchored to the sedimentary substrate (i.e. tubular *Ulva* and *Gracilaria*), and weakly anchored or free-floating algae (i.e. laminar *Ulva* and *P. littoralis*). It is expected that wind and wave action are more likely to influence the transport or movement of free-floating macroalgae. In contrast, the seaweeds anchored to the substrate may be less affected by these factors and more susceptible to the effects of local environmental conditions on their biological performance (see Chapters 5 and 6). Considering that the studied macroalgal blooms were thriving in the sedimentary tidal flats of different estuaries, where the habitat and environmental heterogeneity was relatively low at small spatial scales, the observed patterns partially support this hypothesis. In this case, the biomass of anchored seaweeds varies on bigger spatial scales (i.e. estuaries and sections) than the biomass of free-floating seaweeds (i.e. sampling stations). In the studied green tides, where both tubular and laminar morphologies were thriving in the same sampling locations, this comparison is feasible and supports this idea. For instance, the results obtained showed significant differences between estuaries and the position of the green tide for tubular morphologies. Concerning laminar morphologies, significant differences were observed between sampling stations and sections, but no significant differences were observed between shore positions or between estuaries. This suggests that the spatial patterns of tubular morphologies may be determined by factors affecting the biological performance of the species, such as climatic conditions, desiccation, light and nutrient availability (i.e. factors generating spatial patterns at the scale of estuaries or between positions in the green tide). On the other hand, hydrodynamic conditions, as well as interactions with the substrate morphology and other canopy-forming species, rather than local conditions maximising the biological performance of the species, might determine the spatial distribution of laminar morphologies. The anchorage of tubular morphologies to the substrate could favour this morphological form developing into

green tides in areas where tidal currents favour the export of biomass. Moreover, the burial of the basal part of tubular *Ulva* could provide access to nutrients from pore water, which would not be available to the laminar morphologies (Robertson and Savage, 2018). This could partially explain the dominance of tubular morphologies (e.g. *U. compressa* or *U. prolifera*) in Irish estuaries, despite the higher relative growth rates observed for laminar morphologies (e.g. *U. rigida*) in laboratory experiments (see Chapter 6).

4.4.2 Temporal variability

The red tide affecting the Clonakilty estuary and the green tides affecting the Tolka and Argideen estuaries showed a clear seasonal pattern, suggesting that climatological factors following a similar seasonal pattern could play an essential role in the development of these blooms. In the case of the green tides in the Tolka and Argideen estuaries, a slight mismatch in the occurrence of blooms can be observed. Southern blooms (i.e. Argideen estuary, lower latitude) appear to start, peak and finish before the blooms on the east coast (i.e. Tolka estuary, higher latitude), as can be observed in Figures 4.2 and 4.3 for both *Ulva* morphologies, suggesting a key role of temperature or light as triggers of bloom development (Kalita and Tytlianov, 2003; Abreu *et al*., 2011a,b; Van Alstyne, 2018). These results also revealed a mismatch between the peaks of biomass of tubular and laminar morphologies, suggesting a temporal succession between species with different biological performances that was common to both estuaries (see also Chapters 5 and 6).

These results also suggest important between-year-differences during the peak bloom in green tides, with such differences being less clear in the red tide affecting the Clonakilty estuary. In green tides, these differences were especially relevant between June 2016 [3912.9 ± 2473.8 g m^{-2} and 1193.6 ± 1665.3 g m^{-2} for the Tolka estuary (n = 54) and Argideen estuary (n = 72), respectively] and June 2017 [1851.5 ± 1208.1 g m^{-2} and 889.3 ± 846.4 g m^{-2} for the Tolka and Argideen estuaries, respectively (n = 72)]. In both cases, higher biomasses were observed in June 2016 than in June 2017, which could be related to climatic factors. It is worth noting that from January to May the total rainfall at meteorological stations close to both estuaries (www.met.ie) was noticeably lower in 2017 than in 2016, which may have resulted in suboptimal conditions during the first stages of bloom development in 2017 (i.e. lower nutrient input and higher salinity). Significant between-year variation in macroalgal biomass has been observed in other green tides (Malta and Verschuure, 1997; Lyngby *et al*., 1999), leading to suggestions of a critical role of environmental conditions during the early bloom development, which subsequently determine the total biomass accumulated at peak bloom (Malta and Verschuure, 1997; Gao *et al*., 2018). In the case of the *Gracilaria* bloom affecting the Clonakilty estuary, a similar trend could be observed in the inner section when the biomass from August 2016 (median 2345.3 g m^{-2}) and August 2017 (median 2161.6 g m^{-2}) are compared. However, the opposite pattern was observed in the outer section, showing higher values of biomass during August 2017 (1627.2 g m^{-2}) than in August 2016 (942.2 g m^{-2}).

In the case of the green tide affecting the Tolka estuary, it is possible to perform decadal comparisons because of the existence of a previous study by Jeffrey *et al*. (1995), who monitored the annual dynamics of *Ulva* in this estuary from 1989 to 1990. No changes in the seasonal dynamics were observed, with the peak bloom occurring between June and July and with no biomass over winter. However, when the mean values of biomass observed in the Tolka estuary in 2016 and 2017 during the peak bloom were compared with those obtained by Jeffrey *et al*. (1995) in 1989 (666–750 g m^2 of fresh weight considering a 0.12 ratio of dry to fresh weight) and 1990 (790–885 g m^{-2}), a noticeable increase in biomass was revealed.

5 Monitoring Macroalgal Biomass and Physicochemical Attributes in Four Irish Estuaries Affected by Seaweed Tides

5.1 Background

Areas heavily affected by opportunistic macroalgal blooms usually share a suite of common abiotic traits. These waters are characteristically shallow, exhibit a relatively low rate of water exchange and have high nutrient loadings. These factors lead to high availability of light and the accumulation of nutrients and biomass (Valiela *et al*., 1997). The main abiotic factors controlling the relative growth of opportunistic bloom-forming seaweeds are the same as those for other primary producers: light, nutrients and temperature (e.g. Taylor *et al*., 2001; Nelson *et al*., 2003; Van Alstyne, 2018). In coastal waters, N has been identified as the most important macronutrient constraining primary production (Pedersen and Borum, 1996; Lyngby *et al*., 1999). Light and temperature also play a key role in controlling the productivity and yield of opportunistic macroalgal blooms and determining the observed seasonal patterns, especially in high latitude regions (Pihl *et al*., 1996; Hernandez *et al*., 1997; Malta and Verschuure, 1997). Furthermore, in areas such as estuaries, coastal lagoons or certain bays affected by frequent inputs of freshwater, salinity can also display wide spatial and temporal variability, influencing the composition and productivity of macroalgal blooms (Taylor *et al*., 2001; Choi *et al*., 2006; Rybak, 2018).

One of the main consequences of eutrophication in estuarine areas is the community shift from seagrass meadows to macroalgal or microalgal blooms. This has important consequences in sediment biogeochemistry that lead to non-linear and positive feedback loops, amplifying eutrophication and making it a chronic problem. Changes in light availability as a consequence of the development of the macroalgal or microalgal blooms, organic enrichment of sediments and ammonia toxicity in seagrasses have been identified as key factors explaining this shift (Valiela *et al*., 1997; Koch, 2001; Krause-Jensen *et al*., 2008). Irradiance, concentrations of suspended solids (SS), concentrations of different dissolved inorganic forms of N and P and the percentage of organic matter (%OM) in sediments are usually measured in monitoring programmes to assess the status and impact of anthropogenic eutrophication (Le Moal *et al*., 2019) or potential seagrass restoration (Koch, 2001).

The objective of this chapter was to assess the status and impact of anthropogenic eutrophication and to identify the main factors driving the development and composition of seaweed tides following a correlational approach.

5.2 Methodology

5.2.1 Estimating seaweed biomass and relative growth rate

Following a similar sampling procedure to the one outlined in the previous chapter, seaweed biomass was collected in five different seaweed tides (three green tides: Argideen, Clonakilty and Tolka; one red tide: Clonakilty; one golden tide: Killybegs). However, only seaweed samples collected in the middle shore position of the seaweed bloom were considered in this study.

To estimate the relative net daily growth rate (DGR) an exponential growth was assumed (equation 5.1):

$$\mathrm{DGR}\ (\%\,\mathrm{day}^{-1}) = 100 \ln(\mathrm{FW_f}\,\mathrm{FW_0}^{-1})\,t^{-1} \qquad (5.1)$$

where FW_f is the median fresh weight of seaweed found in the field at the end of the assessment period; FW_0 is the median fresh weight of seaweed found in the field at the beginning of the assessment period; and t is the number of days that the assessment period lasted.

To determine tissue N content and delta N-15 ($\delta^{15}N$), a small fragment (approx. 2 g fresh weight) of seaweed was rinsed with milli-Q water, freeze-dried and ground in a 1.5 ml Eppendorf tube using a pestle. Ground samples were stored in a desiccator until analysed using an isotope ratio mass spectrometer (Finnigan MAT Delta Plus, Thermo®) via an element analyser

(Carlo Erba CHNSO 1108). Three replicates ($n = 3$) per species or morphology, sampling occasion and section of each estuary were analysed. Considering the mean tissue N content and biomass variability, the net N biomass (nNB) was assessed following equation 5.2:

$$nNB\ (g\,N\,m^{-2}\,day^{-1}) = (FW_f\,\%N_f - FW_0\,\%N_0)\,t^{-1} \quad (5.2)$$

where FW_f is the median fresh weight of seaweed found in the field at the end of the assessment period; $\%N_f$ is the mean percentage of tissue N at the end of the assessment period; FW_0 is the median fresh weight of seaweed found in the field at the beginning of the assessment period; $\%N_0$ is the mean percentage of tissue N at the beginning of the assessment period; and t is the number of days that the assessment period lasted.

5.2.2 Assessing the physicochemical attributes of each estuary on a seasonal basis

Daily climatological information (i.e. rainfall, solar radiation, maximum air temperature and minimum air temperature) was obtained from the Irish meteorological service (Met Éireann; www.met.ie/). In the case of the Tolka estuary, all of the climatological information was obtained from the meteorological station at Dublin Airport, located less than 10 km from the estuary. In Killybegs, the climatological data used were obtained from the meteorological stations of Finner Camp (less than 20 km from the estuary). In the case of the Argideen estuary and Clonakilty Bay, rainfall data were taken from the closest pluviometric stations to the Argideen estuary (i.e. Ballinspittle) and Clonakilty Bay (i.e. Rosscarbery). The data for solar radiation and maximum and minimum air temperature were linearly interpolated considering the distance from the sampling site to the two closest meteorological stations (i.e. Sherkin Island and Roche's Point), which were between 35 and 55 km from the study sites on the southern Irish coast, to define the climate variable V_S (equation 5.3):

$$V_S = V_1 + (V_2 - V_1) * (D_{1,S}/D_{1,2}) \quad (5.3)$$

where V_S is the value of the climatic variable in the interpolated site; V_1 is the value in meteorological station 1; V_2 is the value in meteorological station 2; $D_{1,S}$ is the distance between meteorological station 1 and the interpolated site; and $D_{1,2}$ is the distance between meteorological stations 1 and 2.

Sediment and water samples were collected on each sampling occasion. Three replicate sediment samples (3 cm deep, 2.5 cm in diameter) were collected at each section in the estuary along the inner position of the green tide during the sampling for *Ulva* biomass measurements. Subsequently, the %OM was determined by loss of ignition by drying samples until they were a constant weight at 60°C, followed by combustion for 5 hours at 550°C (Crips, 1971). A subsample of 1 g of non-combusted dried sediment was sent to Servizos de Apoio á Investigación at the University of A Coruña (Spain), where the N contents were determined using a Flash combustion EA1108 elemental analyser (Carlo Erba Instruments). Samples of sediments were not collected from the Tolka and Argideen estuaries in February 2017.

Water sampling for physicochemical characteristics (i.e. salinity, SS and dissolved inorganic nutrients) was conducted during the high tide before or after the biomass sampling at all of the estuaries over the six sampling occasions (i.e. data from June/July 2016 were missing). These water samples were collected from the coast at a depth of 20 cm in each sampling site. Salinity was determined using a hand refractometer (ATAGO S–20E). In addition, water samples ($n = 3$) were also collected for the determination of SS and dissolved inorganic nutrients (nitrate, nitrite, ammonium and P). Water samples for the determination of inorganic nutrient concentrations were filtered *in situ* using a syringe and a nylon disposable filter (pore size 0.45 mm; Sarstedt). These samples were stored at –20°C before being analysed. Water samples were analysed for total oxidised N (TON) concentrations on a Thermo Aquakem discrete analyser (Thermo Scientific, Finland), with a detection limit of 0.25 mg L^{-1} for TON. Samples were also analysed for N-nitrite ($N\text{-}NO_2$), N-ammonia ($N\text{-}NH_4^+$) and dissolved reactive P using the same instrument. N-nitrate ($N\text{-}NO_3$) was calculated by subtracting the concentration of $N\text{-}NO_2$ from the concentration of TON. In the case of SS, 5 L of seawater were transported to the laboratory and re-suspended by shaking prior to filtration. Between 0.5 and 0.25 L of water (depending on the amount of SS) were filtered through a glass fibre filter (Whatman GF/F). The filter was dried in an oven at 60°C for at least 24 hours before filtration and for at least 48 hours after filtration. The concentration of SS was calculated as the difference in weight of the dried filter after and before filtration divided by the volume filtered.

5.2.3 Statistical analyses

To assess temporal and spatial differences in dissolved inorganic N (DIN), P and seaweed biomass, a three-way ANOVA was performed for each of the five study sites. The factors considered were sampling occasion (fixed; six levels), section (fixed; two levels) and site, nested in the interaction between section and sampling occasion (random; two levels). In cases of salinity, %OM in sediments, %N in sediments and %N in seaweed tissue, a similar model was followed, but the spatial factor, site, was excluded as the number of replicates per site was insufficient. A post hoc Tukey test, or similar, was applied to compare between levels when the factors exhibited a significant effect. In cases in which more than one factor had a significant effect, the Tukey test was used to compare the levels of temporal variability within each spatial level. Salinity, DIN and P, %OM and %N in sediments, and tissue N content conformed to homoscedasticity (i.e. Levene's test) assumptions, but seaweed biomass did not conform to homoscedasticity even after data transformation and therefore, for seaweed biomass, a PERMANOVA based on Euclidean distances was employed (Anderson *et al*., 2008).

To identify the main environmental factors explaining the development and composition of seaweed tides, a distance-based linear model (distLM) routine (Clarke and Gorley, 2006) was used. A draftsman plot was performed to identify skewed variables or correlated environmental variables ($r > 0.7$). Dissolved nutrients, SS and rainfall showed a skewed distribution and were transformed. In this case, nutrients were $\log(x+1)$ transformed, whereas, for SS and rainfall, a square root transformation was used. Ammonium and nitrite showed a high correlation ($r > 0.7$); thus, only ammonium was considered for the subsequent distLM analysis. In the case of biomass data, a Euclidean distance matrix was used considering four seaweed taxa or morphologies (*Gracilaria*, *Pylaiella* and tubular and laminar *Ulva*). In the case of environmental variables, the mean value obtained in a section for a sampling occasion was used for this analysis. Regarding seaweed biomass, the median value was used instead. The environmental variables considered for this analysis were $\log[(NO_3^-)+1]$, $\log[(NH_4^+)+1]$, $\log[(P)+1]$, $SS^{0.5}$, salinity, solar radiation, maximum air temperature, minimum air temperature and $rainfall^{0.5}$. The data considered comprised six sampling occasions in all cases, except in the area of Clonakilty affected by green tides, where only five complete datasets were available for environmental variables and seaweed biomass. The selection criterion and selection procedure used were the Akaike information criterion (AIC) and stepwise selection procedure. A dbRDA (distance-based redundancy analysis; Anderson *et al*., 2008) plot was performed to visualise the distLM results.

Statistical analyses were performed in R and using the PERMANOVA+ add-on PRIMER 6 (Plymouth Routines in Multivariate Ecological Research) software. In all statistical analyses, significance was set at a probability of $p < 0.05$ and, when necessary, analyses were based on 1999 permutations.

5.3 Results

5.3.1 Spatial and temporal dynamics of seaweed biomass

The PERMANOVA results for the different estuaries and seaweed tides indicated a significant effect of sampling occasion (p-values of < 0.05) for the green tides occurring at the Tolka and Argideen estuaries (tubular and laminar morphologies) and the red tide at Clonakilty. In the case of the green tide affecting Clonakilty, only marginal significance was found for this factor and both morphologies of *Ulva* (PERMANOVA; $0.05 < p < 0.1$). No significance of sampling occasion was found for the biomass of *Pylaiella* occurring at Killybegs. The seasonal pattern revealed a peak bloom during summer and a minimum biomass in winter (Figure 5.1) for the green tides from Tolka and Argideen and the red tide at Clonakilty (as described in the previous chapter). In the case of the green tide affecting the Clonakilty estuary, a similar trend was observed, with minimum biomasses found in winter.

Regarding spatial variability, each estuary and seaweed tide showed a different pattern. The tubular *Ulva* in the Tolka estuary showed significant differences between sections, which was not the case for laminar *Ulva*. At Clonakilty, significant differences were observed between sites and sections for the laminar morphologies, with significant differences observed only between sites for tubular morphologies. Tubular and laminar morphologies showed significant differences between sites in the Argideen estuary, but not between sections. In the case of the red tide

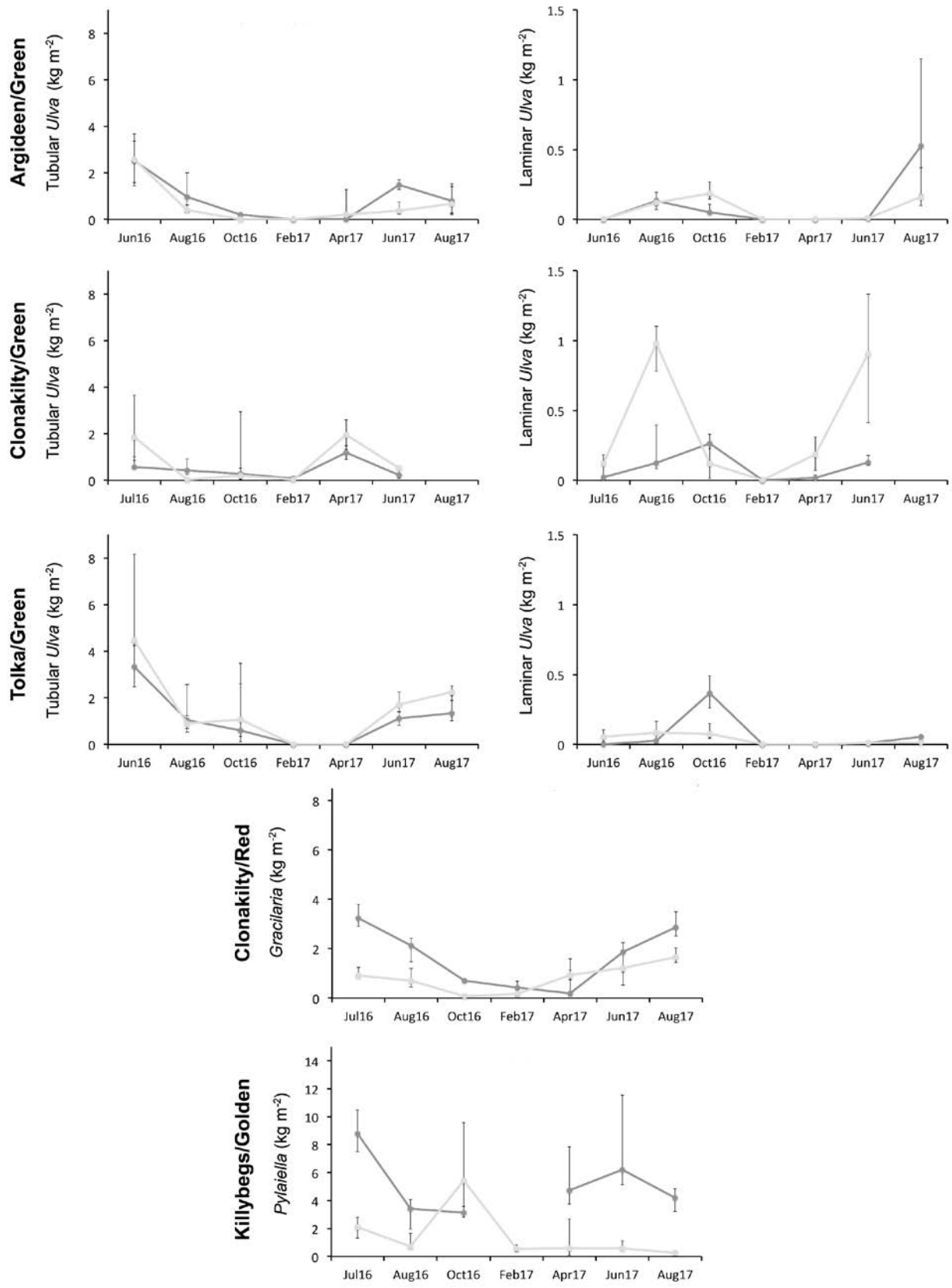

Figure 5.1. Median values for fresh weight of seaweed biomass per square metre in the inner (dark grey) and outer (light grey) sections of the five areas affected by macroalgal blooms during each sampling occasion.

at Clonakilty, there were no significant differences between sections or between sites within sections ($p > 0.05$). The biomass of ectocarpoids in the Killybegs estuary yielded significant differences at the scale of sections.

5.3.2 Spatial and temporal dynamics of tissue N content and isotopic signature

In the three estuaries affected by green tides (i.e. Argideen, Clonakilty and Tolka), the tissue N content showed a significant temporal variability (ANOVA; $p < 0.05$), but no spatial differences between sections were observed (ANOVA; $p > 0.05$). When tubular and laminar morphologies from the same sample (i.e. collected from the same quadrat) were compared, the tubular *Ulva* yielded a higher tissue N content in the Tolka estuary (paired *t*-test; $t = 3.97$; $p < 0.001$) and the Clonakilty estuary (paired *t*-test; $t = 2.04$; $p = 0.049$). In the Argideen estuary, no significant differences between morphologies were found (paired *t*-test; $t = 1.18$; $p = 0.248$) but the trend was similar, with tubular morphologies having a higher tissue N content. Overall, the tissue N content was higher than 2%, with the exception of June 2016 (1.61 ± 0.76% for tubular *Ulva*; 1.20 ± 0.38% for laminar *Ulva*) and August 2016 (1.69 ± 0.46% for laminar *Ulva*) in the Clonakilty estuary (Figure 5.2). The three estuaries followed a similar trend, showing the lowest tissue N contents in summer (June–August), coinciding with the peak biomass (see Figure 5.2). Regarding δ^{15}N, significant temporal variability was observed in the three estuaries (ANOVA; $p < 0.05$), with no spatial differences between sections (ANOVA; $p > 0.05$). When both morphologies from the same sample were compared in the Tolka estuary, tubular morphologies of *Ulva* yielded a lower δ^{15}N (paired *t*-test; $t = -2.92$; $p = 0.007$). No differences in the isotopic signature were found in the Argideen estuary (paired *t*-test; $t = 1.026$; $p = 0.314$) and the Clonakilty estuary (paired *t*-test; $t = 1.678$; $p = 0.103$). Tubular and laminar morphologies followed a similar seasonal pattern, but this pattern was different between estuaries. The Tolka estuary showed the highest δ^{15}N values and the most important seasonal variability (11.19 ± 2.19). The Argideen estuary (9.37 ± 0.75) and the Clonakilty estuary (8.42.19 ± 0.90) showed lower and more stable values of δ^{15}N throughout the year.

Regarding the tissue N content of the *G. vermiculophylla* bloom affecting the Clonakilty estuary, the ANOVA results revealed significant differences between sampling occasions (*F*-value = 24.42; $p < 0.001$), but not between sections (*F*-value = 0.02; $p > 0.05$). The tissue N content followed a seasonal pattern, opposite to the one observed for biomass abundance (see Figure 5.2). The maximum percentages of tissue N content were found in February (4.68 ± 0.31%), coinciding with the minimum biomass abundance, and the minimum percentages of tissue N content were found during the summer (July 2016; 2.27 ± 0.36%), coinciding with the maximum biomass abundance. In the case of δ^{15}N, significant differences were observed between sampling occasions and between sections. The δ^{15}N was higher in the inner section (11.83 ± 0.64) than in the outer section (10.02 ± 0.81). The minimum δ^{15}N was observed in April in both sections (see Figure 5.2), but there was not a clear maximum δ^{15}N in any of the sections. In the inner section, the highest δ^{15}N was found in February, whereas in the outer section the highest δ^{15}N was found during October 2016 and August 2017.

The results did not show any significant scale of temporal or spatial variability for δ^{15}N in the ectocarpoids forming a bloom at Killybegs. The δ^{15}N varied from –3.80 to 3.47, with a mean value of 1.79. Overall, δ^{15}N seemed to be lower in the inner section than in the outer section. Regarding tissue N content, there were significant differences between sampling occasions. The percentage of tissue N tended to increase from summer to winter, with the minimum value in July or August (3.93 ± 0.77% during July 2016) and the maximum in February 2017 (5.54 ± 0.44%).

The change in total nNB associated with the green tide at Tolka was negative from June 2016 to August 2016, and from October 2016 to February 2017 (Table 5.1). The highest loss of N biomass was recorded from June 2016 to August 2016 (–3.31 g N m^{-2} d^{-1}), with the most important gain between April 2017 and June 2017 coinciding with the development of the tubular bloom (1.19 g N m^{-2} d^{-1}). In Killybegs, only data from the outer section were considered. In this estuary, nNB increased from August 2016 to October 2016 and from February 2017 to April 2017. Overall, the changes in the nNB were determined by biomass variability in the case of the golden tide at Killybegs, where nNB and DGR were highly correlated ($r = 0.92$). For the

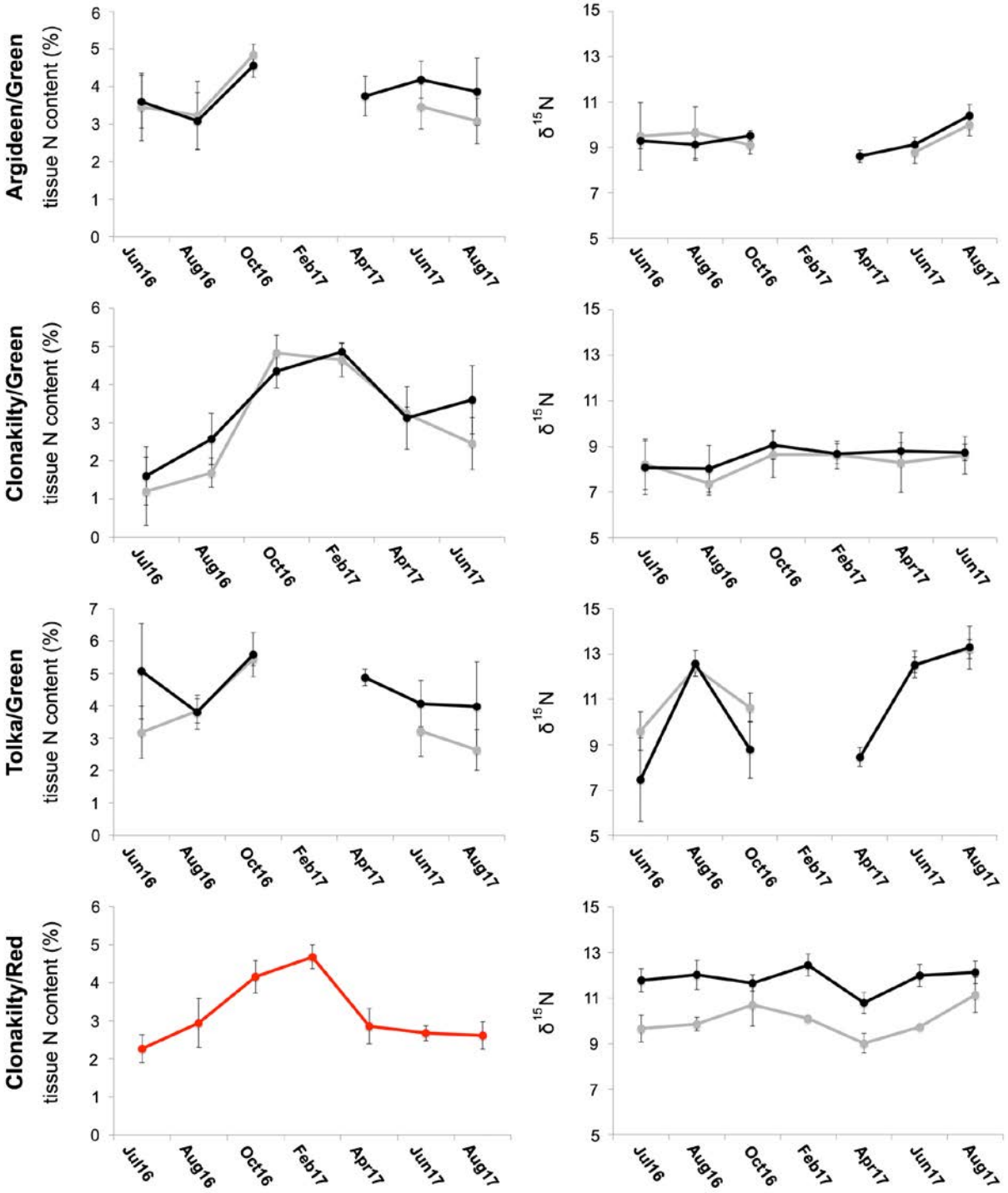

Figure 5.2. Mean values for tissue N content (%) and $\delta^{15}N$ in seaweeds forming green and red tides from the Argideen, Clonakilty and Tolka estuaries during each sampling occasion. Error bars represent standard deviations. In green tides, the lines represent tubular (black lines) and laminar (grey lines) morphologies of *Ulva*. In the case of the red tide affecting the Clonakilty estuary, the lines in the right-hand graph represent the $\delta^{15}N$ for *Gracilaria* thriving in inner (black line) and outer (grey line) sections.

Table 5.1. Net N biomass (g N m^{-2} d^{-1}) and DGR (%) for tubular and laminar *Ulva* from the Tolka estuary and ectocarpoids from the Killybegs estuary during the six different periods studied.

Period	Laminar		Tubular		Ectocarpoid	
	nNB	DGR	nNB	DGR	nNB	DGR
June 2016–August 2016	0.02	5.98	–3.31	–2.78	–1.72	–2.50
August 2016–October 2016	0.22	2.69	0.22	–0.37	8.19	3.58
October 2016–February 2017	–0.09	–5.10	–0.33	–6.20	–3.12	–1.79
February 2017–April 2017	0.00	0.00	0.01	7.88	1.59	1.86
April 2017–June 2017	0.01	9.13	1.19	10.01	–2.66	–2.51
June 2017–August 2017	0.01	2.14	0.26	0.38	–0.51	–1.46

Green shading indicates positive net balance; orange shading indicates negative net balance.

Tolka estuary, although the correlation between DGR and nNB was direct and significant, the coefficient of determination was low, indicating that nNB was explained better by biomass variability, but also by tissue N concentration for both morphologies.

5.3.3 Spatial and temporal dynamics of environmental variables

The seawater physicochemical parameters for each sampling occasion at each study site are presented in Table 5.2. Overall, in the areas affected by green and golden tides, the main source of inorganic N was nitrate followed by ammonia, which surpassed nitrate as the main source at certain times of the year. In the area of the Clonakilty estuary where the annual red tide occurs, nitrate was always the main source of inorganic N followed by ammonia. Regarding total DIN, all study sites showed significant differences in DIN concentrations between sampling occasions (ANOVA; $p < 0.01$). In the Tolka and Argideen estuaries, the maximum DIN concentrations were observed during February (see Table 5.2). Overall, the concentration increased from August to February and decreased sharply from February to April. In the areas of the Clonakilty estuary affected by green and red tides, a similar pattern was observed only in the inner section of the area affected solely by the red seaweed tide. For spatial differences within estuaries for a specific seaweed bloom, only the areas of the Clonakilty estuary affected by red seaweed tides showed significant differences between sections of the estuary, with DIN concentrations higher in the inner section. The areas of the Clonakilty and Argideen estuaries affected by green tides yielded marginal differences in DIN concentrations between sections (ANOVA; $0.05 < p < 0.1$). No differences were found between sites in these estuaries, where the mean DIN concentration ranged between 1.16 and 0.04 mg L^{-1}. When the DIN concentrations were compared between the five areas affected by macroalgal tides, significant differences were found (ANOVA; F-value = 43.07; $p < 0.001$), with the areas of the Clonakilty estuary where the red seaweed tide occurs having the highest concentrations (1.36 ± 0.67 mg L^{-1}). No significant differences were observed between other areas. In the case of P concentrations, significant temporal variability (ANOVA; $p < 0.01$) was observed in the Argideen, Tolka and Clonakilty (areas affected by both green and red seaweed tides) estuaries. A common pattern of temporal variation was not evident, although P concentrations seemed to be higher during the summer of 2017 (June and August) in all study areas (see Table 5.2). Significant differences between sections of the estuary were observed in Clonakilty (ANOVA; $p < 0.05$) in areas affected by both green and red seaweed tides. No temporal or spatial differences were observed in Killybegs for this nutrient. No differences were found between sites within sections. Significant differences between estuaries were found (ANOVA; $p < 0.001$). The Tolka estuary had the highest concentrations of P (38.19 ± 16.15 mg L^{-1}), followed by the areas of the estuary affected by red seaweed tides at Clonakilty (22.95 ± 11.5 mg L^{-1}). No significant differences were found between the other estuaries, where mean P concentrations ranged between 8.53 and 13.50 mg L^{-1}.

The areas affected by green tides had higher salinities than the areas affected by red and golden tides (ANOVA; F-value = 18.18; $p < 0.001$). Salinity in the areas affected by green tides ranged between 21.75 PSU (practical salinity unit; outer section of Tolka during February 2017)

Table 5.2. Summary of water physicochemical attributes (mean ± standard deviation) monitored in all study areas during each sampling occasion

Estuary/tide	SO	Section	$N\text{-}NH_4^+$	$N\text{-}NO_2^-$	$N\text{-}NO_3^-$	DIN	P	Sal	SS
Argideen/green	Aug 2016	Inner	0.07 ± 0.04	22.54 ± 0.92	0.05 ± 0.06	0.14 ± 0.06	8.61 ± 3.26	32.2 ± 0	0.07 ± 0.02
Argideen/green	Aug 2016	Outer	0.13 ± 0.03	23 ± 0.92	0.06 ± 0.01	0.21 ± 0.04	7.72 ± 2.08	32.85 ± 0.07	0.05 ± 0.02
Argideen/green	Oct 2016	Inner	0.06 ± 0.02	23 ± 0.92	0.44 ± 0.61	0.52 ± 0.63	8.61 ± 2.08	30.1 ± 1.13	0.06 ± 0
Argideen/green	Oct 2016	Outer	0.08 ± 0.05	24.38 ± 1.84	0.23 ± 0.09	0.34 ± 0.06	11.28 ± 4.16	30.95 ± 2.19	0.06 ± 0.01
Argideen/green	Feb 2017	Inner	0.08 ± 0.02	24.84 ± 2.3	1.06 ± 0.37	1.16 ± 0.39	13.36 ± 7.12	26.55 ± 4.17	0.45 ± 0.42
Argideen/green	Feb 2017	Outer	0.08 ± 0.02	24.38 ± 2.3	0.58 ± 0.29	0.68 ± 0.3	15.14 ± 9.5	29.2 ± 0.42	0.17 ± 0.04
Argideen/green	Apr 2017	Inner	0.04 ± 0.05	2.3 ± 0.92	0.18 ± 0.05	0.22 ± 0.09	5.34 ± 0.89	32.7 ± 0.14	0.06 ± 0
Argideen/green	Apr 2017	Outer	0.03 ± 0.02	1.84 ± 0.92	0.04 ± 0.06	0.07 ± 0.06	6.53 ± 2.08	33.85 ± 0.07	0.07 ± 0.01
Argideen/green	Jun 2017	Inner	0.05 ± 0.04	5.52 ± 0.46	0.19 ± 0.04	0.25 ± 0.06	13.65 ± 3.56	29.05 ± 1.34	0.07 ± 0.01
Argideen/green	Jun 2017	Outer	0.05 ± 0.05	3.22 ± 1.38	0.13 ± 0.09	0.18 ± 0.14	10.98 ± 3.56	30.8 ± 0.28	0.06 ± 0.01
Argideen/green	Aug 2017	Inner	0.08 ± 0.02	9.66 ± 4.6	0.12 ± 0.02	0.21 ± 0.04	12.47 ± 2.67	31 ± 0	0.06 ± 0.03
Argideen/green	Aug 2017	Outer	0.09 ± 0.05	9.66 ± 6.9	0.04 ± 0.04	0.14 ± 0.1	29.98 ± 23.45	32.5 ± 2.12	0.05 ± 0.04
Overall mean			0.07 ± 0.03	14.53 ± 2.03	0.26 ± 0.15	0.34 ± 0.16	11.97 ± 5.37	30.98 ± 2.04	0.1 ± 0.11
Clonakilty/green	Aug 2016	Inner	0.05 ± 0.02	21.62 ± 0.46	0 ± 0.01	0.07 ± 0.03	7.72 ± 2.97	32.45 ± 0.49	0.07 ± 0.03
Clonakilty/green	Aug 2016	Outer	0.06 ± 0.02	21.16 ± 0.92	0.01 ± 0.02	0.09 ± 0.03	7.72 ± 2.37	28.1 ± 2.26	0.09 ± 0.03
Clonakilty/green	Oct 2016	Inner	0.05 ± 0	21.16 ± 0	0.03 ± 0.02	0.09 ± 0.03	10.09 ± 5.34	27.05 ± 7	0.06 ± 0
Clonakilty/green	Oct 2016	Outer	0.05 ± 0.01	21.62 ± 1.38	0.08 ± 0.06	0.16 ± 0.06	14.25 ± 10.68	30.3 ± 1.56	0.14 ± 0.12
Clonakilty/green	Feb 2017	Inner	0.06 ± 0.04	21.62 ± 0.92	0.21 ± 0.08	0.29 ± 0.13	6.53 ± 0.89	33.45 ± 0.78	0.07 ± 0.01
Clonakilty/green	Feb 2017	Outer	0.09 ± 0.04	23.92 ± 1.38	0.39 ± 0.04	0.51 ± 0.05	8.01 ± 1.78	31.2 ± 0.71	0.27 ± 0.15
Clonakilty/green	Apr 2017	Inner	0.03 ± 0.06	0 ± 0.46	0 ± 0.01	0.03 ± 0.06	4.75 ± 1.19	34.1 ± 0.14	0.07 ± 0.01
Clonakilty/green	Apr 2017	Outer	0.03 ± 0.02	2.76 ± 1.84	0.64 ± 0.71	0.67 ± 0.71	6.83 ± 1.78	33.95 ± 0.21	0.07 ± 0.02
Clonakilty/green	Jun 2017	Inner	0.02 ± 0.01	4.14 ± 1.38	0.26 ± 0.07	0.28 ± 0.08	18.7 ± 2.67	26.2 ± 0.14	0.05 ± 0
Clonakilty/green	Jun 2017	Outer	0.02 ± 0.01	2.3 ± 0.92	0.05 ± 0.01	0.07 ± 0.02	10.68 ± 2.08	30.45 ± 1.77	0.06 ± 0.01
Clonakilty/green	Aug 2017	Inner	0.17 ± 0.07	27.6 ± 23	0.49 ± 0.29	0.69 ± 0.36	49.27 ± 10.39	–	0.09 ± 0.03
Clonakilty/green	Aug 2017	Outer	0.07 ± 0.06	11.5 ± 5.52	0.87 ± 0.41	0.95 ± 0.39	17.51 ± 8.01	–	0.04 ± 0
Overall mean			0.06 ± 0.03	14.95 ± 3.18	0.25 ± 0.15	0.33 ± 0.16	13.5 ± 4.18	30.73 ± 2.86	0.09 ± 0.06

Table 5.2. Continued

Estuary/tide	SO	Section	$N\text{-}NH_4^+$	$N\text{-}NO_2^-$	$N\text{-}NO_3^-$	DIN	P	Sal	SS
Tolka/green	Aug 2016	Inner	0.18±0.06	35.88±9.2	0.03±0.02	0.24±0.08	65.59±54.32	27.15±0.64	0.08±0.03
Tolka/green	Aug 2016	Outer	0.14±0.04	29.9±6.44	0.03±0.05	0.21±0.1	34.73±37.4	34±2.26	0.06±0.02
Tolka/green	Oct 2016	Inner	0.14±0.03	28.98±3.68	0.14±0.02	0.31±0.05	22.26±10.09	29.4±4.24	0.07±0.01
Tolka/green	Oct 2016	Outer	0.22±0.1	36.34±5.52	0.17±0.13	0.43±0.22	43.33±21.37	30.7±6.65	0.07±0.01
Tolka/green	Feb 2017	Inner	0.39±0.13	37.72±2.76	0.55±0.16	0.97±0.27	27.01±7.12	24.15±0.78	0.06±0.01
Tolka/green	Feb 2017	Outer	0.33±0.13	32.2±6.9	0.42±0.21	0.78±0.33	23.74±13.06	21.75±6.01	0.05±0
Tolka/green	Apr 2017	Inner	0.13±0.03	5.52±1.38	0.13±0.06	0.27±0.05	27.9±6.23	30.3±0.42	0.06±0.01
Tolka/green	Apr 2017	Outer	0.11±0.07	4.14±1.38	0.08±0.02	0.2±0.08	25.23±6.23	30.5±0.14	0.06±0.01
Tolka/green	Jun 2017	Inner	0.06±0.06	3.68±4.14	0.05±0.06	0.12±0.12	67.08±13.36	29.2±0.57	0.12±0.07
Tolka/green	Jun 2017	Outer	0.01±0	0±0	0.03±0.05	0.04±0.05	50.46±9.5	29.15±0.07	0.06±0.01
Tolka/green	Aug 2017	Inner	0.03±0.03	1.38±1.38	0.01±0.01	0.04±0.04	34.43±8.31	31.55±0.49	0.07±0.02
Tolka/green	Aug 2017	Outer	0.01±0.02	0.46±0.46	0.28±0.16	0.29±0.17	36.51±6.83	31.55±0.07	0.05±0
Overall mean			0.15±0.06	18.02±3.6	0.16±0.08	0.33±0.13	38.19±16.15	29.12±3.36	0.07±0.02
Clonakilty/red	Aug 2016	Inner	0.31±0.18	26.68±5.52	0.64±0.43	0.99±0.58	20.48±12.47	14.85±4.74	0.05±0.02
Clonakilty/red	Aug 2016	Outer	0.07±0.02	22.54±1.84	0.65±0.78	0.75±0.79	9.79±2.37	19.3±7.35	0.05±0.02
Clonakilty/red	Oct 2016	Inner	0.12±0.06	28.98±6.9	2.29±0.78	2.44±0.8	27.9±24.04	31.5±2.12	0.04±0.01
Clonakilty/red	Oct 2016	Outer	0.05±0.05	23.46±5.06	1.69±1.92	1.77±1.97	10.09±7.12	29.5±5.23	0.06±0.01
Clonakilty/red	Feb 2017	Inner	0.12±0.04	29.9±4.14	2.95±1.35	3.1±1.38	14.25±6.53	15.9±4.38	0.03±0.01
Clonakilty/red	Feb 2017	Outer	0.08±0.07	26.68±9.66	0.71±0.33	0.81±0.25	27.01±46.89	29.55±0.78	0.06±0.01
Clonakilty/red	Apr 2017	Inner	0.07±0.03	7.36±2.3	1.48±0.26	1.56±0.26	19±3.86	31.65±0.92	0.06±0.01
Clonakilty/red	Apr 2017	Outer	0.01±0.03	0.0±0.0	0.26±0.19	0.27±0.21	5.64±1.19	32.5±0.71	0.07±0.01
Clonakilty/red	Jun 2017	Inner	0.1±0.08	11.5±4.6	1.6±0.5	1.71±0.44	32.05±8.01	5.55±0.78	0.02±0.01
Clonakilty/red	Jun 2017	Outer	0.1±0.07	13.34±5.06	0.98±0.35	1.09±0.33	29.98±8.01	14.9±6.65	0.04±0
Clonakilty/red	Aug 2017	Inner	0.18±0.07	32.2±27.6	0.55±0.41	0.76±0.51	53.72±8.31	22.1±10.8	0.06±0.01
Clonakilty/red	Aug 2017	Outer	0.08±0.07	15.18±5.06	0.98±0.53	1.08±0.48	25.53±9.2	14.3±8.7	0.04±0
Overall mean			0.11±0.06	19.82±6.48	1.23±0.65	1.36±0.67	22.95±11.5	22.52±9.55	0.05±0.01

Table 5.2. Continued

Estuary/tide	SO	Section	$N\text{-}NH_4^+$	$N\text{-}NO_2^-$	$N\text{-}NO_3^-$	DIN	P	Sal	SS
Killybegs/golden	Aug 2016	Inner	0.1±0.02	21.62±0.46	0.16±0.24	0.28±0.26	6.53±1.48	10±10.04	0.04±0.01
Killybegs/golden	Aug 2016	Outer	0.18±0.06	22.54±0.92	0.04±0.07	0.24±0.08	5.34±0.59	25.2±0.14	0.03±0.01
Killybegs/golden	Oct 2016	Inner	0.14±0.04	22.54±1.38	0.07±0.04	0.23±0.04	5.05±0.59	13.45±3.18	0.03±0
Killybegs/golden	Oct 2016	Outer	0.14±0.02	22.08±0.92	0.02±0.05	0.18±0.07	4.45±0.89	29.85±0.07	0.06±0.01
Killybegs/golden	Feb 2017	Inner	0.2±0.04	23±0.92	0.08±0.04	0.3±0.06	5.64±0.59	1.15±0.21	0.01±0
Killybegs/golden	Feb 2017	Outer	0.1±0.01	21.16±0.92	0.08±0.02	0.2±0.01	5.94±3.26	1±0.14	0.01±0
Killybegs/golden	Apr 2017	Inner	0.02±0.02	4.14±0	0.01±0.01	0.04±0.03	8.9±1.19	23.85±14.07	0.05±0
Killybegs/golden	Apr 2017	Outer	0.05±0.02	3.68±0.92	0.13±0.08	0.18±0.08	8.01±1.48	30.4±1.27	0.05±0
Killybegs/golden	Jun 2017	Inner	0.03±0.04	1.38±0.92	0.05±0.07	0.09±0.06	20.78±37.4	12.4±0.28	0.07±0.03
Killybegs/golden	Jun 2017	Outer	0.02±0.02	0.92±0.92	0.22±0.14	0.24±0.14	4.75±0.89	13.8±0.57	0.04±0.04
Killybegs/golden	Aug 2017	Inner	0.03±0.02	0.92±0.46	0.04±0.04	0.07±0.04	16.03±8.9	21.45±1.34	0.05±0.02
Killybegs/golden	Aug 2017	Outer	0.03±0.02	0±0	0±0	0.03±0.02	10.98±2.08	26.75±1.48	0.05±0
Overall mean			0.09±0.03	12±0.73	0.08±0.07	0.17±0.07	8.53±4.95	16.11±10.81	0.04±0.02

DIN (mg L^{-1}; $n=6$); NH_4^+, ammonium (mg L^{-1}; $n=6$); NO_2^-, nitrite (mg L^{-1}; $n=6$); NO_3^-, nitrate (mg L^{-1}; $n=6$); P (mg L^{-1}; $n=6$); Sal, salinity (PSU; $n=2$); SO, sampling occasion; SS (mg L^{-1}; $n=4$). For DIN and P concentrations, colours indicate the concentration class according to Irish standards for coastal and transitional waters, following Statutory Instrument (S.I.) 272 (2009) (yellow = moderate ecological status or lower; green = good or high ecological status).

and 34.1 PSU (inner section of Clonakilty affected by the green tide during April 2017), with a mean salinity value of 30.2 PSU (see Table 5.2). In the areas affected by green tides in the Tolka and Argideen estuaries, an annual minimum salinity was observed in February 2017 (ANOVA; $p < 0.01$). No differences between sampling occasions were found in the areas affected by green tides in the Clonakilty estuary (ANOVA; $p > 0.05$). In the case of the areas affected by red seaweed tides in the Clonakilty, the values of salinity ranged from 5.55 to 32.50 PSU, with a mean value of 22.52 PSU. In these areas a higher temporal (ANOVA; *F*-value = 14.06; $p < 0.001$) variability was observed, with two peaks of salinity in October 2016 and April 2017 and a minimum value in June 2017. In Killybegs, significant differences were found between sampling occasions (ANOVA; *F*-value = 9.99; $p < 0.001$). The salinity ranged between 1 PSU (outer section during February 2017) and 30.4 PSU (outer section during April 2017), with a mean value of 16.11 PSU. Regarding spatial differences within estuaries, significant differences between sections were observed in the cases of the Argideen and Killybegs estuaries and the area affected by red tides at Clonakilty.

The areas affected by green tides showed the highest concentrations of SS, with maximum levels recorded for Clonakilty (0.27 g L^{-1}) and Argideen (0.45 g L^{-1}) during February 2017. In these areas, the turbidity ranged between 0.05 g L^{-1} and 0.14 g L^{-1}, excluding data from February 2017. In the areas affected by golden and red tides, the turbidity was lower; concentrations of SS ranged between 0.02 g L^{-1} and 0.07 g L^{-1} in the part of the Clonakilty estuary affected by red tides and between 0.01 g L^{-1} and 0.07 g L^{-1} in Killybegs.

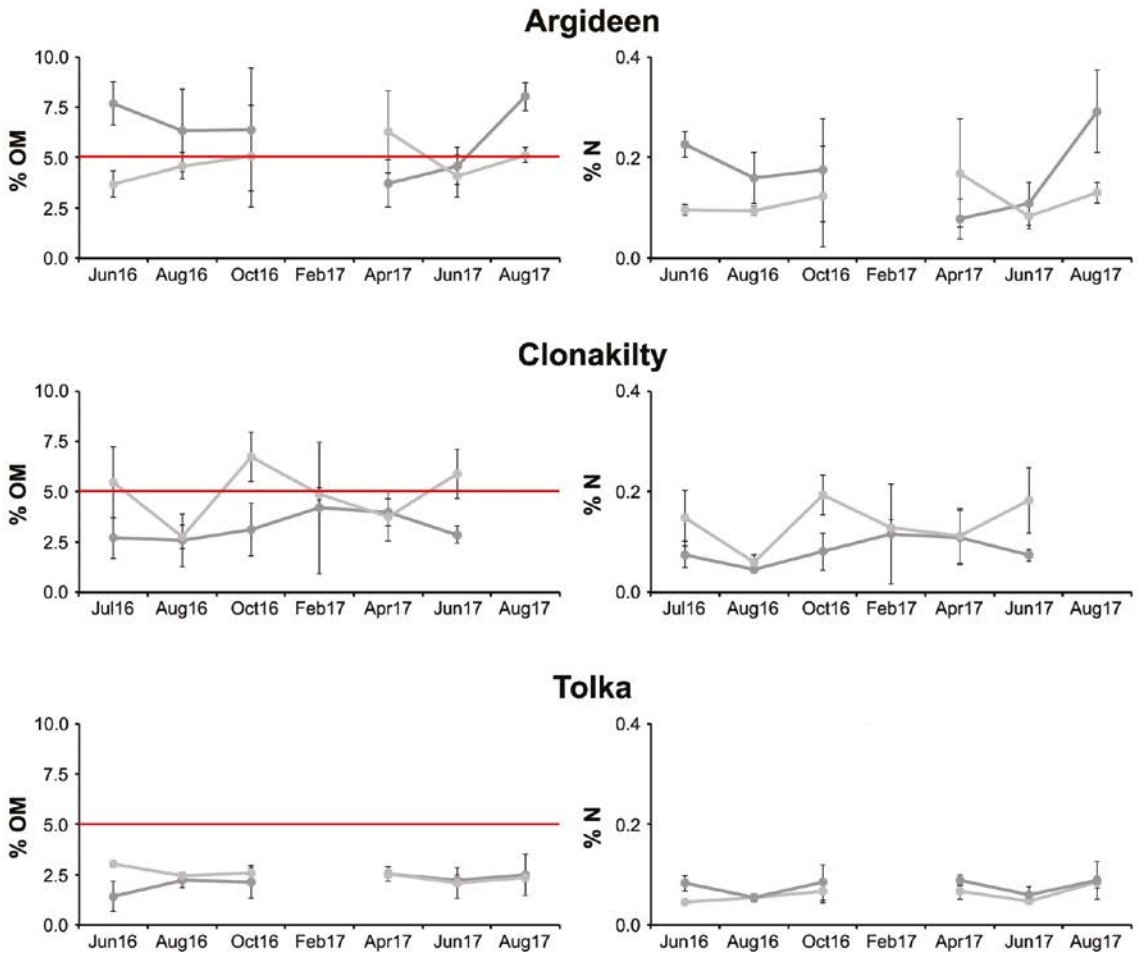

Figure 5.3. The %OM and %N in the inner (dark grey) and outer (light grey) sections of the three estuaries affected by green tides during each sampling occasion. The red horizontal line represents 5% OM content in sediment, which is usually considered the threshold below which seagrass restoration actions are possible (see discussion).

The %OM and %N in sediments (Figure 5.3) from the locations affected by green tides showed a significant correlation ($r = 0.912$; $p < 0.001$; $n = 110$) and yielded similar patterns of spatial and temporal variability. No significant correlations were found between the fresh weight of *Ulva* biomass and the %OM or %N in the sediments for any of the three estuaries investigated ($r < 0.3$; $p > 0.05$). Significant differences were found between estuaries, with the Argideen estuary having the highest values of %OM and %N (%OM 5.46 ± 1.94; %N 0.14 ± 0.08) and the Tolka estuary having the lowest values (%OM 2.35 ± 0.57; %N 0.07 ± 0.02). No significant differences between sampling occasions were found for any of the estuaries. Considering spatial differences within estuaries, the Argideen and Clonakilty estuaries showed significant differences between sections (ANOVA; $p < 0.05$). In the case of the Argideen estuary, the inner section showed higher values than the outer section, with the opposite trend observed at Clonakilty. No differences between sections were found at Tolka.

5.3.4 Distance-based linear model routine

The distLM analysis revealed a significant correlation between the structure of the seaweed tides and four of the nine environmental variables considered (i.e. $N\text{-}NO_3^-$, P, salinity and solar irradiance; Table 5.3) when predictor variables were considered individually. Solar radiation explained the highest percentage of variability (28.221%), followed by salinity (12.640%), nitrate (10.381%) and P (5.917%). Other variables explained < 5% of variability. When variables were added sequentially in order to predict the composition and development of seaweed tides, only solar radiation, nitrate concentration, salinity and ammonia concentration were selected according to the AIC, accounting for 47.896% of the total variation. The inclusion of the other five variables increased the percentage of variability by only 3.058%.

The dbRDA facilitates the identification of correlations between environmental variables and seaweed tide composition (Figure 5.4). Solar radiation was highly

Table 5.3. The distLM results for marginal and sequential tests reflecting the correlation between environmental variables and the composition of seaweed tides

Variable	Pseudo-F	% variability
Marginal tests		
SS	0.72	1.30
$Log[(NH_4^+)+1]$	1.44	2.55
$Log[(NO_3^-)+1]$	6.37**	10.38
$Log[(PO_4^{3-})+1]$	3.46*	5.92
Sal	7.96**	12.64
Rain	2.50	4.35
MaxT	1.59	2.81
MinT	0.73	1.31
Rad	21.62***	28.22
Variable	**Pseudo-F**	**Cumulative % variability**
Sequential tests		
Rad	21.62***	28.22
Log ($[NO_3^-]$+1)	7.02**	36.48
Sal	8.06**	44.86
Log ($[NH_4^+]$+1)	3.03	47.90

MaxT, maximum air temperature the week before the sampling; MinT, minimum air temperature the week before the sampling; Rad, solar radiation; Rain, square root of accumulated rainfall in the week before the sampling; Sal, salinity; SS, square root of SS concentration.

***p* < 0.05; ****p* < 0.01; *****p* < 0.001.**

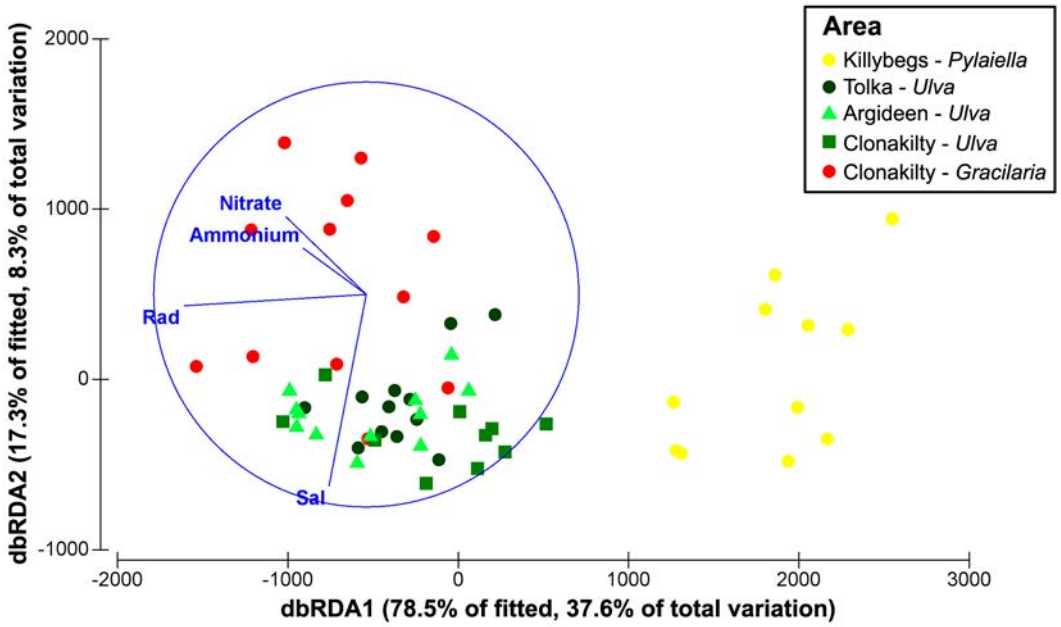

Figure 5.4. The dbRDA showing the correlations between environmental variables and the ordination of the sites based on the composition and abundance of macroalgal blooms. Red dots: blooms dominated by *G. vermiculophylla*; green dots, squares and triangles: blooms dominated by *Ulva* spp.; yellow dots: blooms dominated by *P. littoralis*.

and indirectly correlated with the first dbRDA axis, and salinity with the second dbRDA axis. In the case of nitrate and ammonium, they were equally correlated with both axes, directly with the second and indirectly with the first. Considering the position of the centroid in the dbRDA plot for each studied area affected by seaweed tides, it is possible to identify the most important differences in environmental conditions. The first axis allows Killybegs to be distinguished from other areas affected by seaweed tides. The position of this locality at the far right of the plot indicated that the area affected by the *Pylaiella* bloom received lower radiation than the other areas. This plot also reflected a high dispersion in the second axis for the areas affected by red and golden tides, suggesting that these tides were thriving in a wider salinity range than the green tides, which are located in areas with high and more stable salinities. Finally, the position of the Clonakilty areas affected by red tides in the upper-left corner of the plot indicated that concentrations of nitrates and ammonium were higher in these areas than in areas affected by the other blooms.

5.4 Discussion

Considering the biological index proposed by Scanlan *et al*. (2007), all of the estuaries investigated had a moderate or lower ecological status because of the high biomass observed during the peak bloom and the percentage of the estuary covered by the different seaweed tides. The areas affected by green and red seaweed tides generally showed higher nutrient concentrations in the water column. By contrast, the nutrient concentrations in the Killybegs estuary were low as a consequence of the nutrient uptake by *Pylaiella* bloom occurring in this area. The tissue N content determined in the seaweeds forming macroalgal blooms in the four estuaries studied suggested no N limitation as these values were usually higher than the critical N content described for similar species (Hanisak, 1983; Pedersen and Borum, 1996). A reduction in N loadings, and the enhancement of denitrification activity and nutrient sequestration through different management activities, could limit the development of seaweed tides (e.g. Duarte and Krause-Jensen, 2018). Similar findings were obtained by Ní Longphuirt *et al*. (2015a,b) for

the Argideen estuary based on a modelling approach. The low organic enrichment in sediments from the Tolka estuary and inner part of the Clonakilty estuary (< 5%; Koch, 2001) could allow the development of seagrass meadows. In fact, some stands of *Ruppia* were observed in the Tolka estuary. Considering the relevant role of seagrass meadows for maintenance of ecosystem services and the goods that they provide (Pérez-Lloréns *et al*., 2014), seagrass restoration actions could be considered in further studies.

5.4.1 Status and impact of anthropogenic eutrophication in the studied areas and relevance for management

Although the effects of seaweed tides are very much dependent on local environmental conditions, various studies suggest that an *Ulva* biomass higher than 1000 g fresh weight m^{-2} has significant harmful effects on associated biota (Lowthion *et al*., 1985; Hull, 1987; Wither, 2003). In the context of the European WFD, Scanlan *et al*. (2007) therefore proposed that biomass levels be used as one of the elements for assessing ecological status in transitional water bodies, with 1 kg of wet weight of biomass per square metre during the peak bloom being the threshold between a good and moderate ecological status, even when seaweed cover in the estuary is low. Therefore, considering this 1 kg of wet biomass threshold and the percentage of the estuary covered for the different seaweed tides studied (i.e. green, red and golden), all of the estuaries studied showed a moderate or lower ecological status. The median values of biomass exceeded this threshold five times in the Tolka estuary (June 2016, August 2016, October 2016, June 2017 and August 2017), four times in the red tide from Clonakilty (July 2016, August 2016, June 2017 and August 2017), three times in the green tide from Clonakilty (July 2016, October 2016 and April 2017), six times in the golden tide affecting Killybegs (July 2016, August 2016, October 2016, April 2017, June 2017 and August 2017) and three times in the Argideen estuary (June 2016, August 2016 and August 2017) (see Figure 5.1). This becomes particularly important considering that there are legal implications when a good ecological status is not reached (WFD – 2000/60/EC), necessitating the development of management actions aimed at reducing the total seaweed biomass in order to reach a good ecological status to comply with obligations under the requirements of the WFD.

Regarding dissolved nutrient concentrations, for DIN, the areas of the estuaries affected by red and green tides can be classified as “moderate or lower” at some points of the year, especially in winter, according to Irish standards for coastal and transitional waters, following Statutory Instrument (S.I.) 272 (2009) (see Table 5.2). In the case of P, all estuaries were of a good or higher nutrient class with the exception of the Tolka estuary, where these levels [S.I. 272 (2009)] were exceeded in August 2016 and June 2017. The area of the Killybegs estuary affected by the *Pylaiella* bloom showed the lowest concentrations of nutrients. It is remarkable that this area showed the highest biomass concentrations, especially the inner section (see Figure 5.1). The high biomass concentration found at this locality and the persistence of the bloom throughout the year suggest that the *Pylaiella* biomass might quickly accumulate loadings of nutrients in the estuary, rendering the concentrations of dissolved nutrients both stable and low in the water. In other estuaries, the biofiltration capacity of the bloom might also be important in determining the concentration of dissolved N in the water column during the months when the uptake of nutrients by primary producers is high. The nNB values obtained in the Tolka estuary during the bloom season were of the same order of magnitude as those observed at Killybegs. Although the nNB of *Pylaiella* during the development of the bloom can be eightfold higher than that observed for *Ulva* in the Tolka estuary, uptake rates in *Ulva* could be underestimated because *Ulva* is more susceptible to grazing than *Pylaiella* (Lotze *et al*., 2001). The associated community of invertebrates was more important for *Ulva* (e.g. average values of 2952 *Hydrobia ulvae* individuals m^{-2}; Moya O’Donnell, NUI Galway, 2017, personal observation) or *Gracilaria* than in assemblages dominated by *Pylaiella*, where macrofauna were practically absent (Moya O’Donnell, 2017, personal observation). Furthermore, seaweed biomass and DIN concentration showed a significant and indirect correlation in most of the estuaries studied. This supports the idea that these macroalgal blooms and other estuarine primary producers (e.g. phytoplankton, microbenthos, epiphytes, saltmarsh plants, seagrasses) could accumulate dissolved inorganic nutrients in such quantities that they can reduce the nutrient concentration in surrounding seawaters at medium scales (Viaroli *et al*., 1996; Valiela *et al*., 1997; Xiao *et al*., 2017). This should be considered when management actions are taken.

Macroalgal blooms could act as a buffer, having an important impact on nutrient cycling (Viaroli *et al*., 1996) and reducing the amount of N available in adjacent coastal areas during the period more favourable for the development of toxic microalgal blooms (i.e. late spring to late autumn; Sverdrup, 1953), which could be more harmful to the ecosystem and human activities than seaweed tides (Valiela *et al*., 1997; Smetacek and Zingone, 2013).

The enrichment of organic content in sediments as a consequence of the development of seaweed tides might have an important effect on sediment biogeochemistry and on the associated benthic community, as the decomposition and remineralisation of the OM reduce the oxygen concentration and increase the concentration of nutrients and sulfur compounds in pore water (Rossi, 2006; Corzo *et al*., 2009; Carvalho *et al*., 2011; Robertson and Savage, 2018), acting as a nutrient reservoir fuelling the next bloom event (Corzo *et al*., 2009) and precluding seagrass growth and settlement (Koch, 2001). Seagrass meadows tend to dominate shallow waters under low nutrient inputs, being a key element in the functioning of pristine estuaries (Valiella *et al*., 1997). In nutrient-enriched estuaries, community shifts from seagrass meadows to macroalgal or microalgal tides have been observed in many temperate estuaries globally as a consequence of eutrophication (Valiela *et al*., 1997; Viaroli *et al*., 2008), which has an important impact on biogeochemical cycles (i.e. higher remineralisation and lower nutrient and carbon burial) and other environmental conditions (e.g. increase in water turbidity, anoxic crises, habitat simplification) and could lead to non-linear and positive feedback loops amplifying the eutrophication process and preventing seagrass recolonisation (Viaroli *et al*., 2008). In order to identify suitable conditions for the development of seagrass restoration actions, the percentage of OM content in the sediments is one of the most important parameters considered. Seagrasses can thrive in sediments ranging from 0.5% to 16.5% OM, but mostly occur in those lower than 5% (Koch, 2001), which is considered the threshold to preclude seagrass recolonisation in organically enriched sediments because of eutrophication. Considering the results obtained for sedimentary OM content in the present study (see Figure 5.3), the Tolka estuary and the inner part of the Clonakilty estuary are potential areas where seagrass restoration trials could be developed. In fact, seasonal stands of *Ruppia* cf. *cirrhosa* were observed in the areas sampled at the Tolka estuary during spring and summer. The development of restoration actions may recover and improve ecosystem services, but the use of transplanted seagrasses could also be a tool to monitor the ecological status of transitional water bodies in Ireland. Similarly, biological indices have been used in the Mediterranean using *Posidonia oceanica* (L.) Delile, *Cymodocea nodosa* (Ucria) Ascherson or *Zostera noltei* Hornemann as bioindicators/biomonitors to assess the ecological status of coastal waters (e.g. Romero *et al*., 2007; Oliva *et al*., 2012; García-Marín *et al*., 2013).

No significant correlations were found between organic content in sediments and seaweed biomass across the four estuaries. This supports the notion that the effect of seaweed tides is very much dependent on local environmental conditions (Scanlan *et al*., 2007), such as water motion, sediment granulometry, grazer abundance or eutrophication history, among others (Viaroli *et al*., 2008; Le Moal *et al*., 2019). Despite higher biomass abundances per square metre in the Tolka estuary, the organic content in the sediments was lower than in the Clonakilty and Argideen estuaries. In order to reduce the organic content of sediments and ameliorate the consequences of eutrophication, the removal of seaweed biomass arises as an important action to be considered. *Ulva* and *Gracilaria* species are cultivated for different purposes, such as for the biofiltration of aquaculture wastewaters (Hernandez *et al*., 2002; Abreu *et al*., 2011b), for the production of active biocompounds (Ying-ying *et al*., 2015), biofuels (Trivedi *et al*., 2013), phycocolloids (Orduña-Rojas *et al*., 2008) and animal feed (Wan *et al*., 2017) or for human consumption (Pérez-Lloréns *et al*., 2016). Therefore, the cost of the removal of this biomass could be at least partially compensated by the development of economic activities using the biomass (Charlier *et al*., 2008; Smetacek and Zingone, 2013). Considering the metal concentrations observed by Wan *et al*. (2017) in the *U. rigida* biomass collected at the Tolka, Clonakilty and Argideen estuaries, some of these uses are limited – many of the metals determined in Irish *Ulva* blooms exceed regulatory limits (e.g. for human consumption); however, other uses, such as the production of biofuels or animal feed, are feasible. The removal of this biomass might facilitate the removal of important amounts of N from the

estuary and, in the long or medium term, the reduction of the organic content of the sediment. Previous attempts at the removal and utilisation of this biomass highlighted technical difficulties because of the nature of estuarine environments (Wan *et al*., 2017). For instance, the collection of seaweeds is difficult because of the presence of soft mud, and the collected biomass contains high levels of fine sediments. The collection of seaweed during high tide using boats could overcome or reduce some of these issues. The company Agrival in Brittany has developed a harvest method for *Ulva* blooms: the biomass is collected at high tide using boats and is then washed in a large automated "washing street" at the factory.

The negative correlations found between seaweed biomass and DIN and the high tissue N content found in *Ulva*, *Gracilaria* and *Pylaiella* (>2%, which is higher than the critical N tissue concentration) indicated that there is no N limitation in the estuaries for these seaweeds. Tissue N content was lower than 2% only during July and August 2016 in Clonakilty for *Ulva*, suggesting that the peak bloom was constrained by N limitation during 2016 in this estuary. The reduction in nutrient loadings and the enhancement of bacterial denitrification activity could be helpful to control the development of macroalgal blooms. Various management actions could be taken, such as (1) the establishment of buffer areas (i.e. belts of natural vegetation) between rivers and crops; (2) the recovery of saltmarsh areas and seagrass meadows, which also have an important potential role in fixing N and favouring nutrient burial (Valiela *et al*., 1997; Duarte and Krause-Jensen, 2018); and (3) the development of oyster or seaweed cultures in the estuary, which might improve denitrification activity and the removal of N from the estuary (Humphries *et al*., 2016; Xiao *et al*., 2017).

5.4.2 Factors driving the development and composition of seaweed tides

Important differences in the environmental conditions experienced by the different genera forming macroalgal blooms in Irish estuaries were observed. These preliminary results indicated that *G. vermiculophylla* was located in areas enriched in N and that were less turbid and experienced a wider range of salinity than areas where *Ulva* species were located (see Figure 5.4 and Table 5.3). Similar results were obtained by Sfriso *et al*. (2012) in the lagoons of the north-western Adriatic Sea; the authors identified high nutrient concentrations and moderate salinity as the most characteristic traits of the areas invaded by this species. *G. vermiculophylla* is considered a euryhaline species, that is, able to grow under a wide salinity range (Bolton, 1979), performing best under mesohaline conditions (optimal salinity between 10 and 20 PSU; Rueness, 2005; Weinberger *et al*., 2008) and being more competitive than *Ulva* in areas under variable salinity conditions. Sfriso *et al*. (2012) described the displacement of *U. rigida* by *G. vermiculophylla* in the Sacca di Goro, a Mediterranean lagoon highly influenced by rivers and freshwater inflow. Considering historical data (Task Force, 2010; Wan *et al*., 2017), a similar phenomenon was observed in the inner section of the Clonakilty, where *Gracilaria* displaced *Ulva* (see Figure 4.1a, area 1). Furthermore, *G. vermiculophylla* was also able to settle in areas where *Ulva* was unable to bloom (see Figure 4.1a, area 2).

In the case of *Pylaiella*, an important variability in salinity was observed in the areas of the Killybegs estuary covered by this seaweed. The turbidity was also lower than in the areas affected by green tides and similar to the turbidity in the areas where *Gracilaria* blooms. The most important factor explaining the dominance of this species in comparison with green and red tides was the low solar radiation found at Killybegs. However, Killybegs was the only studied locality affected by this bloom, and no other blooms occurred there. Thus, the observed differences could be a consequence of local environmental conditions rather than a consequence of the effect of solar radiation on the composition of seaweed tides. Further studies should consider more localities and, if possible, select localities containing different blooms (e.g. the Clonakilty estuary, which contains red and green tides) in a geographical range as large as possible. In any case, *Pylaiella* can grow under lower irradiance and temperature conditions than other species, being the first species blooming after ice break-up in areas of the Baltic Sea that freeze during winter (Paalme and Kukk, 2003). This species is also considered to be euryhaline.

Considering the high marine influence of the four studied estuaries, and the previous results obtained by Jeffrey *et al*. (1995) and Ní Longphuirt *et al*. (2015a), P limitation seems to be unlikely. In these

estuaries with short residence times, P might be replenished at each tidal cycle, sustaining macroalgal growth (Ní Longphuirt *et al*., 2015a). The results of this study revealed that the tissue N content is higher than the estimated critical tissue N concentration (i.e. minimum tissue N concentration necessary to support maximum growth) for similar species (Hanisak, 1983; Pedersen and Borum, 1996), indicating no N limitation in the studied areas. In the case of the Tolka estuary, *Ulva* with a tubular morphology showed higher tissue N concentrations and a lower $\delta^{15}N$, supporting the idea that the burial of the basal part of the tubular morphology could allow access to pore water nutrients in the sediment (e.g. Corzo *et al*., 2009; Robertson and Savage, 2018). This could partially explain tubular *Ulva* dominance despite better performance of laminar *Ulva* in laboratory experiments (see Chapter 6), and would support the key role of pore water nutrients (e.g. sediment as a reservoir of nutrients) in the maintenance of Irish macroalgal blooms. Nevertheless, more detailed studies will be necessary to test this hypothesis and its importance for the development of the green tide. The results obtained also reflect a seasonal variation in the isotopic signal and tissue N content, with both *Ulva* morphologies following a similar pattern, which suggests a change in the activities producing N enrichment of the Tolka estuary through the bloom development. In the Argideen and Clonakilty estuaries, the seasonal differences were small, suggesting that the nutrient enrichment of these estuaries is produced by the same activities throughout the year or, alternatively, that all N sources showed similar isotopic signatures. In the case of *Pylaiella*, a much lower $\delta^{15}N$ was observed, suggesting a different N source from that in other estuaries. No significant temporal differences in the isotopic signal were found in this estuary.

6 Understanding the Conditions Controlling the Development of Green Tides in Ireland: Ecophysiological Experiments

6.1 Background

Irish green tides are multispecific and they are dominated by three main species: *U. compressa*, *U. prolifera* and *U. rigida* (see Chapter 2). The composition and dominance pattern of the main species forming green tides change seasonally, with seaweed tides dominated by tubular morphologies (i.e. *U. compressa* and *U. prolifera*) at the beginning of the bloom and co-dominated by tubular (i.e. *U. compressa* and *U. prolifera*) and laminar (i.e. *U. rigida*) morphologies at the end of the bloom (see Chapters 4 and 5). The occurrence of temporal or spatial successions is usually indicative of different ecophysiological traits (Fong *et al*., 1996; Lotze and Schramm, 2000; Nelson *et al*., 2008). A change in environmental conditions could lead to a shift in the composition and structure of the bloom (Lavery *et al*., 1991), which could have important consequences for the balance of biomass (and nutrients) in the estuary, as previously discussed (see Chapters 4 and 5).

Similar to other aquatic primary producers, the biological performance of opportunistic bloom-forming seaweeds is mainly determined by nutrients, light and temperature (Valiela *et al*., 1997). In estuarine and marine environments such as the ones affected by *Ulva* blooms in Ireland, N is considered the main limiting nutrient constraining primary production (Valiela *et al*., 1997; Lyngby *et al*., 1999; Sfriso *et al*., 2003). However, according to the preliminary results obtained during the course of this study, green tides are not limited by N availability, at least in the Tolka and Killybegs estuaries, as the tissue N content remained above the critical concentration (see Chapter 5). Thus, other environmental factors such as temperature and irradiance could play an important role in controlling the development of green tides (Kim *et al*., 2010; Fan *et al*., 2014; Gao *et al*., 2018).

According to the Intergovernmental Panel on Climate Change (IPCC), climate change is predicted to increase the water temperature of Irish coastal waters by between 1.2°C and 3.6°C by the year 2100. This increase will not be homogeneously distributed over the year but will be more important during late spring and early summer, coinciding with the early stages of development of *Ulva* blooms in Ireland (Jeffrey *et al*., 1995). Environmental conditions during the early bloom development stage play a critical role in determining the total biomass accumulated during the peak bloom (Schories and Reise, 1993; Malta and Verschuure, 1997; Valiela *et al*., 1997). According to previous physiological and ecological studies, an increase in temperature during this period will enhance the growth of two of the main Irish green bloom-forming species (i.e. *U. prolifera* and *U. rigida*) (Wang *et al*., 2012; Gao *et al*., 2016). Moreover, an increase in temperature could accelerate the metabolism of microbial benthic communities, favouring remineralisation processes and the release of nutrients from the sediment to the water column (Jeffrey *et al*., 1995), amplifying the eutrophication process. Nutrient release from agricultural land is already a significant source of surface water pollution (Fanning *et al*., 2017) and is predicted to increase with an increasing demand for food. The government's response, envisioned in Food Wise 2025 (https://www.agriculture.gov.ie/foodwise2025/), is for agricultural intensification to satisfy domestic demand and increase exports, possibly at the expense of water quality and greenhouse gas emission targets. It is likely that these issues combined will result in increased eutrophication and hence increased incidences and severity of extraordinary macroalgal blooms, as is supported by Environmental Protection Agency modelling approaches (dynamic combined phytoplankton macroalgae model; Ní Longphuirt *et al*., 2015b; O'Boyle *et al*., 2017) and direct observations (Ní Longphuirt *et al*., 2015a).

Therefore, different experiments were performed to assess the ecophysiological response (i.e. DGR and tissue N content) and the interaction between two of the main species of *Ulva*-forming green tides in Ireland (*U. compressa* and *U. rigida*) in a scenario of global warming and eutrophication.

6.2 Methodology

Specimens of *U. compressa* and *U. rigida* collected from the Argideen estuary in August 2016 were used to perform all of the experiments. The taxonomic identity was confirmed using genetic barcoding (i.e. the *rbc*L marker; see Chapter 2). The seaweeds were collected by hand at low tide, placed in clear plastic bags wrapped in damp laboratory tissue paper and transported to the laboratory in a cool box under conditions of darkness. Both species were then placed in artificial seawater under controlled conditions and left to acclimatise for 1 month prior to the beginning of the experiment. This initial stock material was maintained at an irradiance of approximately 90 µmol photons m^{-2} s^{-1}, a photoperiod of 15:9, a temperature of 15°C and salinity of 32‰. The culture medium, which was modified f/2 diluted 1:2 (Guillard, 1975), was changed twice a week. The *Ulva* were kept in a 15 L aquarium with a water pump to ensure water motion, favouring nutrient uptake and avoiding bacterial growth.

All of the experiments were performed in a constant temperature room in which the ambient temperature was maintained at 20°C. In order to retain the temperature at 13.5°C or 17°C, four thermal baths, which consisted of two 50 L containers connected to an aquarium chiller (TK150, TECO®) through a system of pumps and silicone tubing, were used. Baths were placed under panels of fluorescent lights (Blau Aquaristic Lumina 1080) with adjustable irradiance, which was set at 90 µmol photons m^{-2} s^{-1}. Using electric timers, the photoperiod was adjusted to 16:8, 14:10 or 12:12. The baths were surrounded with dark blinds or covers to avoid external light influences. Irradiance, salinity and water temperature were monitored twice daily. To measure irradiance, a LI-COR LI-1500 Spherical Light Sensor was used. In the case of salinity and water temperature, a portable multiparametric sonde (sensION+, HACH©) was used. No significant deviations from experimental conditions were observed during the monitoring of experimental parameters and factors. Each experimental treatment was replicated four times. A replicate consisted of a 500 ml glass beaker.

6.2.1 Experiment 1

To determine the ecophysiological performance and to assess the biological interaction between two species under different conditions of temperature and photoperiod, a factorial design was followed. Two levels of temperature (13.5°C and 17.0°C), two photoperiods (14:10 and 16:8) and two kinds of culture (monospecific: *U. compressa* or *U. rigida*; multispecific: *U. compressa* and *U. rigida*) were considered. The seaweeds were cultivated for 10 days at an initial density of 0.2 g L^{-1} in half-modified f/2 medium at a salinity of 32‰ and irradiance of 90 µmol photons m^{-2} s^{-1}. The medium was replaced every 2 days to avoid nutrient limitation. All of the treatments were performed simultaneously. The chosen conditions of temperature and photoperiod corresponded to the current mean water temperature and photoperiod observed at the time of the highest relative growth rates for tubular (May–June; 13.5°C and 16:8) and laminar (July–August; 17°C and 14:10) morphologies of *Ulva*, and those predicted by the IPCC for June 2100 (17°C and 16:8). The final combination (13.5°C and 14:10) does not correspond to observed or predicted conditions, but allows assessment of the interaction between these factors and their importance for the biological performance of *Ulva*. Although the number of replicates for each treatment was four, during the development of the experiment, one replicate of the treatment "*U. compressa* monospecific at 14:10 and 17°C" was lost; hence, there were three replicates for this treatment.

6.2.2 Experiment 2

Another experimental design was established in order to assess herbivore susceptibility and the role of grazing in the composition of multispecific *Ulva* assemblages (*U. compressa* and *U. rigida*) under different conditions of photoperiod (12:12 and 16:8) and temperature (13.5°C and 17°C). Two grazing scenarios were assessed: no grazing and moderate grazing (10 adult individuals of *Gammarus* species per gram of *Ulva*; Andersson *et al*., 2009). Multispecific cultures of 0.05 g of *U. rigida* and 0.05 g of *U. compressa* were incubated together for 1 week in 500 mL of half-modified f/2 media at a salinity of 32‰ and irradiance of 90 µmol photons m^{-2} s^{-1}. To reduce the stress to grazers, the medium was not replaced but was refreshed every 3 days, adding nutrients. In this experiment, a layer of bacteria at the surface of the beakers was observed in replicates after day 4 at 17°C.

6.2.3 Ecophysiological response

The relative DGR and tissue N content were determined for each replicate. The DGR was calculated assuming an exponential growth (equation 6.1):

$$\text{DGR}\ (\%\,\text{day}^{-1}) = 100\ln(\text{FW}_f\text{FW}_0^{-1})\,t^{-1} \quad (6.1)$$

where FW_f is the fresh weight of seaweed at the end of the experiment, FW_0 is the fresh weight of seaweed at the beginning of the experiment and t is the number of days (10 in this case). The initial and final fresh weights were measured using a precision weight scale accurate to 0.0001 g. Before weighing, the specimens were dried with filter paper until wet spots disappeared.

In order to assess the tissue N content before and after the experiment, a small amount of *Ulva* (approx. 0.1 g) was freeze-dried at –52°C (FreeZone 12, Labconco) and ground in Eppendorf tubes using a tissue lyser (TissueLyser, Qiagen) and tungsten balls. These ground samples were stored in a desiccator with silica gel and sent to Servizos de Apoio á Investigación at the University of A Coruña (Spain), where tissue N content was determined using a Flash combustion EA1108 elemental analyser (Carlo Erba Instruments).

6.2.4 Data analyses

In order to assess the effects of the different factors and their interactions on the DGR and tissue N content, factorial ANOVA was performed. Assumptions of normality and homoscedasticity were assessed using the Shapiro–Wilk's and Levene's tests, respectively. A post hoc Tukey test was applied to compare levels of treatment factors when main factors had a significant effect. In the case of significant interactions or when more than one factor showed a significant effect, the Tukey test was used to compare the levels of each factor within each level of the other factor and vice versa. Tissue N content in *U. rigida* (experiment 1) and DGR in *U. compressa* (experiment 2) did not meet homoscedasticity assumptions, even after data transformation. For this reason, a PERMANOVA was used instead. The PERMANOVAs were based on Euclidean distances.

To assess the impact of grazing, temperature and photoperiod on the composition of multispecific cultures, a three-way PERMANOVA was performed. This analysis was based on Euclidean distances considering the DGR of the two species (i.e. *U. compressa* and *U. rigida*). The three factors considered were temperature (fixed; two levels: 13.5°C and 17°C), photoperiod (fixed; two levels: 12:12 and 16:8) and grazing (fixed; two levels: moderate and no grazing). In the case of significant effects for a factor, a PERMDISP (Anderson *et al*., 2008) and a pairwise PERMANOVA test (Anderson *et al*., 2008) were performed to interpret patterns.

Statistical analyses were performed using R software version 3.2.1 (R Development Core Team, 2017) and PERMANOVA+ add-on PRIMER 6 (Plymouth Routines in Multivariate Ecological Research) software (Anderson *et al*., 2008). In all statistical analyses, significance was set at a probability of $p < 0.05$ and, when necessary, analyses were based on 9999 permutations.

6.3 Results

6.3.1 Experiment 1

The ANOVA results revealed a significant effect of temperature and biotic interaction on the DGR of *U. rigida*. No other factors or interactions between factors showed a significant effect on this species (Table 6.1). *U. rigida* had a higher DGR at 17°C than at 13.5°C. Furthermore, the growth rate improved in the presence of *U. compressa* independently of the experimental conditions assayed (Figure 6.1). In the case of *U. compressa*, photoperiod was the only factor that had a significant effect on growth. It is remarkable that the presence of *U. rigida* did not have any significant effect on the DGR of *U. compressa*.

Regarding tissue N content in *U. rigida* and *U. compressa*, significant differences were found only between temperatures (Table 6.2), with both showing a higher tissue N content at 13.5°C than at 17°C. In the case of *U. rigida*, the tissue N content was 4.37 ± 0.09% at 17°C and 4.52 ± 0.2% at 13.5°C. For *U. compressa*, the tissue N content was 4.63 ± 0.28% at 17°C and 4.83 ± 0.22% at 13.5°C. It should be noted that the nNB accumulated at the end of the experiment for monospecific cultures was 5.30 ± 1.31 mg N for *U. compressa* and 10.26 ± 1.41 mg N for *U. rigida*.

Table 6.1. Results of the three-way ANOVA testing the effects of the factors "biotic interaction", "photoperiod" and "temperature" on the DGR of *U. rigida* and *U. prolifera*

Factor	*U. rigida*			*U. compressa*		
	df	MS	*F*-value	df	MS	*F*-value
Biotic interaction (BI)	1	21.735	21.64***	1	0.001	0
Photoperiod (Ph)	1	0.013	0.01	1	6.977	4.79*
Temperature (t^a)	1	9.837	9.80**	1	0.742	0.51
BI x Ph	1	1.640	1.63	1	0.795	0.55
BI x t^a	1	0.091	0.09	1	0.004	0
Ph x t^a	1	0.826	0.82	1	2.722	1.87
BI x Ph x t^a	1	0.323	0.32	1	0.035	0.02
Residual	23	1.004		22	1.455	

df, degrees of freedom; MS, mean squares.
***p*<0.05; ****p*<0.01; *****p*<0.001.**

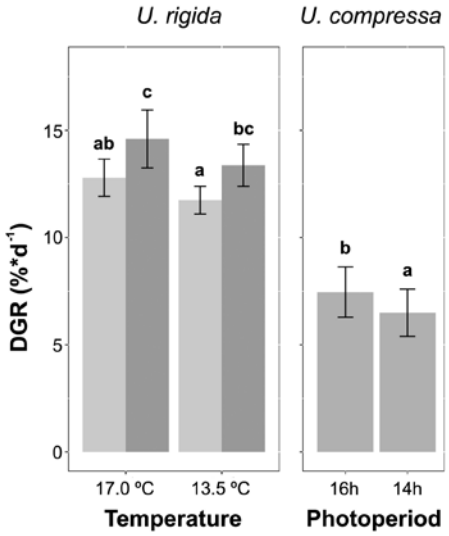

Figure 6.1. Mean DGRs for *U. rigida* and *U. compressa* for the factors yielding a significant effect in the ANOVA. In the case of *U. rigida*, light grey and dark grey bars represent the absence or presence of *U. compressa*, respectively. Lower and upper error bars represent ± standard deviation; letters over the bars represent significant differences.

6.3.2 Experiment 2

When the biological performance of the multispecific assemblage was assessed, grazing was the only factor showing a significant effect on the structure of the assemblage (PERMANOVA; Ps-F = 13.12; $p > 0.001$). The PERMDISP results yielded significant differences (PERMDISP; $p < 0.001$) in the dispersion between no grazing (3.01 ± 0.42) and moderate grazing (8.97 ± 1.52) conditions. When species were assessed separately, the results for *U. compressa* revealed a significant effect of grazing (PERMANOVA; Ps-F = 4.37; $p < 0.05$) and for the interaction between the three factors assessed (PERMANOVA; Ps-F = 5.34; $p < 0.05$). In the case of *U. rigida*, grazing was the only factor showing a significant effect on the DGR (ANOVA; *F*-value = 21.14; $p < 0.001$). In both cases, the DGR was greater in the absence of grazers. In the absence of grazers, *U. rigida* (12.92 ± 2.69% d^{-1}) grew faster than *U. compressa* (7.57 ± 2.30% d^{-1}), but in the presence of grazers no differences were observed between *U. rigida* (3.31 ± 7.57% d^{-1}) and *U. compressa* (3.38 ± 8.11% d^{-1}). In the absence of grazers, temperature was the only factor that had a significant effect on the growth of *U. rigida* (ANOVA; *F*-value = 26.07; $p < 0.001$), which agreed with

Table 6.2. Results of the three-way ANOVA testing the effects of the factors "biotic interaction", "photoperiod" and "temperature" on the tissue N content of *U. rigida* and *U. prolifera*

Factor	*U. rigida*			*U. compressa*		
	df	MS	*F*-value	df	MS	*F*-value
Biotic interaction (BI)	1	0.072	2.90	1	0.045	0.74
Photoperiod (Ph)	1	0.002	0.09	1	0.213	3.50
Temperature (t^a)	1	0.188	7.61*	1	0.275	4.51*
BI x Ph	1	0	0	1	0.005	0.09
BI x t^a	1	0.052	2.09	1	0.029	0.48
Ph x t^a	1	0.005	0.22	1	0.228	3.74
BI x Ph x t^a	1	0.008	0.34	1	0.008	0.13
Residual	23	0.025		22	0.061	

df, degrees of freedom; MS, mean squares.
***$p < 0.05$; **$p < 0.01$; ***$p < 0.001$.**

experiment 1. However, in the case of *U. compressa*, photoperiod (ANOVA; F-value = 9.02; $p < 0.05$) and the interaction of photoperiod and temperature (ANOVA; F-value = 19.06; $p < 0.001$) had a significant effect on the growth of this species. It is remarkable that this significant interaction between temperature and photoperiod on the growth of *U. compressa* was not observed in experiment 1. In high-temperature scenarios (17°C), the growth of *U. compressa* seemed to be promoted under short photoperiod (12:12) and reduced under long photoperiod (16:8) conditions. Some caution is needed in the interpretation of these results as bacterial growth was observed in treatments at 17°C.

6.4 Discussion

This experiment indicated that, during Irish summer conditions, temperature might control the development of *U. rigida*, whereas photoperiod played a more important role in triggering the growth of *U. compressa*. Furthermore, the potential growth of *U. rigida* was more constrained by grazing than the potential growth of *U. compressa* at moderate grazer densities (Andersson *et al*., 2009). This partially explains the seasonal patterns found in the field, with the most important increase in biomass of tubular morphologies (i.e. *U. compressa* and *U. prolifera*) occurring during the months of longer photoperiods, and the most important accumulation of laminar *Ulva* (i.e. *U. rigida*) occurring when the water temperature is raised in midsummer (see Chapters 4 and 5). Nevertheless, important differences in growth were observed between species, with *U. rigida* (12.27 ± 0.91% – experiment 1) having a higher DGR than *U. compressa* (6.75 ± 1.58% – experiment 1). This contrasts with the biomass dominance of tubular *Ulva* observed in the field. The higher transport rates of biomass (removal from the bay to the open sea) expected for the free-living laminar *Ulva* (see Chapter 4), higher grazer susceptibility and generalised sporulation events of *U. rigida* may account for this. Comparing the results observed in this study with those of similar studies assessing the growth of *U. compressa* under similar experimental conditions, this study yielded much lower values for DGR than those observed by Wang *et al*. (2018; between 20% d^{-1} and 25% d^{-1}) using seaweeds from Asia, but similar values to those obtained by Taylor *et al*. (2001; 5–8% d^{-1}) for specimens from Britain and Lotze and Schramm (2000; 9–11% d^{-1}) for seaweeds from the Baltic Sea. This could be indicative of important differences in biological performance between European and Asian strains of *U. compressa* and have potentially important implications, as the arrival of Asiatic strains could favour the development of green tides.

Assuming the scenario of global warming proposed by the IPCC for early summer (i.e. June) in the year 2100 and the expected increase in nutrient loading in Irish estuaries (O'Boyle *et al*., 2017), the results support the idea of a change in the structure and seasonality of green tides. This agrees with the results of Gao *et al*. (2016), who predicted an increase in green tides dominated by *U. rigida* in a context of global warming and eutrophication based on laboratory studies. In this case, we expect an earlier development in summer

of *U. rigida* blooms, which might increase the total biomass of *Ulva* per square metre at this time of the year because of the simultaneous occurrence of the peak bloom of tubular and laminar morphologies. Moreover, if the duration of the *U. rigida* blooming season is also extended, this could enhance the exportation of *Ulva* biomass. An increased biomass export of *Ulva* could have a positive local impact on estuaries, having a similar effect to the removal of seaweed biomass (see Chapter 5 discussion).

Finally, the biotic interactions between these two species in the context of no nutrient limitations were neutral (i.e. *U. compressa*) or positive (i.e. *U. rigida*). The growth of *U. rigida* seems to be enhanced by the presence of *U. compressa* (see Figure 6.1). Fong *et al*. (1996), in a scenario of nutrient deprivation, found that *U. expansa* facilitated the growth of *U. intestinalis*, which was attributed to the release of dissolved organic N (DON) when *U. expansa* does not have enough tissue N for growth. Although the release of DON cannot be ruled out as the mechanism explaining this facilitation, it was not due to nutrient limitation as the tissue N in both species was relatively high (>4%). As other variables (e.g. the presence of allelopathic compounds, DON and dissolved organic carbon) were not measured during the development of the experiment, the mechanisms regulating this interaction remain unexplained. It would be interesting to assess the interactions between these species in a context of nutrient limitation, as non-linear responses could occur, with possible implications for the development of management strategies.

7 Recommendations

Nitrogen limitation is the main constraint for primary producers in temperate estuarine waters with a strong marine influence. When estuarine waters become N over-enriched as a result of human activities (e.g. agricultural run-off; the presence of urban and industrial sewage), the growth of some taxa is no longer constrained by N limitation and they can bloom, producing important accumulations of seaweed biomasses. The size and persistence of these blooms is then constrained by other biotic and abiotic factors. Overall, the results obtained in this study revealed that the development of seaweed tides in Ireland is not limited by N at any time of the year. Moreover, considering the strong marine influence in the estuaries studied, it is unlikely that P is limiting the growth of bloom-forming species, as previously demonstrated by Ní Longphuirt (2015a) in the Argideen estuary and by Jeffrey *et al*. (1995) in the Tolka estuary. Thus, the potential development of macroalgal blooms in Ireland is currently constrained by a combination of other abiotic factors (e.g. hydrographical, geomorphological, meteorological and climatological conditions) and biotic factors (e.g. grazing, inter- and intraspecific competition, or ecophysiological performance of bloom-forming species). Considering that there are nutrients available, the arrival of new alien species capable of forming a bloom, or changes in environmental conditions (e.g. global warming, acidification), could increase the size and duration of the blooms. Management actions to control the spreading, and especially the arrival, of alien seaweeds are recommended. Moreover, the development of models to predict the effects of global changes on Irish estuaries, considering the presence of multiple species with different ecophysiological requirements, is also recommended in order to identify the most suitable management actions. To reduce the size and development of macroalgal blooms, the restoration of N-limited conditions, which were present before nutrient over-enrichment of Irish estuaries, is the preferred choice. Although it would be possible to constrain bloom development through hydrological modifications (e.g. increased river flushing, reduction in water residence times, enhancing tidal currents, enhancing turbidity) or geoengineering actions (e.g. injection of aluminium in sediment) (Duarte and Krause-Jensen, 2018), the ecological consequences in the estuary and surrounding coastal waters are difficult to predict, and in some cases could be even more harmful for the environment and human activities than seaweed tides.

The nutrient stock available in Irish estuaries fuelling macroalgal blooms arises from a combination of current loadings and reservoirs (e.g. estuarine sediments, underground waters), with the specific contribution of each source being difficult to estimate. As the contribution of N reservoirs to the development of macroalgal tides could be important, it would not be surprising if the effects of management actions were not immediate, making it more difficult to assess the suitability of management actions. Therefore, to control the size of green tides it would be necessary to reduce the stock of available nutrients (i.e. current loads and reservoirs), especially N, and ameliorate the consequences of nutrient enrichment. In order to achieve this aim, different actions could be taken:

- Reduce current loadings – the development and identification of best agriculture practices, the creation of buffer areas (e.g. belts of natural vegetation between crops and rivers) and an increase in the effectiveness of wastewater treatment facilities should be prioritised among the main actions. These actions will affect current loads, but their impact on estuarine reservoirs will be limited.
- Active removal of nutrients from estuaries – the removal of biomass from the ecosystem during the peak of biomass, harvesting seaweeds or developing seaweed cultures might reduce the amount of nutrients and OM in estuarine sediments. The identification of biotechnological applications for seaweed biomass and the development of valuable products taking advantage of the nutrient enrichment could make this action feasible and inexpensive.
- Passive removal of nutrients from estuaries – the restoration of saltmarshes, seagrass meadows or riverine vegetation may favour nutrient and carbon

sequestration, also enhancing the denitrification processes. The development of oyster cultures or the restoration of oyster beds has also been proven to increase denitrification rates (Duarte and Krause-Jensen, 2018).

Although the development of productive activities taking advantage of eutrophication (e.g. seaweed and oyster culture, seaweed harvesting) could be profitable and may help to ameliorate the negative effects of eutrophication, the final aim of management strategies should be the restoration of the estuary to pre-impact conditions, restoring biodiversity and ecological functions and making the ecosystem self-sustainable (Moss, 2007). In order to achieve this aim, it will be necessary to:

- Define baseline conditions based on historical data and paleo-ecological studies. The study of herbarium material and historical documents may be useful to identify the dominant vegetation in pre-impact conditions.
- Identify effective management actions and strategies. The development of management actions (e.g. best agriculture practices, new wastewater treatments or harvesting of seaweeds) in representative model estuaries, which are fully monitored, would provide useful information about management actions that could be applied in similar cases.
- Develop and implement faster and inexpensive methods for the monitoring of green tides and nutrients that allow assessment of the suitability of management strategies and produce valuable information for model simulation of bloom predictions. The creation of a network of volunteers in combination with the use of Earth observation technologies could help to reduce the cost and increase monitoring frequency.
- Test the feasibility and convenience of restoration actions. Considering that seagrasses or saltmarsh plants play a key role in nutrient cycling from estuarine environments and enhance nutrient sequestration in sediments, as well as enhancing denitrification activity, the application of indices to assess the ecological status of Irish estuaries based on the physiological status of seagrasses or saltmarsh plants will provide information about ecological status, and also about the feasibility of restoration actions.

References

Abreu, M.H., Pereira, R., Buschmann, A.H., Sousa-pinto, I. and Yarish, C., 2011a. Nitrogen uptake responses of *Gracilaria vermiculophylla* (Ohmi) Papenfuss under combined and single addition of nitrate and ammonium. J*ournal of Experimental Marine Biology and Ecology* 407: 190–199.

Abreu, M.H., Pereira, R., Yarish, C., Buschmann, A.H. and Sousa-pinto, I., 2011b. IMTA with *Gracilaria vermiculophylla*: productivity and nutrient removal performance of the seaweed in a land-based pilot scale system. *Aquaculture* 312: 77–87.

Aldridge, J.N. and Trimmer, M., 2009. Modelling the distribution and growth of “problem” green seaweed in the Medway estuary, UK. *Hydrobiologia* 629: 107–122.

Anderson, M.J., Gorley, R.N. and Clarke, K.R., 2008. PERMANOVA+ for PRIMER: *Guide to Software and Statistical Methods*. PRIMER-E, Plymouth.

Andersson, S., Persson, M., Moksnes, P.O. and Baden, S., 2009. The role of the amphipod *Gammarus locusta* as a grazer on macroalgae in Swedish seagrass meadows. *Marine Biology* 156: 969–981.

Andrew N.L. and Mapstone, B.D., 1987. Sampling and the description of spatial pattern in marine ecology. *Oceanography and Marine Biology* 25: 39–90.

Atkinson, P.M. and Lewis, P., 2000. Geostatistical classification for remote sensing: an introduction. *Computers and Geosciences* 26: 361–371.

Baamonde-López, S., Baspino-Fernández, I., Barreiro-Lozano, R. and Cremades-Ugarte, J., 2007. Is the cryptic alien seaweed *Ulva pertusa* (Ulvales, Chlorophyta) widely distributed along European Atlantic coasts? *Botanica Marina* 50: 267–274.

Bárbara, I., Díaz-Tapia, P., Peteiro, C., Berecibar, E., Peña, V., Sánchez, N., Tavares, A.M., Santos, R., Secilla, A., Riera Fernández, P., Bermejo, R. and García, V., 2012. Nuevas citas y aportaciones corológicas para la flora bentónica marina del atlántico de la península ibérica. *Acta Botanica Malacitana* 37: 5–32.

Benedetti-Cecchi, L., Rindi, F., Bertocci, I., Bulleri, F. and Cinelli, F., 2001. Spatial variation in development of epibenthic assemblages in a coastal lagoon. *Estuarine, Coastal and Shelf Science* 52: 659–668.

Bermejo, R., Ramírez-Romero, E., Vergara, J.J. and Hernández, I., 2015. Spatial patterns of macrophyte composition and landscape along the rocky shores of northern coasts of the Alboran Sea. *Estuarine, Coastal and Shelf Science* 155: 17–28.

Bermejo, R., Heesch, S., MacMonagail, M., O’Donnell, M., Daly, E., Wilkes, R.J. and Morrison, L., 2019. Spatial and temporal variability of biomass and composition of green tides in Ireland. *Harmful Algae* 81: 94–105.

Billard, E., Daguin, C., Pearson, G.A., Serrão, E.A., Engel, C. and Valero, M., 2005. Genetic isolation between three closely related taxa: *Fucus vesiculosus*, *F. spiralis* and *F. ceranoides* (Phaeophyceae). *Journal of Phycology* 41: 900–905.

Bolton, J.J., 1979. Estuarine adaptation in populations of *Pilayella littoralis* (L.) Kjellm. (Phaeophyta, Ectocarpales). *Estuarine and Coastal Marine Science* 9: 273–280.

Bonsdorff, E., 1992. Drifting algae and zoobenthos – effects on settling and community structure. *Netherlands Journal of Sea Research* 62: 57–62.

Burkhardt, E. and Peters, A.F., 1998. Molecular evidence from nrDNA its sequences that *Laminariocolax* (Phaeophyceae, Ectocarpales *sensu lato*) is a worldwide clade of closely related kelp endophytes. *Journal of Phycology* 34: 682–691.

Carvalho, S., Pereira, P., Pereira, F., de Pablo, H., Vale, C. and Gaspar, M.B., 2011. Factors structuring temporal and spatial dynamics of macrobenthic communities in a eutrophic coastal lagoon (Óbidos lagoon, Portugal). *Marine Environmental Research* 71: 97–110.

Charlier, R.H., Morand, P. and Finkl, C.W., 2008. How Brittany and Florida coasts cope with green tides. *International Journal of Environmental Studies* 65: 191–208.

Choi, H.G., Kim, Y.S., Kim, J.H., Lee, S.J., Park, E.J., Ryu, J. and Nam, K.W., 2006. Effects of temperature and salinity on the growth of *Gracilaria verrucosa* and *G. chorda*, with the potential for mariculture in Korea. *Journal of Applied Phycology* 18: 269–277.

Clabby, K.J., Bradley, C., Craig, M., Daly, D., Lucey, J., McGarrigle, M., O'Boyle, S., Tierney, D. and Bowman, J., 2008. *Water Quality in Ireland 2004–2006*. Available online: https://www.epa.ie/pubs/reports/water/waterqua/waterrep/ (accessed 18 June 2019).

Clarke, K.R. and Gorley, R.N., 2006. *PRIMER v6: User Manual/Tutorial*. PRIMER-E, Plymouth.

Corzo, A., Van Bergeijk, S.A. and García-Robledo, E., 2009. Effects of green macroalgal blooms on intertidal sediments: net metabolism and carbon and nitrogen contents. *Marine Ecology Progress Series* 380: 81–93.

Crips, D.J., 1971. Energy flow measurements. In Holme, N.A. and Mclntyre, A.D. (eds), *Methods for the Study of Marine Benthos*. IBP Handbook 16. Blackwell Scientific Publishing, Oxford. pp. 197–279.

Defries, R.S., and Townshend, J.R., 1994. NDVI-derived land cover classifications at a global scale. *International Journal of Remote Sensing* 15: 3567–3586.

Dekker, A., Brando, V., Anstee, J., Fyfe, S., Malthus, T. and Karpouzli, E., 2006. Remote sensing of seagrass ecosystems: use of spaceborne and airborne sensors. In *Seagrasses: Biology, Ecology and Conservation*, A.W.D. Larkum *et al*. (eds.). Springer, Dordrecht. pp. 347–359.

Duarte, C.M. and Krause-Jensen, D., 2018. Intervention options to accelerate ecosystem recovery from coastal eutrophication. *Frontiers in Marine Science* 5: 1–8.

Fan, X., Xu, D., Wang, Y., Zhang, X., Cao, S., Mou, S. and Ye, N., 2014. The effect of nutrient concentrations, nutrient ratios and temperature on photosynthesis and nutrient uptake by *Ulva prolifera*: implications for the explosion in green tides. *Journal of Applied Phycology* 26: 537–544.

Fanning, A., Craig, M., Webster, P., Bradley, C., Tierney, D., Wilkes, R. and Mannix, A., 2017. *Water Quality in Ireland 2010–2015*. Available online: https://www.epa.ie/pubs/reports/water/waterqua/waterqualityinireland2010-2015.html (accessed 18 June 2019).

Fong, P., Boyer, K.E., Desmond, J.S. and Zelder, J.B., 1996. Salinity stress, nitrogen competition and facilitation: what controls seasonal succession of 2 opportunistic green macroalgae? *Journal of Experimental Marine Biology and Ecology* 206: 203–221.

Foody, G.M., 1992. Derivation and applications of probabalistic measures of class membership from maximum-likelihood classification. *Photogrammetric Engineering and Remote Sensing* 58: 1335–1341.

Gandhi, G.M., Parthiban, S., Thummalu, N. and Christy, A., 2015. Ndvi: vegetation change detection using remote sensing and GIS – a case study of Vellore District. *Procedia Computer Science* 57: 1199–1210.

Gao, G., Clare, A.S., Rose, C. and Caldwell, G.S., 2016. Eutrophication and warming-driven green tides (*Ulva rigida*) are predicted to increase under future climate change scenarios. *Marine Pollution Bulletin* 114: 439–447.

Gao, G., Beardall, J., Bao, M., Wang, C., Ren, W. and Xu, J., 2018. Ocean acidification and nutrient limitation synergistically reduce growth and photosynthetic performances of a green tide alga *Ulva linza. Biogeosciences Discussions* 86: 1–43.

Garcia, R.A., Fearns, P., Keesing, J.K. and Liu, D., 2013. Quantification of floating macroalgae blooms using the scaled algae index. *Journal of Geophysical Research: Oceans* 118: 26–42.

García-Marín, P., Cabaço, S., Hernández, I., Vergara, J.J., Silva, J. and Santos, R., 2013. Multi-metric index based on the seagrass *Zostera noltii* (ZoNI) for ecological quality assessment of coastal and estuarine systems in SW Iberian Peninsula. *Marine Pollution Bulletin* 68: 46–54.

Geoffroy, A., Mauger, S., De Jode, A., Le Gall, L. and Destombe, C., 2015. Molecular evidence for the coexistence of two sibling species in *Pylaiella littoralis* (Ectocarpales, Phaeophyceae) along the Brittany coast. *Journal of Phycology* 51: 480–489.

Gonçalves, J.A. and Henriques, R., 2015. UAV photogrammetry for topographic monitoring of coastal areas. *ISPRS Journal of Photogrammetry and Remote Sensing* 104: 101–111.

Guidone, M. and Thornber, C.S., 2013. Examination of *Ulva* bloom species richness and relative abundance reveals two cryptically co-occurring bloom species in Narragansett Bay, Rhode Island. *Harmful Algae* 24: 1–9.

Guidone, M., Thornber, C., Wysor, B. and O'Kelly, C.J., 2013. Molecular and morphological diversity of Narragansett Bay (RI, USA) *Ulva* (Ulvales, Chlorophyta) populations. *Journal of Phycology* 49: 979–995.

Guillard, R., 1975. Culture of phytoplankton for feeding marine invertebrates. In Chanley, M.H. and Smith, W.L. (eds), *Culture of Marine Invertebrate Animals*. Plenum Press, New York. Pp. 26–60.

Guillemin, M.-L., Akki, S.A., Givernaud, T., Mouradi, A., Valero, M. and Destombe, C., 2008. Molecular characterisation and development of rapid molecular methods to identify species of Gracilariaceae from the Atlantic coast of Morocco. *Aquatic Botany* 89: 324–330.

Guiry, M.D. & Guiry, G.M. 2019. *AlgaeBase*. World-wide electronic publication, National University of Ireland, Galway. http://www.algaebase.org; searched on 30 January 2018.

Hanisak, M.D., 1983. The nitrogen relationships of marine macroalgae. In Carpenter, E.J. and Capone, D.G., (eds), N*itrogen in the Marine Environment*. Academic Press, New York. pp. 699–730.

Hansen, M.C., Sohlberg, R., Defries, R.S. and Townshend, J.R.G., 2000. Global land cover classification at 1 km spatial resolution using a classification tree approach. *International Journal of Remote Sensing* 21: 1331–1364.

Hayden, H.S., Blomster, J., Maggs, C.A., Silva, P.C., Stanhope, M.J. and Waaland, J.R., 2003. Linnaeus was right all along: *Ulva* and *Enteromorpha* are not distinct genera. *European Journal of Phycology* 38: 277–294.

Heesch, S., Broom, J.E.S., Neill, K.F., Farr, T.J., Dalen, J.L. and Nelson, W.A., 2009. *Ulva*, *Umbraulva* and *Gemina*: genetic survey of New Zealand taxa reveals diversity and introduced species. *European Journal of Phycology* 44: 143–154.

Heesch, S., Pažoutová, M., Moniz, M.B.J. and Rindi, F., 2016. Prasiolales (Trebouxiophyceae, Chlorophyta) of the Svalbard Archipelago: diversity, biogeography and description of the new genera *Prasionella* and *Prasionema*. *European Journal of Phycology* 51: 171–187.

Hering, D., Borja, A., Carstensen, J., Carvalho, L., Elliott, M., Feld, C.K., Heiskanen, A.-S., Johnson, R.K., Moe, J., Pont, D., Solheim, A.L. and Van de Bund, W., 2010. The European Water Framework Directive at the age of 10: a critical review of the achievements with recommendations for the future. *Science of the Total Environment* 408: 4007–4019.

Hernandez, I., Peralta, G., Perez-Llorens, J.L., Vergara, J.J. and Niell, F.X., 1997. Biomass and growth dynamics of *Ulva* species in Palmones River estuary. *Journal of Phycology* 33: 764–772.

Hernandez, I., Martinez-Aragon, J.F., Tovar, A., Terez-Llorens, J.L. and Vergara, J.J., 2002. Biofiltering efficiency in removal of dissolved nutrients by the three species of estuarine macroalgae with sea bass (*Dicentrarchus labrax*) waste waters. 2. Ammonium. *Journal of Applied Phycology* 14: 375–384.

Hu, C., 2009. A novel ocean color index to detect floating algae in the global oceans. *Remote Sensing of Environment* 113: 2118–2129.

Hu, C., Li, D., Chen, C., Ge, J., Muller-Karger, F.E., Liu, J., Yu, F. and He, M.X., 2010. On the recurrent *Ulva prolifera* blooms in the Yellow Sea and East China Sea. *Journal of Geophysical Research*: *Oceans* 115: 1–8.

Hull, S.C., 1987. Macroalgal mats and species abundance: a field experiment. *Estuarine Coastal Shelf Sciences* 25: 519–532.

Humphries, A.T., Ayvazian, S.G., Carey, J.C., Hancock, B.T., Grabbert, S., Cobb, D., Strobel, C.J. and Fulweiler, R.W., 2016. Directly measured denitrification reveals oyster aquaculture and restored oyster reefs remove nitrogen at comparable high rates. *Frontiers in Marine Science* 3: 74.

Ismail, M.H. and Jusoff, K., 2008. Satellite data classification accuracy assessment based from reference dataset. *World Academy of Science, Engineering and Technology* 15: 527–533.

Jeffrey, D.W., Brennan, M.T., Jennings, E., Madden, B. and Wilson, J.G., 1995. Nutrient sources for in-shore nuisance macroalgae: the Dublin bay case. *Ophelia* 42: 147–161.

Jensen, A., Clemens, S.R., McKee, M. and Zaman, B., 2014. Retrieval of spectral reflectance of high resolution multispectral imagery acquired with an autonomous unmanned aerial vehicle. *Photogrammetric Engineering & Remote Sensing* 80: 1139–1150.

Jorgensen, P., Ibarra-Obando, S.E. and Carriquiry, J.D., 2010. Management of natural *Ulva* spp. blooms in San Quintin Bay, Baja California: is it justified? *Journal of Applied Phycology* 22: 549–558.

Kalita, T.L. and Tytlianov, E.A., 2003. Effect of temperature and illumination on growth and reproduction of the green alga *Ulva fenestrata. Russian Journal of Marine Biology* 29: 316–322.

Kim, J.-H., Kang, E.J., Park, M.G., Lee, B.-G. and Kim, K.Y., 2010. Effects of temperature and irradiance on photosynthesis and growth of a green-tide-forming species (*Ulva linza*) in the Yellow Sea. *Journal of Applied Phycology* 23: 421–432.

Koch, E.W., 2001. Beyond light: physical, geological, and geochemical parameters as possible submersed aquatic vegetation habitat requirements. *Estuaries* 24: 1–17.

Kogan, F., Stark, R., Gitelson, A., Jargalsaikhan, L., Dugrajav, C. and Tsooj, S., 2004. Derivation of pasture biomass in Mongolia from AVHRR-based vegetation health indices. *International Journal of Remote Sensing* 25: 2889–2896.

Krause-Jensen, D., Sagert, S., Schubert, H. and Boström, C., 2008. Empirical relationships linking distribution and abundance of marine vegetation to eutrophication. *Ecological Indicators* 8: 515–529.

Krueger-Hadfield, S.A., Magill, C.L., Bunker, F., Mieszkowska, N., Sotka, E. and Maggs, C.A., 2017. When invaders go unnoticed: the case of *Gracilaria vermiculophylla* in the British Isles. *Cryptogamie, Algologie* 38: 379–400.

Krueger-Hadfield, S.A., Stephens, T.A., Ryan, W.H. and Heiser, S., 2018. Everywhere you look, everywhere you go, there's an estuary invaded by the red seaweed *Gracilaria vermiculophylla (Ohmi) Papenfuss, 1967*. *Bioinvasions Records* 7: 343-355.

Kucera, H. and Saunders, G.W., 2008. Assigning morphological variants of *Fucus* (Fucales, Phaeophyceae) in Canadian waters to recognized species using DNA barcoding. *Botany* 86: 1065–1079.

Lanari, M. and Copertino, M., 2017. Drift macroalgae in the Patos Lagoon Estuary (southern Brazil): effects of climate, hydrology and wind action on the onset and magnitude of blooms. *Marine Biology Research* 13: 36–47.

Lavery, P.S., Lukatelich, R.J. and McComb, A.J., 1991. Changes in the biomass and species composition of macroalgae in a eutrophic estuary. *Estuarine, Coastal and Shelf Science* 33: 1–22.

Le Moal, M., Gascuel-Odoux, C., Ménesguen, A., Souchon, Y., Étrillard, C., Levain, A., Moatar, F., Pannard, A., Souchu, P., Lefebvre, A. and Pinay, G., 2019. Eutrophication: a new wine in an old bottle? *Science of the Total Environment* 651: 1–11.

Liu, X., Li, Y., Wang, Z., Zhang, Q. and Cai, X., 2015. Cruise observation of *Ulva prolifera* bloom in the southern Yellow Sea, China. *Estuarine, Coastal and Shelf Science* 163: 17–22.

Long, N., Millescamps, B., Guillot, B., Pouget, F. and Bertin, X., 2016. Monitoring the topography of a dynamic tidal inlet using UAV imagery. *Remote Sensing* 8: 387.

Lotze, H.K. and Schramm, W., 2000. Ecophysiological traits explain species dominance patterns in macroalgal blooms. *Journal of Phycology* 295: 287–295.

Lotze, H.K., Schramm, W., Schories, D. and Worm, B., 1999. Control of macroalgal blooms at early developmental stages: *Pilayella littoralis* versus *Enteromorpha* spp. *Oecologia* 119: 46–54.

Lotze, H.K., Worm, B. and Sommer, U., 2000. Propagule banks, herbivory and nutrient supply control population development and dominance patterns in macroalgal blooms. *Oikos* 89: 46–58.

Lotze, H.K., Worm, B. and Sommer, U., 2001. Strong bottom-up and top-down control of early life stages of macroalgae. *Limnology and Oceanography* 46: 749–757.

Lowthion, D., Soulsby, P.G. and Houston, M.C.M., 1985. Investigation of a eutrophic tidal basin: 1. Factors affecting the distribution and biomass of macroalgae. *Marine Environmental Research* 15: 263–284.

Lyngby, J.E., Mortensen, S. and Ahrensberg, N., 1999. Bioassessment techniques for monitoring of eutrophication and nutrient limitation in coastal ecosystems. *Marine Pollution Bulletin* 39: 212–223.

McDevit, D.C. and Saunders, G.W., 2009. On the utility of DNA barcoding for species differentiation among brown macroalgae (Phaeophyceae) including a novel extraction protocol. *Phycological Research* 57: 131–141.

Malta, E.-J. and Verschuure, J.M., 1997. Effects of environmental variables on between-year variation of *Ulva* growth and biomass in a eutrophic brackish lake. *Journal of Sea Research* 38: 71–84.

Malta, E.-J., Draisma, S.G.A. and Kamermans, P., 1999. Free-floating *Ulva* in the southwest Netherlands: species or morphotypes? A morphological, molecular and ecological comparison. *European Journal of Phycology* 34: 443–454.

Mancini, F., Dubbini, M., Gattelli, M., Stecchi, F., Fabbri, S. and Gabbianelli, G., 2013. Using unmanned aerial vehicles (UAV) for high-resolution reconstruction of topography: the structure from motion approach on coastal environments. *Remote Sensing* 5: 6880–6898.

Mehrtens, C., Kaschell, T., Tardeck, F., Graser, N., Borowy, C. and Bartsch, I., 2009. Differentiation of brown seaweeds by hyperspectral airborne remote sensing and field spectrometry in a rocky intertidal. 6th EARSeL SIG-Imaging Spectroscopy Workshop. from 16th to 19th March 2009. Tel-Aviv University (Tel-Aviv, Israel).

Merceron, M., Antoine, V., Auby, I. and Morand, P., 2007. *In situ* growth potential of the subtidal part of green tide forming *Ulva* spp. stocks. *Science of the Total Environment* 384: 293–305.

Mineur, F., De Clerck, O., Le Roux, A., Maggs, C.A. and Velarque, M., 2010. *Polyopes lancifolius* (Halymeniales, Rhodophyta), a new component of the Japanese marine flora introduced to Europe. *Phycologia* 49: 86–96.

Mollet, J., Rahaoui, A. and Lemoine, Y., 1998. Yield, chemical composition and gel strength of agarocolloids of *Gracilaria gracilis*, *Gracilariopsis longissima* and the newly reported *Gracilaria cf. vermiculophylla* from Roscoff (Brittany, France). *Jounal of Applied Phycology* 10: 59–66.

Moss, B., 2007. Shallow lakes, the Water Framework Directive and life. What should it all be about? *Hydrobiologia* 584: 381–394.

Neiva, J., Pearson, G.A., Valero, M. and Serrão, E.A., 2010. Surfing the wave on a borrowed board: range expansion and spread of introgressed organellar genomes in the seaweed *Fucus ceranoides* L. *Molecular Ecology* 19: 4812–4822.

Nelson, T.A., Nelson, A.V and Tjoelker, M., 2003. Seasonal and spatial patterns of “green tides” (ulvoid algal blooms) and related water quality parameters in the coastal waters of Washington State, USA. *Botanica Marina* 46: 263–275.

Nelson, T.A., Haberlin, K., Nelson, A.V., Ribarich, H., Hotchkiss, R., Van Alstyne, K.L., Buckingham, L., Simunds, D.J. and Fredrickson, K., 2008. Ecological and physiological controls of species composition in green macroalgal blooms. *Ecology* 89: 1287–1298.

Ní Longphuirt, S., O’Boyle, S., Wilkes, R., Dabrowski, T. and Stengel, D.B., 2015a. Influence of hydrological regime in determining the response of macroalgal blooms to nutrient loading in two Irish estuaries. *Estuaries and Coasts* 39: 478–494.

Ní Longphuirt, S., O’Boyle, S. and Stengel, D.B., 2015b. Environmental response of an Irish estuary to changing land management practices. *Science of the Total Environment* 521–522: 388–399.

O’Boyle, S., Wilkes, R., Mcdermott, G. and Ní Longphuirt, S., 2017. Will recent improvements in estuarine water quality in Ireland be compromised by plans for increased agricultural production? A case study of the Blackwater estuary in southern Ireland. *Ocean and Coastal Management* 143: 87–95.

Oksanen, J., Guillaume-Blanchet, F., Roeland-Kindt, P., Legendre, P., Minchin, R., O’Hara, R.B., Simpson, G.L., Solymos, P., Henry, M., Stevens, H. and Wagner, H., 2012. Package “Vegan”, p. 255. Available online: https://cran.r-project.org/web/packages/vegan/vegan.pdf (accessed 20 May 2018).

Oliva, S., Mascaró, O., Llagostera, I., Pérez, M. and Romero, J., 2012. Selection of metrics based on the seagrass C*ymodocea nodosa* and development of a biotic index (CYMOX) for assessing ecological status of coastal and transitional waters. *Estuarine, Coastal and Shelf Science* 114: 7–17.

Orduña-Rojas, J., García-Camacho, K.Y., Orozco-Meyer, P., Ríosmena-Rodríguez, R., Pacheco-Ruiz, I., Zertuche-González, J.A. and Meling-López, A.E., 2008. Agar properties of two species of *Gracilaria*ceae from the Gulf of California, Mexico. *Journal of Applied Phycology* 20: 169–175.

Paalme, T. and Kukk, H., 2003. Comparison of net primary production rates of *Pilayella littoralis* (L.) Kjellm. and other dominating macroalgal species in Koiguste Bay, northeastern Baltic Sea. *Proceedings of the Estonian Academy of Sciences, Biology and Ecology* 52: 125–133.

Pang, S.J., Liu, F., Shan, T.F., Xu, N., Zhang, Z.H., Gao, S.Q., Chopin, T. and Sun, S., 2010. Tracking the algal origin of the *Ulva* bloom in the Yellow Sea by a combination of molecular, morphological and physiological analyses. *Marine Environmental Research* 69: 207–215.

Park, S.R., Kang, Y.H., Lee, H.J., Ko, Y.W. and Kim, J.H., 2014. The importance of substratum and elevation in recruitment and persistence of ulvoid algal blooms on rocky intertidal shores of the southern Korean coast. *Botanica Marina* 57: 55–66.

Pedersen, M.F. and Borum, J., 1996. Nutrient control of algal growth in estuarine waters. Nutrient limitation and the importance of nitrogen requirements and nitrogen storage among phytoplankton and species of macroalgae. *Marine Ecology Progress Series* 142: 261–272.

Pérez-Lloréns, J.L., Vergara, J.J., Olivé, I., Mercado, J.M. and Conde-álvarez, R., 2014. Autochthonous seagrasses. In Goffredo, S. and Dubinsky, Z. (eds), *The Mediterranean Sea: Its History and Present Challenges*. Springer Netherlands, Dordrecht. pp. 137–158.

Pérez-Lloréns, J.L., Hernández, I., Vergara, J.J., Brun, F.G. and León, Á., 2016. *Those Curious and Delicious Seaweeds. A Fascinating Voyage from Biology to Gastronomy*. Servicio de Publicaciones de la Universidad de Cádiz, Cádiz. pp. 390.

Pihl, L., Magnusson, G., Isaksson, I. and Wallentinus, I., 1996. Distribution and growth dynamics of ephemeral macroalgae in shallow bays on the Swedish west coast. *Journal of Sea Research* 35: 169–180.

Rapinel, S., Clément, B., Magnanon, S., Sellin, V. and Hubert-Moy, L., 2014. Identification and mapping of natural vegetation on a coastal site using a Worldview-2 satellite image. *Journal of Environmental Management* 114: 236–246.

Robertson, B.P. and Savage, C., 2018. Mud-entrained macroalgae utilise porewater and overlying water column nutrients to grow in a eutrophic intertidal estuary. *Biogeochemistry* 139: 1–16.

Romero, J., Martínez-Crego, B., Alcoverro, T. and Pérez, M., 2007. A multivariate index based on the seagrass *Posidonia oceanica* (POMI) to assess ecological status of coastal waters under the Water Framework Directive (WFD). *Marine Pollution Bulletin* 55: 196–204.

Rossi, F., 2006. Small-scale burial of macroalgal detritus in marine sediments: effects of *Ulva* spp. on the spatial distribution of macrofauna assemblages. *Journal of Experimental Marine Biology and Ecology* 332: 84–95.

Rueness, J., 2005. Life history and molecular sequences of *Gracilaria vermiculophylla* (Gracilariales, Rhodophyta), a new introduction to European waters. *Phycologia* 44: 120–128.

Rybak, A.S., 2018. Species of *Ulva* (Ulvophyceae, Chlorophyta) as indicators of salinity. *Ecological Indicators* 85: 253–261.

Saunders, G.W. and Kucera, H., 2010. An evaluation of *rbc*L, *tuf*A, UPA, LSU and ITS as DNA barcode markers for the marine green macroalgae. *Cryptogamie*, *Algologie* 31: 487–528.

Scanlan, C.M., Foden, J., Wells, E. and Best, M.A., 2007. The monitoring of opportunistic macroalgal blooms for the Water Framework Directive. *Marine Pollution Bulletin* 55: 162–171.

Schories, D. and Reise, K., 1993. Germination and anchorage of *Enteromorpha* spp. in sediments of the Wadden Sea. *Helgoländer Meeresuntersuchungen* 47: 275–285.

Setyawidati, N.A.R., Puspita, M., Kaimuddin, A.H., Widowati, I., Deslandes, E., Bourgougnon, N. and Stiger-Pouvreau, V., 2018. Seasonal biomass and alginate stock assessment of three abundant genera of brown macroalgae using multispectral high resolution satellite remote sensing: a case study at Ekas Bay (Lombok, Indonesia). *Marine Pollution Bulletin* 131: 40–48.

Sfriso, A., Facca, C. and Ghetti, P.F., 2003. Temporal and spatial changes of macroalgae and phytoplankton in a Mediterranean coastal area: the Venice lagoon as a case study. *Marine Environmental Research* 56: 617–636.

Sfriso, A., Wolf, M.A., Maistro, S., Sciuto, K. and Moro, I., 2012. Spreading and autoecology of the invasive species *Gracilaria vermiculophylla* (Gracilariales, Rhodophyta) in the lagoons of the north-western Adriatic Sea (Mediterranean Sea, Italy). *Estuarine, Coastal and Shelf Science* 114: 192–198.

Silva, T.S.F., Costa, M.P.F., Melack, J.M. and Novo, E.M.L.M., 2008. Remote sensing of aquatic vegetation: theory and applications. *Environmental Monitoring and Assessment* 140: 131–145.

Sims, D.A. and Gamon, J.A., 2003. Estimation of vegetation water content and photosynthetic tissue area from spectral reflectance: a comparison of indices based on liquid water and chlorophyll absorption features. *Remote Sensing of Environment* 84: 526–537.

Smayda, T.J., 1997. Harmful algal blooms: their ecophysiology and general relevance to phytoplankton blooms in the sea. *Limnology and Oceanography* 42: 1137–1153.

Smetacek, V. and Zingone, A., 2013. Green and golden seaweed tides on the rise. *Nature* 504: 84–88.

Son, Y.B., Min, J.E. and Ryu, J.H., 2012. Detecting massive green algae (*Ulva prolifera*) blooms in the Yellow Sea and East China Sea using Geostationary Ocean Color Imager (GOCI) data. *Ocean Science Journal* 47: 359–375.

Steentoft, M., Irvine, L.M. and Farnham, W.F., 1995. Two terete species of *Gracilaria* and *Gracilariopsis* (Gracilariales, Rhodophyta) in Britain. *Phycologia* 34: 113–127.

Sverdrup, H.U., 1953. On conditions for the vernal blooming of phytoplankton. *Journal du Conseil Permanent International pour l'Exploration de la Mer* 18: 287–295.

Task Force, 2010. *Sea Lettuce Task Force Report*. Available online: https://www.housing.gov.ie/sites/default/files/migrated-files/en/Foreshore/ApplicationsandDeterminations/CorkCoCl-RemovalSeaLettuce/ApplicationDetails/FileDownLoad%2C30556%2Cen.pdf (accessed 30 May 2019).

Taylor, R., Fletcher, R. and Raven, J., 2001. Preliminary studies on the growth of selected "green tide" algae in laboratory culture: effects of irradiance, temperature, salinity and nutrients on growth rate. *Botanica Marina* 44: 327–336.

Teichberg, M., Fox, S.E., Olsen, Y.S., Valiela, I., Martinetto, P., Iribarne, O., Muto, E.Y., Petti, M.A.V, Corbisier, T.N., Soto-Jiménez, M., Páez-Osuna, F., Castro, P., Freitas, H., Zitelli, A., Cardinaletti, M. and Tagliapietra, D., 2010. Eutrophication and macroalgal blooms in temperate and tropical coastal waters: Nutrient enrichment experiments with *Ulva* spp. *Global Change Biology* 16: 2624–2637.

Terlizzi, A., Anderson, M.J., Fraschetti, S. and Benedetti-Cecchi, L., 2007. Scales of spatial variation in Mediterranean subtidal sessile assemblages at different depths. *Marine Ecology Progress Series* 332: 25–39.

Thornber, C.S., Guidone, M., Deacutis, C., Green, L., Ramsay, C.N. and Palmisciano, M., 2017. Spatial and temporal variability in macroalgal blooms in a eutrophied coastal estuary. *Harmful Algae* 68: 82–96.

Trivedi, N., Gupta, V., Reddy, C.R.K. and Jha, B., 2013. Enzymatic hydrolysis and production of bioethanol from common macrophytic green alga *Ulva fasciata* Delile. *Bioresource Technology* 150: 106–112.

Uhl, F., Bartsch, I. and Oppelt, N., 2016. Submerged kelp detection with hyperspectral data. *Remote Sensing* 8: 487.

Valiela, I., Mcclelland, J., Hauxwell, J., Behr, P.J., Hersh, D. and Foreman, K., 1997. Macroalgal blooms in shallow estuaries: controls and ecophysiological and ecosystem consequences. *Limnology and Oceanography* 42: 1105–1118.

Vallet, J., Panissod, F., Strecha, C. and Tracol, M., 2012. Photogrammetric performance of an ultra light weight swinglet "UAV". *International Archives of the Photogrammetry, Remote Sensing and Spatial Information Sciences* XXXVIII-1/C22: 253–258.

Van Alstyne, K.L., 2018. Seawater nitrogen concentration and light independently alter performance, growth, and resource allocation in the bloom-forming seaweeds *Ulva lactuca* and *Ulvaria obscura* (Chlorophyta). Harmful Algae 78: 27–35.

Van Alstyne, K.L., Nelson, T.A., and Ridgway, R.L., 2015. Environmental chemistry and chemical ecology of "green tide" seaweed blooms. *Integrative and Comparative Biology* 55: 518–533.

Van der Wal, D., Van Dalen, J., Wielemaker-van den Dool, A., Dijkstra, J.T. and Ysebaert, T., 2014. Biophysical control of intertidal benthic macroalgae revealed by high-frequency multispectral camera images. *Journal of Sea Research* 90: 111–120.

Viaroli, P., Naldi, M., Bondavalli, C. and Bencivelli, S., 1996. Growth of the seaweed *Ulva rigida* C. Agardh in relation to biomass densities, internal nutrient pools and external nutrient supply in the Sacca di Goro lagoon (Northern Italy). *Hydrobiologia* 329: 93–103.

Viaroli, P., Bartoli, M., Giordani, G. and Naldi, M., 2008. Community shifts, alternative stable states, biogeochemical controls and feedbacks in eutrophic coastal lagoons: a brief overview. *Aquatic Conservation: Marine and Freshwater Ecosystems* 18: 105–117.

Wan, A.H.L., Wilkes, R.J., Heesch, S., Bermejo, R., Johnson, M.P. and Morrison, L., 2017. Assessment and characterisation of Irelands green tides (*Ulva* species). *PLOS ONE* 12: e0169049.

Wang, S., Huo, Y., Zhang, J., Cui, J., Wang, Y., Yang, L., Zhou, Q., Lu, Y., Yu, K. and He, P., 2018. Variations of dominant free-floating *Ulva* species in the source area for the world's largest macroalgal blooms, China: differences of ecological tolerance. *Harmful Algae* 74: 58–66.

Wang, Y., Wang, Y., Zhu, L., Zhou, B. and Tang, X., 2012. Comparative studies on the ecophysiological differences of two green tide macroalgae under controlled laboratory conditions. *PLOS ONE* 7: e38245.

Wang, Z., Xiao, J., Fan, S., Li, Y., Liu, X. and Liu, D., 2015. Who made the world's largest green tide in China? An integrated study on the initiation and early development of the green tide in Yellow Sea. *Limnology and Oceanography* 60: 1105–1117.

Weinberger, F., Buchholz, B., Karez, R. and Wahl, M., 2008. The invasive red alga *Gracilaria vermiculophylla* in the Baltic Sea: adaptation to brackish water may compensate for light limitation. *Aquatic Biology* 3: 251–264.

Wessels, K.J., Prince, S.D., Zambatis, N., MacFadyen, S., Frost, P.E. and Van Zyl, D., 2006. Relationship between herbaceous biomass and 1-km^2 Advanced Very High Resolution Radiometer (AVHRR) NDVI in Kruger National Park, South Africa. *International Journal of Remote Sensing* 27: 951–973.

West, H., Quinn, N., Horswell, M. and White, P., 2018. Assessing vegetation response to soil moisture fluctuation under extreme drought using sentinel-2. *Water* 10: 838.

Wilkes, R.J., Morabito, M. and Gargiulo, G.M., 2006. Taxonomic considerations of a foliose *Grateloupia* species from the Straits of Messina. *Journal of Applied Phycology* 18: 663–669.

Wilson-Freshwater, D. and Rueness, J., 1994. Phylogenetic relationships of some European *Gelidium* (Gelidiales , Rhodophyta) species, based on *rbcL* nucleotide sequence analysis. *Phycologia* 33: 187–194.

Wither, A., 2003. *Guidance for Sites Potentially Impacted by Algal Mats (Green Seaweed)*. EC Habitats Directive Technical Advisory Group report WQTAG07c.

Xiao, X., Agusti, S., Lin, F., Li, K., Pan, Y., Yu, Y., Zheng, Y. and Wu, J., 2017. Nutrient removal from Chinese coastal waters by large-scale seaweed aquaculture. S*cientific Reports* 7: 46613.

Yabe, T., Ishii, Y., Amano, Y., Koga, T., Hayashi, S. and Nohara, S., 2009. Green tide formed by free-floating *Ulva* spp. at Yatsu tidal flat, Japan. *Limnology* 10: 239–245.

Yang, M.Y., Macaya, E.C. and Kim, M.S., 2015. Molecular evidence for verifying the distribution of *Chondracanthus chamissoi* and *C. teedei* (Gigartinaceae, Rhodophyta). *Botanica Marina* 58: 103–113.

Ying-ying, S., Hui, W., Gan-lin, G., Yin-fang, P., Bin-lun, Y. and Chang-hai, W., 2015. Green alga *Ulva pertusa* – a new source of bioactive compounds with antialgal activity. *Environmental Science and Pollution Research* 22: 10351–10359.

Yoshida, G., Uchimura, M. and Hiraoka, M., 2015. Persistent occurrence of floating *Ulva* green tide in Hiroshima Bay, Japan: seasonal succession and growth patterns of *Ulva pertusa* and *Ulva* spp. (Chlorophyta, *Ulva*les). *Hydrobiologia* 758: 223–233.

Zhao, K., García, M., Liu, S., Guo, Q., Chen, G., Zhang, X., Zhou, Y. and Meng, X., 2015. Terrestrial lidar remote sensing of forests: maximum likelihood estimates of canopy profile, leaf area index, and leaf angle distribution. *Agricultural and Forest Meteorology* 209: 100–113.

Abbreviations

δ^{15}N	Delta nitrogen-15
AIC	Akaike information criterion
ANOVA	Analysis of variance
dbRDA	Distance-based redundancy analysis
DGR	Daily growth rate
DIN	Dissolved inorganic nitrogen
distLM	Distance-based linear model
DON	Dissolved organic nitrogen
GCP	Ground control point
GPS	Global positioning system
GSD	Ground sampling distance
IPCC	Intergovernmental Panel on Climate Change
ITS	Internal transcribed spacers of the nuclear-encoded ribosomal operon
MD	Minimum distance
ML	Maximum likelihood
N	Nitrogen
NDVI	Normalised difference vegetation index
nNB	Net nitrogen biomass
OM	Organic matter
P	Phosphorus
PCR	Polymerase chain reaction
PERMANOVA	Permutational analysis of variance
PERMDISP	Permutational distance-based test for homogeneity of multivariate dispersion
PSU	Practical salinity unit
***rbc*L**	Large subunit of the plastic-encoded ribulose-1,5-bisphosphate carboxylase/oxygenase
RS	Remote sensing
S.I.	Statutory Instrument
SS	Suspended solids
TON	Total oxidised nitrogen
UAV	Unmanned aerial vehicle
WFD	Water Framework Directive

AN GHNÍOMHAIREACHT UM CHAOMHNÚ COMHSHAOIL
Tá an Ghníomhaireacht um Chaomhnú Comhshaoil (GCC) freagrach as an gcomhshaol a chaomhnú agus a fheabhsú mar shócmhainn luachmhar do mhuintir na hÉireann. Táimid tiomanta do dhaoine agus don chomhshaol a chosaint ó éifeachtaí díobhálacha na radaíochta agus an truaillithe.

Is féidir obair na Gníomhaireachta a roinnt ina trí phríomhréimse:

Rialú: *Déanaimid córais éifeachtacha rialaithe agus comhlíonta comhshaoil a chur i bhfeidhm chun torthaí maithe comhshaoil a sholáthar agus chun díriú orthu siúd nach gcloíonn leis na córais sin.*

Eolas: *Soláthraímid sonraí, faisnéis agus measúnú comhshaoil atá ar ardchaighdeán, spriocdhírithe agus tráthúil chun bonn eolais a chur faoin gcinnteoireacht ar gach leibhéal.*

Tacaíocht: *Bímid ag saothrú i gcomhar le grúpaí eile chun tacú le comhshaol atá glan, táirgiúil agus cosanta go maith, agus le hiompar a chuirfidh le comhshaol inbhuanaithe.*

Ár bhFreagrachtaí

Ceadúnú
Déanaimid na gníomhaíochtaí seo a leanas a rialú ionas nach ndéanann siad dochar do shláinte an phobail ná don chomhshaol:
- saoráidí dramhaíola *(m.sh. láithreáin líonta talún, loisceoirí, stáisiúin aistrithe dramhaíola)*;
- gníomhaíochtaí tionsclaíocha ar scála mór *(m.sh. déantúsaíocht cógaisíochta, déantúsaíocht stroighne, stáisiúin chumhachta)*;
- an diantalmhaíocht *(m.sh. muca, éanlaith)*;
- úsáid shrianta agus scaoileadh rialaithe Orgánach Géinmhodhnaithe *(OGM)*;
- foinsí radaíochta ianúcháin *(m.sh. trealamh x-gha agus radaiteiripe, foinsí tionsclaíocha)*;
- áiseanna móra stórála peitril;
- scardadh dramhuisce;
- gníomhaíochtaí dumpála ar farraige.

Forfheidhmiú Náisiúnta i leith Cúrsaí Comhshaoil
- Clár náisiúnta iniúchtaí agus cigireachtaí a dhéanamh gach bliain ar shaoráidí a bhfuil ceadúnas ón nGníomhaireacht acu.
- Maoirseacht a dhéanamh ar fhreagrachtaí cosanta comhshaoil na n-údarás áitiúil.
- Caighdeán an uisce óil, arna sholáthar ag soláthraithe uisce phoiblí, a mhaoirsiú.
- Obair le húdaráis áitiúla agus le gníomhaireachtaí eile chun dul i ngleic le coireanna comhshaoil trí chomhordú a dhéanamh ar líonra forfheidhmiúcháin náisiúnta, trí dhíriú ar chiontóirí, agus trí mhaoirsiú a dhéanamh ar leasúchán.
- Cur i bhfeidhm rialachán ar nós na Rialachán um Dhramhthrealamh Leictreach agus Leictreonach (DTLL), um Shrian ar Shubstaintí Guaiseacha agus na Rialachán um rialú ar shubstaintí a ídíonn an ciseal ózóin.
- An dlí a chur orthu siúd a bhriseann dlí an chomhshaoil agus a dhéanann dochar don chomhshaol.

Bainistíocht Uisce
- Monatóireacht agus tuairisciú a dhéanamh ar cháilíocht aibhneacha, lochanna, uiscí idirchriosacha agus cósta na hÉireann, agus screamhuiscí; leibhéil uisce agus sruthanna aibhneacha a thomhas.
- Comhordú náisiúnta agus maoirsiú a dhéanamh ar an gCreat-Treoir Uisce.
- Monatóireacht agus tuairisciú a dhéanamh ar Cháilíocht an Uisce Snámha.

Monatóireacht, Anailís agus Tuairisciú ar an gComhshaol
- Monatóireacht a dhéanamh ar cháilíocht an aeir agus Treoir an AE maidir le hAer Glan don Eoraip (CAFÉ) a chur chun feidhme.
- Tuairisciú neamhspleách le cabhrú le cinnteoireacht an rialtais náisiúnta agus na n-údarás áitiúil *(m.sh. tuairisciú tréimhsiúil ar staid Chomhshaol na hÉireann agus Tuarascálacha ar Tháscairí)*.

Rialú Astaíochtaí na nGás Ceaptha Teasa in Éirinn
- Fardail agus réamh-mheastacháin na hÉireann maidir le gáis cheaptha teasa a ullmhú.
- An Treoir maidir le Trádáil Astaíochtaí a chur chun feidhme i gcomhair breis agus 100 de na táirgeoirí dé-ocsaíde carbóin is mó in Éirinn.

Taighde agus Forbairt Comhshaoil
- Taighde comhshaoil a chistiú chun brúnna a shainaithint, bonn eolais a chur faoi bheartais, agus réitigh a sholáthar i réimsí na haeráide, an uisce agus na hinbhuanaitheachta.

Measúnacht Straitéiseach Timpeallachta
- Measúnacht a dhéanamh ar thionchar pleananna agus clár beartaithe ar an gcomhshaol in Éirinn *(m.sh. mórphleananna forbartha)*.

Cosaint Raideolaíoch
- Monatóireacht a dhéanamh ar leibhéil radaíochta, measúnacht a dhéanamh ar nochtadh mhuintir na hÉireann don radaíocht ianúcháin.
- Cabhrú le pleananna náisiúnta a fhorbairt le haghaidh éigeandálaí ag eascairt as taismí núicléacha.
- Monatóireacht a dhéanamh ar fhorbairtí thar lear a bhaineann le saoráidí núicléacha agus leis an tsábháilteacht raideolaíochta.
- Sainseirbhísí cosanta ar an radaíocht a sholáthar, nó maoirsiú a dhéanamh ar sholáthar na seirbhísí sin.

Treoir, Faisnéis Inrochtana agus Oideachas
- Comhairle agus treoir a chur ar fáil d'earnáil na tionsclaíochta agus don phobal maidir le hábhair a bhaineann le caomhnú an chomhshaoil agus leis an gcosaint raideolaíoch.
- Faisnéis thráthúil ar an gcomhshaol ar a bhfuil fáil éasca a chur ar fáil chun rannpháirtíocht an phobail a spreagadh sa chinnteoireacht i ndáil leis an gcomhshaol *(m.sh. Timpeall an Tí, léarscáileanna radóin)*.
- Comhairle a chur ar fáil don Rialtas maidir le hábhair a bhaineann leis an tsábháilteacht raideolaíoch agus le cúrsaí práinnfhreagartha.
- Plean Náisiúnta Bainistíochta Dramhaíola Guaisí a fhorbairt chun dramhaíl ghuaiseach a chosc agus a bhainistiú.

Múscailt Feasachta agus Athrú Iompraíochta
- Feasacht chomhshaoil níos fearr a ghiniúint agus dul i bhfeidhm ar athrú iompraíochta dearfach trí thacú le gnóthais, le pobail agus le teaghlaigh a bheith níos éifeachtúla ar acmhainní.
- Tástáil le haghaidh radóin a chur chun cinn i dtithe agus in ionaid oibre, agus gníomhartha leasúcháin a spreagadh nuair is gá.

Bainistíocht agus struchtúr na Gníomhaireachta um Chaomhnú Comhshaoil
Tá an ghníomhaíocht á bainistiú ag Bord lánaimseartha, ar a bhfuil Ard-Stiúrthóir agus cúigear Stiúrthóirí. Déantar an obair ar fud cúig cinn d'Oifigí:
- An Oifig um Inmharthanacht Comhshaoil
- An Oifig Forfheidhmithe i leith cúrsaí Comhshaoil
- An Oifig um Fianaise is Measúnú
- Oifig um Chosaint Radaíochta agus Monatóireachta Comhshaoil
- An Oifig Cumarsáide agus Seirbhísí Corparáideacha

Tá Coiste Comhairleach ag an nGníomhaireacht le cabhrú léi. Tá dáréag comhaltaí air agus tagann siad le chéile go rialta le plé a dhéanamh ar ábhair imní agus le comhairle a chur ar an mBord.

EPA Research Report 285

Nutrient Dynamics and Ecophysiology of Opportunistic Macroalgal Blooms in Irish Estuaries and Coastal Bays (Sea-MAT)

Authors: Ricardo Bermejo, Svenja Heesch, Moya O'Donnell, Nessa Golden, Michéal MacMonagail, Maeve Edwards, Edna Curley, Owen Fenton, Eve Daly and Liam Morrison

Identifying pressures

Eutrophication is still a challenge for Europe and, in 2017, 100,000 km2 of coastal ecosystems remained affected. This equates to an area almost one and a half times the size of Ireland. In Ireland, 16% of transitional and coastal waters are classified as potentially eutrophic. The Sea-MAT project monitored four estuarine locations affected by macroalgal blooms (green tides). Macroalgal coverage and biomass abundances were considerably higher than the threshold values according to the monitoring tool used for the European Union Water Framework Directive (WFD, 2000/60/EC). Green tides comprise laminar and tubular *Ulva* spp., with tubular morphologies more numerous and less susceptible to transportation out of the estuary. Tubular morphologies appear to be buried at the end of the bloom, favouring accumulation of organic matter and nutrients in sediments. These can be a potential source of nutrients for subsequent blooms, perpetuating the eutrophication problem. The arrival of the non-native species *Gracilaria vermiculophylla* is an additional pressure as this species is able to bloom in areas where native species cannot.

Informing policy

In Ireland, the ecological status of transitional waters is assessed via the European Union WFD, based on physicochemical and biological parameters, which stipulates that good status must be achieved in order to protect associated ecosystems. The findings of the Sea-MAT project have implications for WFD assessment and provide information on future blooms in the context of climate change, as proposed by the Intergovernmental Panel on Climate Change for Irish coastal waters, forecasting earlier blooms with greater biomasses. These blooms are of great concern to the Local Authority Waters Programme (LAWPRO), which focuses on the protection and improvement of water quality, including estuarine and coastal waters, by engaging public bodies, stakeholders and local communities, and also to An Fóram Uisce, a statutory body established to represent all stakeholders interested in water quality.

Developing solutions

The Sea-MAT project has provided an understanding of the role of local environmental conditions in the development of macroalgal blooms in Ireland. Recommendations to reduce the impact of seaweed tides and control their development are proposed. Molecular tools successfully revealed the multispecific composition of Irish green tides and confirmed the presence of the alien species *G. vermiculophylla* along Irish coasts. The determination of the nitrogen content of the seaweeds forming blooms in Ireland revealed that nitrogen levels were above that needed to sustain the blooms and that other controlling factors limited growth throughout year. Remote sensing techniques are an effective and accurate method for monitoring the spatial extent of bloom events in Irish estuaries.

EPA Research: McCumiskey House, Richiew, Clonskeagh, Dublin 14.

Phone: 01 268 0100
Twitter: @EPAResearchNews
Email: research@epa.ie

www.epa.ie

EPA Research Webpages
www.epa.ie/researchandeducation/research/